Sustainable Anode Design for High-Rate and Flexible Lithium-Ion Batteries

by

Heeju Jin

A thesis submitted in conformity with the requirements
for the degree of Master of Applied Science

Department of Mechanical and Industrial Engineering
University of Toronto

Sustainable Anode Design for High-Rate and Flexible Lithium-Ion Batteries

Heeju Jin
Master of Applied Science

Department of Mechanical and Industrial Engineering
University of Toronto
2025

Abstract

Lithium-ion batteries are a widely used class of rechargeable batteries, commonly employed in everyday applications. Beyond their well-established role as a replacement for traditional internal combustion engines in the automotive industry, lithium-ion batteries have garnered significant attention for emerging applications in wearable devices, biomedical equipment, and flexible electronics. Although widely used, conventional lithium-ion batteries are inherently rigid and unable to accommodate mechanical deformations such as bending or folding, which are essential for flexible electronic applications. Beyond structural limitations, they also pose environmental challenges, as the conventional slurry-casting method for electrode fabrication typically relies on toxic solvents. To overcome these limitations, this thesis aimed to design flexible, fast charging, and high-performance anodes while also addressing environmental concerns. The first study demonstrated the integration of niobium oxide as a fast-charging anode material for lithium-ion batteries using a sustainable solvent-free electrode processing technique, achieving mechanical durability and high mass loading, while delivering excellent electrochemical performance even under high-rate charging and discharging conditions. For the second study, hydrothermal/solvothermal synthesis were employed to directly grow titanium dioxide on flexible carbon fiber substrates for the fabrication of a freestanding anode. Given their shared objectives, both studies highlight environmentally friendly aspects while simultaneously enabling flexibility and fast-charging capabilities. In summary, this research seeks to contribute to the advancement of technologies in the expanding rechargeable battery sector.

Acknowledgements

I dedicate this thesis to all those around me who have provided limitless support and encouragement along the way. Your kindness and presence helped me overcome challenges and complete this work, and I truly appreciate to each one of you for being there for me.

First and foremost, I would like to express my deepest gratitude to my supervisor, Professor Hani Naguib. Thank you for giving me the incredible opportunity to work under your guidance. I am deeply grateful for your assistance and excellent mentorship. I especially appreciate your encouragement to explore and advocate for my own ideas, supporting my growth as an independent researcher. Your willingness to engage in numerous one-on-one discussions and brainstorming sessions has been instrumental in shaping my academic development. I would also like to extend my sincere appreciation to both the current and former members of the TSMART Lab. It has been a privilege to have worked with such amazing individuals and will remain as memorable experience for me.

My exceptional mentor, Yoojin, from the very beginning of our work together, your guidance has taught me not only technical skills but also countless invaluable lessons through every aspect of our work. Despite being inexperienced as a master's student, you were always opened to my ideas with respect, offering insightful feedback and encouragement. As you know, we encountered numerous challenges throughout our study, but I was able to navigate through because you consistently stood by my side, facing every obstacle together with me. In addition, my adorable Yi-Chen, thank you for always uplifting me with your bright energy, I am extremely glad we met through Yoojin and hope we cross path one day.

To my loving parents and my brother, Wonik, I truly would not be where I am today without your unconditional support. I have always shared both the highs and lows with you, and I deeply appreciate your constant understanding, guidance, empathy, and care. Since I was little, you have taught me perseverance to pursue my goals and that has been the key foundation in completing this degree. I love you all deeply and am incredibly proud to be your daughter.

Last but certainly not least, I would like to thank my dear friends who have always brought joy and love into my life. Sue and Shinwon, I am truly grateful to have met you all at the University of Toronto. Your positive energy has always kept me cheerful and entertained, while our heartfelt conversations and shared concerns provided comfort and support along the way. Tina, Laura, Hari, Doowon, and Vasant – our endless jokes, teasing, and shared laughter have been a constant source of joy for me. Those moments gave me the strength and energy to start each new week, and I am truly grateful for the happiness you have brought into my life in Toronto. Safwan, it was such a relief knowing I had someone here when I was just starting out at the University of Toronto, and I am really grateful for our friendship. To John, my best friend Katrina, and Brandon, thank you for always cheering me on and making the effort to visit me in Toronto. You guys always know how to make me smile, and my life would not be the same without you all.

Table of Contents

List of Tables

List of Figures

Chapter 1: Introduction

1.1 Preamble

Greenhouse gas emissions and global warming continue to be significant ongoing concerns. To mitigate these issues, there is an urgent need to develop sustainable energy solutions that can effectively reduce fossil fuel consumptions [1,2]. Numerous energy storage systems are currently being explored and under the development, with portable energy storage devices having introduced the concept of batteries [3,4]. Batteries can be categorized into two types: primary and secondary batteries [5]. Primary batteries are non-rechargeable, meaning they can only be used once, while secondary batteries are rechargeable energy systems capable of undergoing multiple charging and discharging cycles [6]. The development of rechargeable battery-based technologies is aimed at significantly reducing greenhouse gas emissions, playing a vital role in advancing sustainable energy sources [7,8]. Among these, lithium-ion batteries (LIBs) have emerged as the most widely used energy storage system, particularly in electric vehicles and portable electronic devices such as mobile phones, laptops, and handheld power tools, owing to their advantages of high energy density and long cycle life [9–11]. Since the commercialization of the first LIB by Sony in the 1990s, the battery market has undergone a significant growth [12]. Despite its advantages, the rising demand for advanced energy storage solutions underscores the limitations of current LIBs in meeting market requirements. The need for LIBs with fast charging and discharging capabilities, combined with high energy density, is steadily increasing [13–15]. Moreover, the expanding use of wearable and biomedical devices has driven consumer demand for flexible electronic devices, highlighting the necessity for flexible, foldable, and stretchable energy storage systems [16,17]. Hence, the development of innovative advanced materials that can meet these growing requirements is essential [18,19].

1.2 Thesis Objectives / Motivation

Ongoing development of anode materials is being driven by the increasing usage of lithium-ion batteries in everyday applications. In addition to achieving higher specific capacities, growing consumer demands for reduced charging and discharging times have further emphasized the need for high-rate capable anode materials. Furthermore, the advancement of wearable and flexible electronics has necessitated a shift from traditional rigid battery designs toward flexible battery technologies capable of integrating into these emerging applications. As a result, the motivation of this study was to explore anode materials with both high-rate capability and mechanical resilience, suitable for incorporation into flexible lithium-ion batteries. Beyond conventional electrochemical evaluations, this study employs mechanical analysis to systematically assess the robustness of the anode material. The effects of external mechanical deformation on electrochemical performance are investigated, offering a comprehensive understanding of the material's mechanical and electrochemical stability. The primary objective of the first study is to incorporate niobium oxide as an anode material into flexible lithium-ion batteries using a dry electrode fabrication technique, aiming to demonstrate its fast-charging performance, high mass loading capability, and structural flexibility. In the second study, a comparative analysis of hydrothermal and solvothermal syntheses was conducted to optimize the growth of titanium oxide on carbon fiber for application as a flexible, freestanding anode material.

1.3 Lithium-Ion Batteries (LIBs)

In lithium-ion battery systems, multiple single unit cells are interconnected to form a module, and several of these modules can be assembled to construct a complete battery pack [20]. Each individual unit cell consists of an anode and a cathode, serving as the negative and positive electrodes, respectively, along with the electrolyte and separator [21]. Here, the movement of ions is supported by electrolytes, separators, and current collectors [22]. During the charging process, lithium ions migrate from the cathode to the anode through the electrolyte, while electrons flow in the same direction through the external circuit. In contrast, during discharging, the intercalation process occurs in the opposite direction [23]. The separator component is employed to maintain a barrier between the electrodes, preventing direct contact and subsequent internal short-circuiting, while permitting the free movement of ions [23,24]. Therefore, the separator is a critical component that directly influences the overall safety of the battery system. Currently, the most widely adopted commercial separators are polyolefin-based microporous membranes, which are primarily polyethylene (PE) and polypropylene (PP) [25]. Their widespread use is attributed to their cost-effectiveness, excellent mechanical strength, chemical stability, and non-toxic nature [26]. Finally, the current collectors serve to gather the electrical current produced by both electrodes and integrate this generated current to the external circuit [27]. In conventional LIBs, aluminum foil is generally used as the current collector for the cathode, while copper foil serves as the current collector for the anode. The use of different current collectors for each electrode side is attributed to the natural tendency of copper to easily oxidize at higher potentials, making it unsuitable for the cathode. Thus, copper is primarily employed as the current collector for the negative side [28]. In contrast, aluminum has demonstrated stability even at potentials greater than 4V vs. Li/Li+, making it an ideal candidate for use as the cathode current collector [29]. The transport of lithium ions between electrodes occurs through an electrolyte composed of conductive lithium salts, such as $LiPF_6$, dissolved in non-aqueous solvents like ethylene carbonate (EC) and dimethyl carbonate (DMC) [30,31].

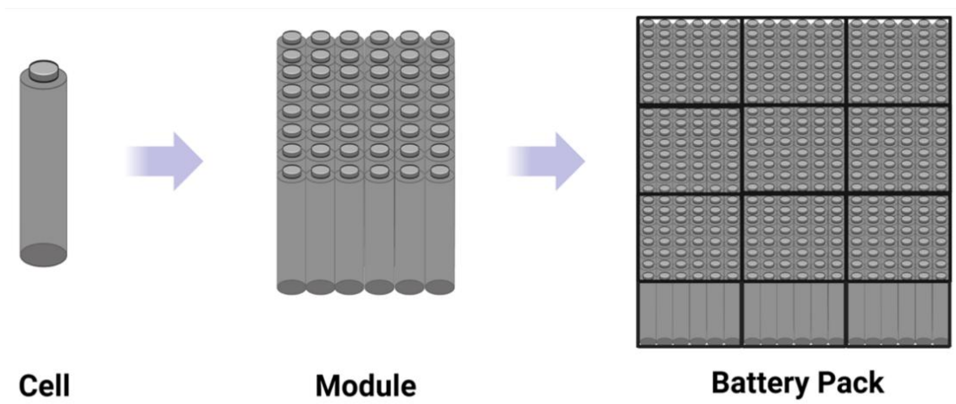

Figure 1-1. Illustration of lithium-ion cell, module, and battery pack

1.3.1 Basic Fundamental of LIB

In LIBs, upon assembly and prior to any charge-discharge cycles, a lithium-ion battery is at its discharged state, where all the lithium ions remain at the cathode, the source of lithium ions [32]. During the charging process, lithium ions de-intercalate from the cathode and migrate toward the anode, driven by the electrochemical potential differences across the cell [33]. This process is accompanied by an oxidation half-reaction at the cathode, as it loses electrons by releasing to the external circuit to maintain overall charge balance across the cell. At the same time, anode accepts lithium ions and gains electrons through an external circuit where it undergoes a reduction half-reaction. In contrast, during the discharging process, the anode is oxidized as lithium ions travel back to the cathode, while cathode experiences a reduction half-reaction by accepting the lithium ions [34,35].

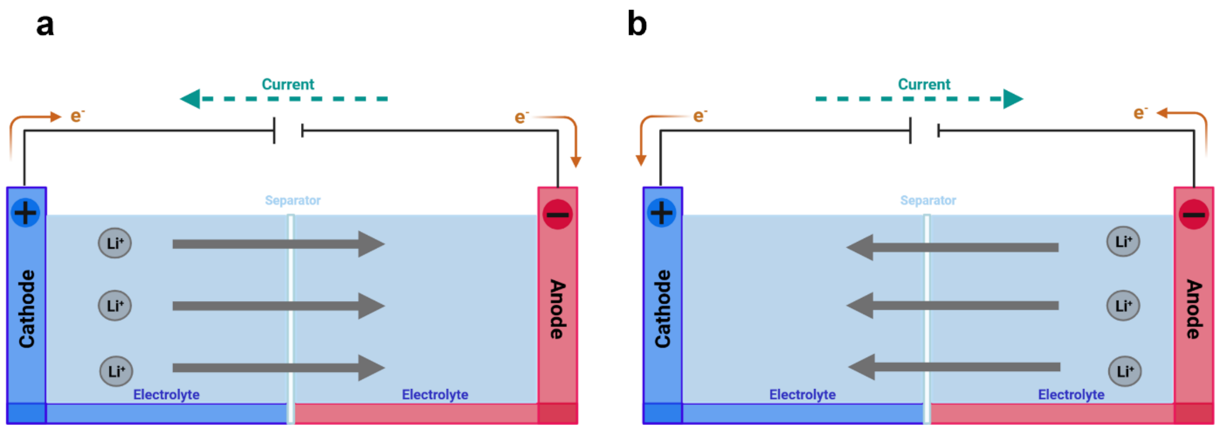

Figure 1-2. Basic Lithium-ion Battery Electrochemistry Fundamentals a) Charging b) Discharging

Throughout the charge-discharge cycles, there are few side reactions that are detrimental, leading to capacity degradation and reduced electrochemical performance. Among the side reactions, the formation of a solid electrolyte interphase (SEI) occurs as the electrolyte reduction happens at the surface of the anode, producing a passivation layer [36]. Theses layers are typically formed during the initial cycle when the electrolyte interacts with the electrode surface. The formation of these layers takes place when the operating voltage of the cell is beyond the electrochemical stability voltage window of the electrolyte [37]. The SEI layer is essential for chemical and electrochemical stability within the cell. Once established, the SEI acts as an electronically insulating yet ionically conductive layer that inhibits electron interaction with the electrolyte, thereby suppressing further electrolyte decomposition and maintaining interfacial stability at the electrode-electrolyte interface [38,39]. However, it can undergo continuous growth through ongoing electrolyte decomposition and the consumption of active lithium ions, leading to increased battery resistance, capacity degradation, and low power density [40]. Moreover, the formed SEI typically exhibits microstructural heterogeneity and can result in non-uniform lithium deposition across the anode surface [41]. This phenomenon, referred to as lithium plating, involves the deposition of metallic lithium on the anode surface rather than intercalation. It is initiated when the anode potential drops below 0V vs. Li/LI^+ due to the extremely close potential difference between lithium metal and the intercalated anode, making lithium deposition favorable over intercalation [42,43]. Such plating can occur when the battery operates in low-temperature environments, under fast charging conditions, or in the event of experiencing overcharging [44]. Ultimately, lithium plating reduces the amount of active lithium available for reversible intercalation processes, thereby directly impacting battery performance, increased rate of capacity fade, and shortening cycle life [45]. This uneven lithium deposition can lead to creating needle-like lithium dendrites [46]. The growth of such dendritic structures poses a significant safety concern, as they can penetrate the separator, leading to internal short circuits [47,48].

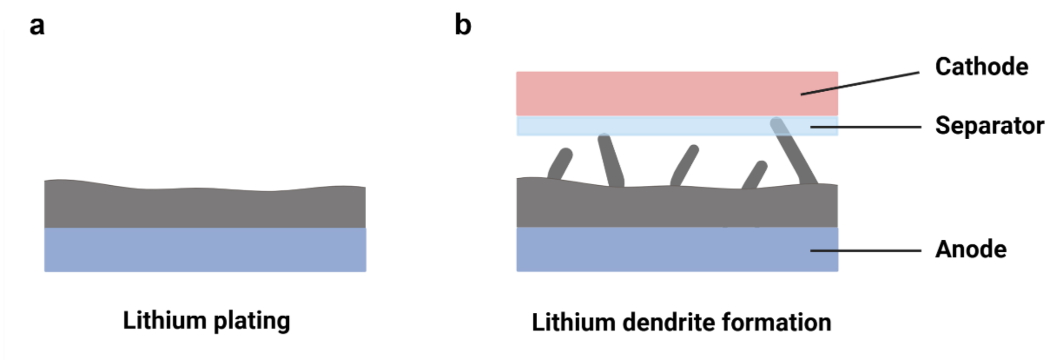

Figure 1-3. SEI layer a) lithium plating b) lithium dendrite formation

1.3.2 LIB Cell Structures

In battery testing, two main cell configurations are typically employed: half-cells and full cells. In a half-cell setup, the fabricated working electrode is paired with lithium metal as the counter and reference electrode, allowing evaluation of the working electrode's electrochemical performance. In the half-cell configuration, lithium metal, owing to its exceptionally low redox potential of -3.04 V (vs. standard hydrogen electrode), serves as the anode in practical operation [49,50]. On the other hand, the full cell comprises both a fabricated anode and cathode, instead of using lithium metal as a reference or counter electrode [51,52]. Evaluating both half-cell and full-cell configurations is essential, as half-cell measurements alone may not provide sufficient insight into the practical applicability of the fabricated electrode in a complete battery system [53]. For example, the review by Li et al. (2022) demonstrated that, in half-cell assembly using a silicon anode, the issue of low coulombic efficiency was mitigated due to the excess lithium provided by the lithium metal counter electrode. In contrast, when the same silicon anode was integrated in a full cell, the absence of lithium metal and the resulting limitation in lithium supply raised a problem of having a low coulombic efficiency [54].

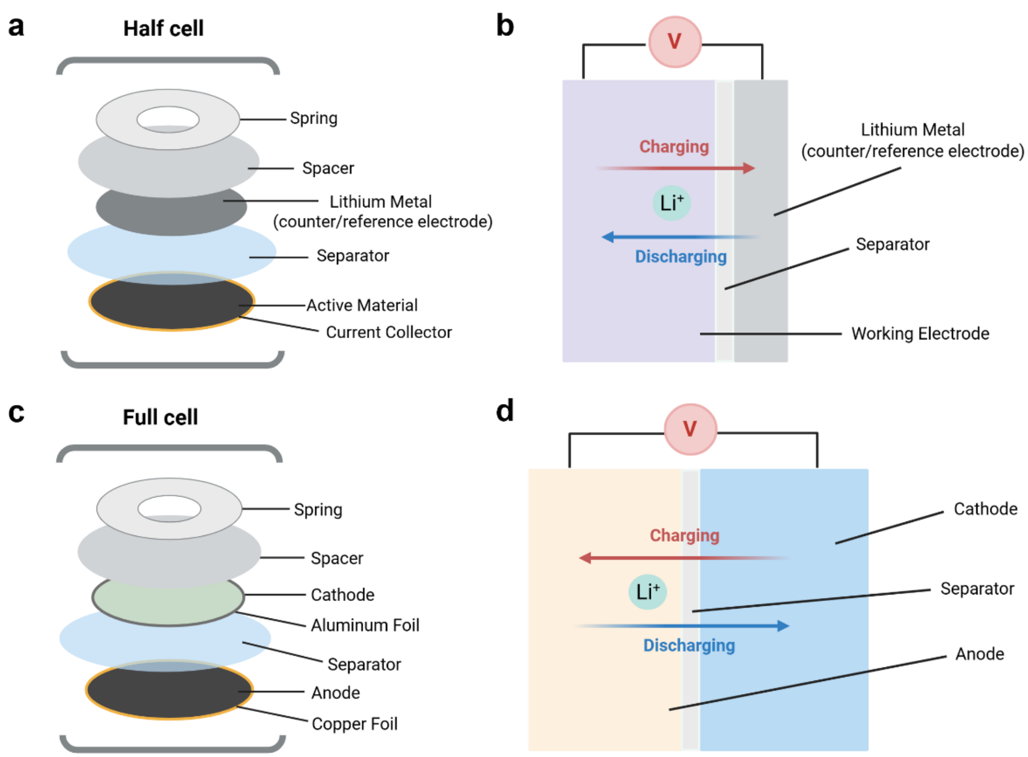

Figure 1-4. Configurations of a) half-cell assembly b) half-cell mechanism c) full cell assembly d) full cell mechanism

1.3.3 LIB Cell Configurations

Lithium-ion batteries are available in various outer configurations, enhancing their compatibility with a diverse array of commercial applications [55]. In large scale applications, such as electric vehicles, multiple cells are combined and assembled into a module. The design of this module is determined by the size and shape of the application products, with the additional consideration of interconnecting circuits, safety, and temperature management [56]. Primarily, the types of cells commonly found are coin, cylindrical, pouch, and prismatic cells [57]. Coin cell batteries feature a disc-shaped design and are commonly used in small electronics due to their compact size and compatibility with portable devices [55]. Cylindrical cells, commonly used in Tesla Motors' vehicles, employ the standardized 18650 cell configuration, with a diameter of

18mm in diameter and a height of 65mm. Laminated current collectors and separators are placed within a steel or aluminum alloy prismatic-shaped structure, with the electrolyte inserted [58]. The pouch cell encapsulates the electrodes, separator, and current collectors with a flexible laminate material, replacing the conventional rigid casing. Electrical connections are established by attaching metallic tabs to the current collectors, which extend outside the pouch cell to accommodate external connections [59]. Lastly, the prismatic shape of LIBs is designed similarly to cylindrical cells, with the main difference being the winding shape, which resembles the elliptical form of a pouch cell. Both cylindrical and prismatic cells are typically encased in a solid hard case made of aluminum or stainless steel [60].

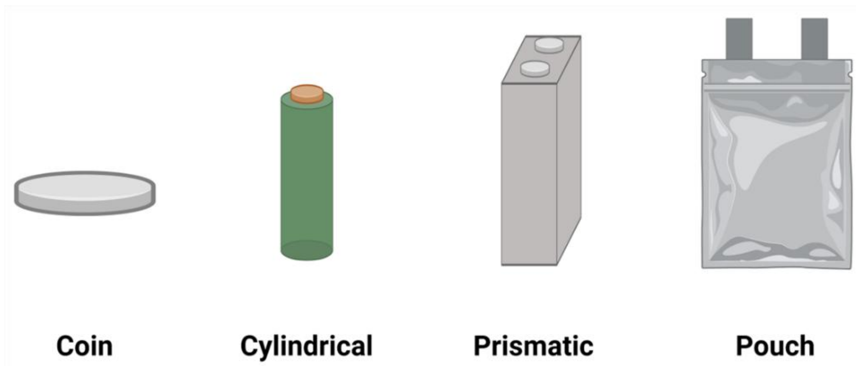

Figure 1-5. Different types of cell configurations

1.3.4 Key Factors Affecting Cell Assembly

Cell assembly involves several critical factors that must be considered, as they directly influence cell quality and ensure repeatability. Electrode alignment plays a critical role in determining cell stability during long-term cycling [61]. In practice, achieving perfect alignment between the anode and cathode is challenging. To address this issue, designing the anode with a larger surface area than the cathode can ensure a full utilization of cathode active material (or counter electrode), thereby minimizing the risk of inactive regions [62]. This parameter is commonly referred to as the N/P ratio, which denotes the capacity ratio between the negative and positive electrodes [63]. Furthermore, the quantity of electrolyte used during cell assembly significantly influences the long-term cycling performance. A larger electrolyte volume has been shown to support prolonged cycle life. For example, a study done by Chen et al. (2019) reported that when a limited amount of electrolyte was used in NMC 622-coin cell tests, stable cycling was sustained for only 12 cycles, after which the capacity rapidly dropped until it reached near zero [64]. Finally, the application of appropriate crimping pressure during the final stage of cell assembly is essential [65]. This pressure serves to enhance the interfacial contact between the electrolyte and electrodes. Although, excessive pressure can be detrimental, as it may induce cracks that compromise battery performance and increase the risk of thermal runaway or failure [66].

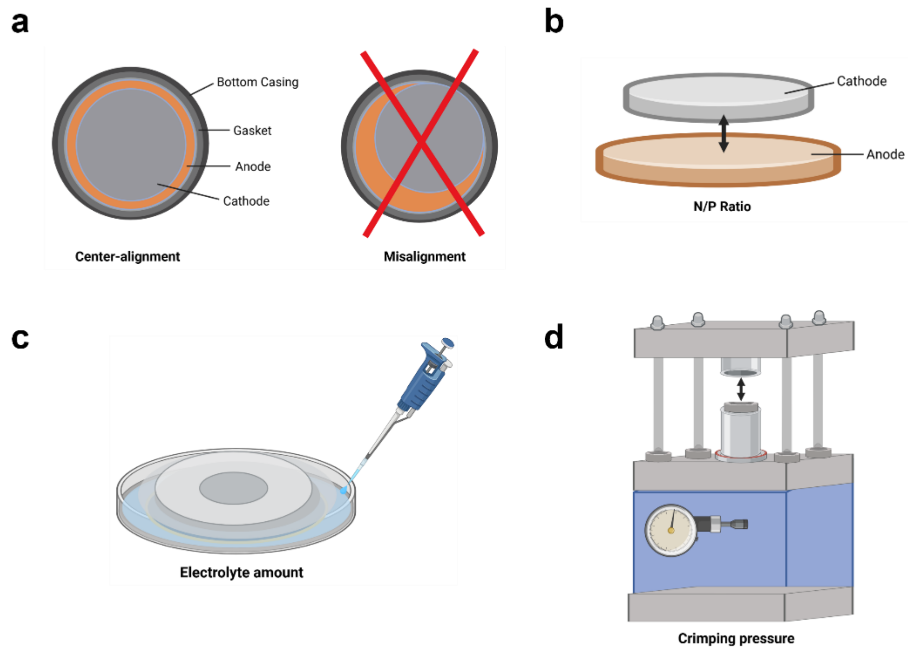

Figure 1-6. Cell assembly affected by a) electrode alignment b) N/P ratio c) amount of electrolytes d) crimping pressure

1.4 Fast Charging

In recent years, the rising demand for rechargeable batteries, coupled with the desire to achieve higher power density, had also led to increasing interest in fast-charging capabilities. Fast-charging characteristics are garnering significant attention due to the convenience and time efficiency they offer. One of the areas where fast-charging batteries are in high demand are the automotive industry. When comparing the charging times of electric vehicles to those of conventional internal combustion engine vehicles, the significantly longer charging times required by electric vehicles lead to considerable inconvenience for consumers [67]. To achieve this goal, extensive research has been focused on the design of high-rate anode materials to enable fast-charging LIBs. Among the various anode materials extensively studied, transition metal oxides have garnered considerable interest for fast charging applications due to their multivalent characteristic, wherein the presence of multiple oxidation states allows for multiple electron transfer processes [68,69]. This allows for faster (de)intercalation kinetics, enabling higher c-rate performance and contributing to higher theoretical capacity [70]. Accordingly, this section of the paper will explore different transition metal oxides utilized in the following studies.

1.4.1 Graphite (conventional anode material)

Graphite-based materials are commonly used for LIB anodes in commercial applications due to their low cost and the abundance of carbon. The widespread use of graphite as an anode material can attributed to its excellent electrical conductivity, high reversible lithium storage capacity, and low electrochemical potential. As a result, they retain their capacity even after repeated charge and discharge cycles [71]. On the other hand, the low operating potential leads to challenges at high charging rates (C-rate), limiting its ability to support fast charging [72]. It poses challenges in achieving high-rate performance (exceeding 1C) due to its inherently sluggish kinetics and low operating potential close to lithium metal (0.1V vs. Li/Li^+) [72,73]. This then causes the graphite anode to undergo a build-up of lithium ions on the surface of the graphite electrodes, resulting in lithium plating [74]. To mitigate the issue with graphite when fast charging, alternative materials capable of accommodating rapid lithium-ion transport were explored in this study.

1.4.2 Titanium Oxide / Lithium Titanate

Titanium oxide (TiO_2) and lithium titanate ($Li_4Ti_5O_{12}$, LTO) exhibit great rate capability and long-term cycling stability, making them promising candidates to replace conventional graphite anodes in fast-charging LIBs [75]. Lithium titanate ($Li_4Ti_5O_{12}$) is a well-established fast charging material candidate, offering high-rate capability also operating at a relatively high potential (~1.55V vs. Li/Li^+). Nevertheless, despite its outstanding high-rate performance, LTO suffers from a low theoretical specific capacity (~175mAh g^{-1}), presenting a trade-off that constrains from attaining a high energy density in LIBs [76]. On the other hand, TiO_2 offers a theoretical specific capacity of 335mAh g^{-1} and operates at a relatively high potential range of 1.5-1.7V vs. Li/Li^+ [77,78]. Additionally, it undergoes a small volume change (~4%) during cycling, demonstrate excellent capacity retention and long-term stability [78]. Although, the inherently poor ionic and electronic conductivities of TiO_2 significantly hinder its rate performance under rapid charging and discharging conditions, thereby constraining its viability for fast-charging LIB systems [79]. Titanium dioxide primarily crystallizes in four distinct phases which are anatase, rutile, brookite, and TiO_2 (B), each exhibiting distinct structural characteristics [80,81]. Among the four crystalline phases of TiO_2, rutile is the most thermodynamically stable [82,83]. However, bulk rutile exhibits relatively poor electronic conductivity [84]. To mitigate this issue, TiO2 must be synthesized and engineered at the nanoscale to improve its electrochemical performance, enabling higher capacity at high charge-discharge rates [84,85].

1.4.3 Niobium Oxide

Niobium can exist in four distinct oxidation states, namely 0, 2+, 4+, and 5+. Among these, niobium pentoxide (Nb_2O_5) is the most thermodynamically stable form [86]. Niobium pentoxide can be synthesized in several crystalline phases, including hexagonal (TT-phase), orthorhombic (T-phase), tetragonal (M-phase), and monoclinic (H-phase) structures, with each phase offering different electrochemical performance. The M-phase is an intermediate state between the T- and H-phases and therefore, the synthesis of a pure M-phase extremely difficult [87]. The TT-phase and T-phase have been reported to deliver capacities of 200mAhg^{-1} at 0.1C, while the H-phase attained the highest capacity of 242mAhg^{-1} [88]. Here, the electrochemical performance difference is attributed to the structural configurations of each phase, with the T-phase possessing a bronze structure, while the H-phase has shown Wadsley-Roth shear structure [89]. The T-phase offers two-dimensional diffusion pathways, while the Wadsley-Roth shear structure of the H-phase permits three-dimensional diffusion, thereby enhancing high-rate performance and enabling rapid charging [90,91]. In addition, the Wadsley-Roth shear structure has larger number of lithium active sites, leading to an increased theoretical specific capacity when compared to the bronze structured phase [91]. Overall, niobium oxide offers a high operating voltage window (1-3V vs. Li/Li^+), which helps avoid lithium dendrite growth and minimizes solid electrolyte interphase (SEI) formation [92]. Furthermore, it has a higher theoretical specific capacity compared to LTO (~175mAhg^{-1}) [93]. As a result, niobium pentoxide (Nb_2O_5) has emerged as a promising alternative fast-charging anode material.

1.5 Flexible Lithium-Ion Batteries (FLIBs)

The increasing demand for miniaturization, high speed, and integration in portable electronics has led to the development of flexible electronic devices, which are now utilized across various sections, including communications, healthcare, and wearable consumer electronics. Flexible batteries are defined as batteries that retain all the functional attributes of conventional batteries while possessing the ability to withstand mechanical deformations, such as bending, stretching, distortion, and folding. The ability to withstand mechanical deformations offers a significant benefit, enabling electronic products integrated with flexible batteries to operate under various conditions [94]. Flexible electronics must not only endure deformation but also maintain their electrochemical and safety performance, requiring extensive research efforts to achieve these objectives. Considering that LIBs are among the leading candidates for powering portable electronics, and conventional LIBs fall short of meeting the requirements of flexible electronics, the focus should be directed towards the design and fabrication of flexible lithium-ion batteries (FLIBs) [95].

Figure 1-7. Prospective real-life applications of flexible batteries

1.6 Electrode Fabrication

The electrode fabrication of commercial LIBs typically involves four distinct steps: slurry mixing, coating, electrode drying, and calendaring. The three primary components which are active materials, conductive agents, and binders are thoroughly mixed with a selected solvent to form a slurry, ensuring the uniform distribution of particles [96]. The prepared slurries are then coated onto current collectors to form uniform electrode films. These films are subsequently heated to fully evaporate the solvents from the slurry. Finally, the films are compressed using two metal rollers to achieve the desired thickness and uniformity [97]. However, several challenges are associated with the conventional slurry-based electrode fabrication method. One primary issue arises during the solvent drying process, where uneven evaporation rates can lead to severe cracking, particularly when the electrode thickness is beyond the critical threshold thickness for cracking [98]. Furthermore, although LIBs are considered a clean energy storage solution, they remain distant from being fully sustainable due to the use of toxic solvent in the slurry mixture. Polyvinylidene fluoride (PVDF) is commonly combined with the volatile solvent N-methyl pyrrolidone (NMP), as PVDF is insoluble in water, to be used in the slurry casting fabrication method as a binder [99]. To overcome this issue, carboxymethyl cellulose (CMC) binder, a promising alternative, has recently been increasingly used to replace toxic NMP, as CMC is water-soluble. Unfortunately, binders such as PVDF and CMC, commonly used in the slurry casting method, are ineffective in preventing crack formation during the electrode drying process, especially as the electrode thickness increases [98,100]. On top of that, this approach does not address all the issues, as cathode materials must avoid water-based formulations and therefore, replacing PVDF with CMC binder is not a viable solution. This is because nickel-based NCM (nickel-cobalt-manganese) active materials in the cathode are moisture sensitive [101]. Consequently, conventional fabrication methods have demonstrated limitations in producing effective electrodes, hindering further advancements in the development of next-generation LIBs.

1.6.1 Components in Electrode Fabrication

An electrode is generally composed of four key components: an active material, a binder, conductive additives, and a current collector [102]. The active material, comprising the majority of the electrode's composition, predominantly determines the cell capacity and operating voltage [103]. The binder serves to preserve the structural integrity of the electrode by ensuring the adhesion of the active material and conductive additives, thereby ensuring the mechanical stability of the electrode [104]. Next, the use of conductive additives enhances the overall electrical conductivity while reducing the internal resistance [105]. Lastly, the current collector functions as an electrical pathway for electron transport between the two electrodes through the external circuit [106]. Overall, the formulation of electrode components is typically tailored to meet the desired performance, as it directly influences the energy density, cycle life, and electrochemical performance of LIBs. In particular, increasing the proportion of active material within the electrode can enhance the specific energy, thus providing excellent electrochemical performance [107].

1.6.2 Solvent-Free Electrode Processing

Increasing electrode thickness or mass loading is an effective strategy for enhancing the energy density of the cell [108,109]. Although it has been established that achieving this goal is challenging with the conventional fabrication approach. As an alternative, the dry electrode fabrication process has shown significant advantages in terms of operating cost and energy efficiency when compared to the traditional solvent-based process [110]. Moreover, the dry electrode fabrication process has demonstrated the ability to increase active mass loading, enabling the production of thicker electrodes. The removal of solvents in the electrode the fabrication process has effectively increased the maximum limit for active mass loading [111]. The solvent-free dry electrode fabrication process utilizes distinct binding technique, employing a binder that fibrillates to bind the active material and conductive agents together [112]. The dry electrode processing involves mixing the powdered active material, conductive additives, and binder together [113]. During this process, the chosen binder is pre-fibrillated through the shear forces generated during mixing. The functionality of the binder plays a crucial role in the formation of the desired electrode microstructure, as it dictates both mechanical strength and battery performance [114]. Polytetrafluoroethylene (PTFE), a commonly used binder in dry electrode fabrication, is a deformable material that transforms into fibrous structures under shear force, effectively interconnecting the particles within the electrode [115]. The resulting freestanding film is then transferred onto the current collector, completing the electrode fabrication process.

Studies have shown that parameters such as duration and intensity are critical in the solvent-free electrode fabrication, as they dictate the morphology and distribution of the fibrous binder [113,116]. For instance, insufficient mixing time results inadequate fibrillation and uneven distribution of materials within the mixture. On the other hand, excessive mixing duration can result in cracks and poor binding, making it difficult to form a stable film. Hence, this indicates that optimal mixing is essential for forming a strong fibrillated matrix, which will exhibit high tensile and adhesion strength that can demonstrate structural stability even after repeated charging and discharging cycles [117]. To establish the connection between dry electrode processing and flexible batteries, it has been demonstrated that enhancing the mechanical properties is a viable strategy for developing new flexible electrode materials [118]. It has been shown that the dry electrode method exhibits significantly improved mechanical strength compared to the conventional slurry coating technique [119].

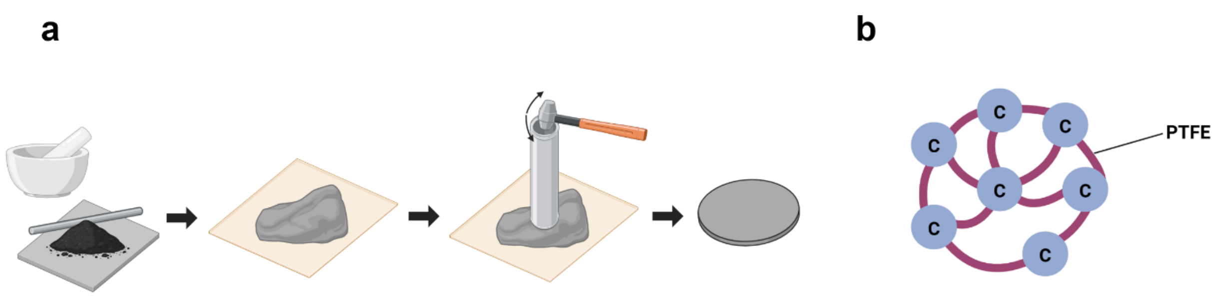

Figure 1-8. (a) Dry electrode process technique (b) fibrillation

1.6.3 Hydrothermal / Solvothermal Synthesis

Hydrothermal synthesis involves conducting chemical reactions in an aqueous solution at elevated temperatures, whereas solvothermal synthesis is carried out in a non-aqueous solvent under high temperature conditions [120]. The hydrothermal / solvothermal synthesis processes typically involve nucleation followed by particle growth. The resulting particle size and morphology can be precisely controlled by adjusting various experimental parameters, including reaction temperature, precursor concentration, and other processing conditions [121]. These synthesis methods enable the formation and growth of nanoparticles by enclosing chemical solvents within a sealed vessel, such as an autoclave, and increasing the temperature which consequently increases the internal pressure. Under these conditions, chemical reactions occur, and it results particle growth [122]. Consequently, as this synthesis approach enables direct particle growth on substrates, a notable advantage in electrode fabrication is the capability to synthesize binder-free electrodes. Furthermore, when employed with flexible substrates, this method facilitates the fabrication of flexible electrodes, expanding its applicability in flexible energy storage devices [123].

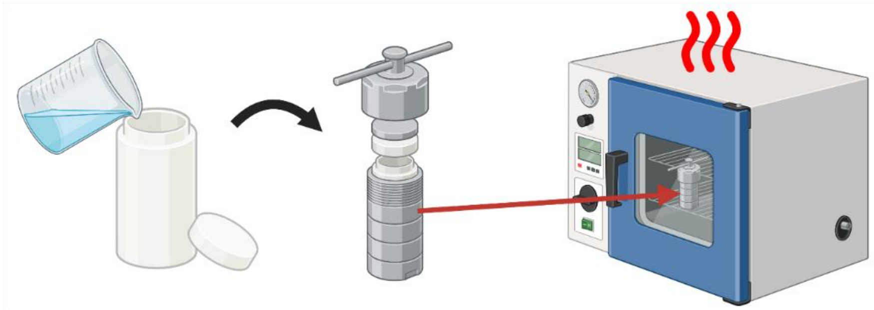

Figure 1-9. Hydrothermal/solvothermal synthesis procedure

1.7 Thesis Organization

Chapter 2 introduces a flexible lithium-ion battery design featuring a niobium oxide-based anode, demonstrating both fast-charging capability and mechanical flexibility. This study will discuss the use of a dry electrode processing technique, which eliminates the need for solvents, thereby enabling higher active material mass loading and resulting in enhanced capacity performance. Additionally, the study highlights the environmentally friendly aspect of the approach through the application of a selected polymer adhesive as a binder to adhere the fabricated anode onto current collectors, effectively eliminating the use of toxic materials commonly employed in conventional electrode fabrication processes. The study overall demonstrated stable electrochemical performance even after 100 cycles of mechanical bending, while also maintaining excellent fast-charging capability, operating reliably at high current rates of 5C. Moreover, the study validated long-term cycling stability, with bent pouch cells sustaining performance over 1000 cycles, thereby confirming their mechanical flexibility. The electrochemical performance was evaluated in both half-cell and full-cell configurations, validating the potential for practical use of the proposed battery design in conjunction with the fabricated flexible anode for real-life energy storage applications.

Chapter 3 further explores the development of flexible lithium-ion battery anode designs. This study also focuses on creating an anode that offers rapid charging capability and mechanical durability, capable of maintaining stable performance under external mechanical deformation. Titanium dioxide, another fast-charging capable material, was integrated into the electrode design through a hydrothermal synthesis approach. Unlike the method taken in Chapter 2, where fabricated electrodes were adhered to current collectors, this synthesizing technique was selected to allow the direct growth of titanium dioxide onto a flexible current collector, specifically carbon fiber. This approach also offers an environmentally friendly alternative by removing the need for hazardous solvents commonly employed in commercial electrode manufacturing.

In the final chapter, it outlines the key research findings presented in the preceding chapters and concludes the thesis by proposing potential future research directions that can be considered to further advance the development of fast charging and flexible lithium-ion batteries.

1.8 References

(1) Wulandari, T.; Fawcett, D.; Majumder, S. B.; Poinern, G. E. J. Lithium-Based Batteries, History, Current Status, Challenges, and Future Perspectives. *Battery Energy*. John Wiley and Sons Inc November 1, 2023. https://doi.org/10.1002/bte2.20230030.

(2) Deng, J.; Li, K.; Laverty, D.; Deng, W.; Xue, Y. Li-Ion Battery Management System for Electric Vehicles - A Practical Guide. *Springer Nature Link* **2014**.

(3) Grey, C. P.; Hall, D. S. Prospects for Lithium-Ion Batteries and beyond—a 2030 Vision. *Nature Communications*. Nature Research December 1, 2020. https://doi.org/10.1038/s41467-020-19991-4.

(4) Liang, Y.; Zhao, C. Z.; Yuan, H.; Chen, Y.; Zhang, W.; Huang, J. Q.; Yu, D.; Liu, Y.; Titirici, M. M.; Chueh, Y. L.; Yu, H.; Zhang, Q. A Review of Rechargeable Batteries for Portable Electronic Devices. *InfoMat*. Blackwell Publishing Ltd March 1, 2019, pp 6–32. https://doi.org/10.1002/inf2.12000.

(5) Yoshino, A. The Birth of the Lithium-Ion Battery. *Angewandte Chemie - International Edition*. June 11, 2012, pp 5798–5800. https://doi.org/10.1002/anie.201105006.

(6) Balakrishnan, N. T. M.; Prasanth, R. *Materials Horizons: From Nature to Nanomaterials Electrospinning for Advanced Energy Storage Applications*. http://www.springer.com/series/16122.

(7) Zhu, Z.; Jiang, T.; Ali, M.; Meng, Y.; Jin, Y.; Cui, Y.; Chen, W. Rechargeable Batteries for Grid Scale Energy Storage. *Chemical Reviews*. American Chemical Society November 23, 2022, pp 16610–16751. https://doi.org/10.1021/acs.chemrev.2c00289.

(8) Chen, S.; Liu, C.; Feng, R.; Chen, Z.; Lu, Y.; Chen, L.; Huang, Q.; Guan, Y.; Yan, W.; Su, Y.; Li, N.; Wu, F. Natural Graphite Anode for Advanced Lithium-Ion Batteries: Challenges, Progress, and Perspectives. *Chemical Engineering Journal*. Elsevier B.V. January 1, 2025. https://doi.org/10.1016/j.cej.2024.158116.

(9) Ding, X.; Zhou, Q.; Li, X.; Xiong, X. Fast-Charging Anodes for Lithium Ion Batteries: Progress and Challenges. *Chemical Communications* **2024**, *60* (18), 2472–2488. https://doi.org/10.1039/d4cc00110a.

(10) Wang, Y.; Liu, B.; Li, Q.; Cartmell, S.; Ferrara, S.; Deng, Z. D.; Xiao, J. Lithium and Lithium Ion Batteries for Applications in Microelectronic Devices: A Review. *Journal of Power Sources*. Elsevier July 15, 2015, pp 330–345. https://doi.org/10.1016/j.jpowsour.2015.03.164.

(11) Mohammadi Moradian, J.; Ali, A.; Yan, X.; Pei, G.; Zhang, S.; Naveed, A.; Shehzad, K.; Shahnavaz, Z.; Ahmad, F.; Yousaf, B. Sensors Innovations for Smart Lithium-Based Batteries: Advancements, Opportunities, and Potential Challenges. *Nano-Micro Letters*.

Springer Science and Business Media B.V. December 1, 2025. https://doi.org/10.1007/s40820-025-01786-1.

(12) Velasquez Carballo, K.; Singh, M.; Meng, X. Accurately Constituting Robust Interfaces for High-Performance High-Energy Lithium Metal Batteries. *Chemical Communications* **2024**. https://doi.org/10.1039/d4cc05705h.

(13) Xu, J.; Cai, X.; Cai, S.; Shao, Y.; Hu, C.; Lu, S.; Ding, S. High-Energy Lithium-Ion Batteries: Recent Progress and a Promising Future in Applications. *Energy and Environmental Materials*. John Wiley and Sons Inc September 1, 2023. https://doi.org/10.1002/eem2.12450.

(14) Weiss, M.; Ruess, R.; Kasnatscheew, J.; Levartovsky, Y.; Levy, N. R.; Minnmann, P.; Stolz, L.; Waldmann, T.; Wohlfahrt-Mehrens, M.; Aurbach, D.; Winter, M.; Ein-Eli, Y.; Janek, J. Fast Charging of Lithium-Ion Batteries: A Review of Materials Aspects. *Advanced Energy Materials*. John Wiley and Sons Inc September 1, 2021. https://doi.org/10.1002/aenm.202101126.

(15) Wu, Y.; Wang, W.; Ming, J.; Li, M.; Xie, L.; He, X.; Wang, J.; Liang, S.; Wu, Y. An Exploration of New Energy Storage System: High Energy Density, High Safety, and Fast Charging Lithium Ion Battery. *Adv Funct Mater* **2019**, *29* (1). https://doi.org/10.1002/adfm.201805978.

(16) Xiao, B. H.; Xiao, K.; Li, J. X.; Xiao, C. F.; Cao, S.; Liu, Z. Q. Flexible Electrochemical Energy Storage Devices and Related Applications: Recent Progress and Challenges. *Chemical Science*. Royal Society of Chemistry June 28, 2024, pp 11229–11266. https://doi.org/10.1039/d4sc02139h.

(17) Zhang, Q.; Soham, D.; Liang, Z.; Wan, J. Advances in Wearable Energy Storage and Harvesting Systems. *Med-X* **2025**, *3* (1). https://doi.org/10.1007/s44258-024-00048-w.

(18) Sun, Y.; Wang, L.; Li, Y.; Li, Y.; Lee, H. R.; Pei, A.; He, X.; Cui, Y. Design of Red Phosphorus Nanostructured Electrode for Fast-Charging Lithium-Ion Batteries with High Energy Density. *Joule* **2019**, *3* (4), 1080–1093. https://doi.org/10.1016/j.joule.2019.01.017.

(19) Wang, B.; Ryu, J.; Choi, S.; Zhang, X.; Pribat, D.; Li, X.; Zhi, L.; Park, S.; Ruoff, R. S. Ultrafast-Charging Silicon-Based Coral-like Network Anodes for Lithium-Ion Batteries with High Energy and Power Densities. *ACS Nano* **2019**, *13* (2), 2307–2315. https://doi.org/10.1021/acsnano.8b09034.

(20) Thompson, D. L.; Hartley, J. M.; Lambert, S. M.; Shiref, M.; Harper, G. D. J.; Kendrick, E.; Anderson, P.; Ryder, K. S.; Gaines, L.; Abbott, A. P. The Importance of Design in Lithium Ion Battery Recycling-a Critical Review. *Green Chemistry*. Royal Society of Chemistry November 21, 2020, pp 7585–7603. https://doi.org/10.1039/d0gc02745f.

(21) Nasajpour-Esfahani, N.; Garmestani, H.; Bagheritabar, M.; Jasim, D. J.; Toghraie, D.; Dadkhah, S.; Firoozeh, H. Comprehensive Review of Lithium-Ion Battery Materials and Development Challenges. *Renewable and Sustainable Energy Reviews*. Elsevier Ltd October 1, 2024. https://doi.org/10.1016/j.rser.2024.114783.

(22) Koech, A. K.; Mwandila, G.; Mulolani, F.; Mwaanga, P. Lithium-Ion Battery Fundamentals and Exploration of Cathode Materials: A Review. *South African Journal of Chemical Engineering*. Elsevier B.V. October 1, 2024, pp 321–339. https://doi.org/10.1016/j.sajce.2024.09.008.

(23) Arote, S. A. Fundamentals and Perspectives of Lithium-Ion Batteries. In *Lithium-ion and Lithium–Sulfur Batteries*; IOP Publishing, 2022; pp 1-1-1–26. https://doi.org/10.1088/978-0-7503-4881-2ch1.

(24) Zhang, X.; Sahraei, E.; Wang, K. Li-Ion Battery Separators, Mechanical Integrity and Failure Mechanisms Leading to Soft and Hard Internal Shorts. *Sci Rep* **2016**, *6*. https://doi.org/10.1038/srep32578.

(25) Liu, Z.; Jiang, Y.; Hu, Q.; Guo, S.; Yu, L.; Li, Q.; Liu, Q.; Hu, X. Safer Lithium-Ion Batteries from the Separator Aspect: Development and Future Perspectives. *Energy and Environmental Materials*. John Wiley and Sons Inc July 1, 2021, pp 336–362. https://doi.org/10.1002/eem2.12129.

(26) Liu, F.; Chuan, X. Recent Developments in Natural Mineral-Based Separators for Lithium-Ion Batteries. *RSC Advances*. Royal Society of Chemistry April 27, 2021, pp 16633–16644. https://doi.org/10.1039/d1ra02845f.

(27) Zhu, P.; Gastol, D.; Marshall, J.; Sommerville, R.; Goodship, V.; Kendrick, E. A Review of Current Collectors for Lithium-Ion Batteries. *Journal of Power Sources*. Elsevier B.V. February 15, 2021. https://doi.org/10.1016/j.jpowsour.2020.229321.

(28) Li, Y. Research Progress of Lithium-Ion Battery Current Collectors. In *IOP Conference Series: Earth and Environmental Science*; Institute of Physics Publishing, 2020; Vol. 514. https://doi.org/10.1088/1755-1315/514/4/042019.

(29) Theivaprakasam, S.; Girard, G.; Howlett, P.; Forsyth, M.; Mitra, S.; MacFarlane, D. Passivation Behaviour of Aluminium Current Collector in Ionic Liquid Alkyl Carbonate (Hybrid) Electrolytes. *Npj Mater Degrad* **2018**, *2* (1). https://doi.org/10.1038/s41529-018-0033-6.

(30) Liu, Y. K.; Zhao, C. Z.; Du, J.; Zhang, X. Q.; Chen, A. B.; Zhang, Q. Research Progresses of Liquid Electrolytes in Lithium-Ion Batteries. *Small*. John Wiley and Sons Inc February 22, 2023. https://doi.org/10.1002/smll.202205315.

(31) Haregewoin, A. M.; Wotango, A. S.; Hwang, B. J. Electrolyte Additives for Lithium Ion Battery Electrodes: Progress and Perspectives. *Energy and Environmental Science*. Royal Society of Chemistry June 1, 2016, pp 1955–1988. https://doi.org/10.1039/c6ee00123h.

(32) Koech, A. K.; Mwandila, G.; Mulolani, F.; Mwaanga, P. Lithium-Ion Battery Fundamentals and Exploration of Cathode Materials: A Review. *South African Journal of Chemical Engineering*. Elsevier B.V. October 1, 2024, pp 321–339. https://doi.org/10.1016/j.sajce.2024.09.008.

(33) Salah, M.; Hall, C.; Francis, C.; Rollo-Walker, G.; Fabretto, M. Binary Silicon-Based Thin-Film Anodes for Lithium-Ion Batteries: A Review. *Journal of Power Sources*. Elsevier B.V. February 1, 2022. https://doi.org/10.1016/j.jpowsour.2021.230871.

(34) Gao, T.; Han, Y.; Fraggedakis, D.; Das, S.; Zhou, T.; Yeh, C. N.; Xu, S.; Chueh, W. C.; Li, J.; Bazant, M. Z. Interplay of Lithium Intercalation and Plating on a Single Graphite Particle. *Joule* **2021**, *5* (2), 393–414. https://doi.org/10.1016/j.joule.2020.12.020.

(35) Wagner, R.; Preschitschek, N.; Passerini, S.; Leker, J.; Winter, M. Current Research Trends and Prospects among the Various Materials and Designs Used in Lithium-Based Batteries. *Journal of Applied Electrochemistry*. Kluwer Academic Publishers May 1, 2013, pp 481–496. https://doi.org/10.1007/s10800-013-0533-6.

(36) Luchkin, S. Y.; Lipovskikh, S. A.; Katorova, N. S.; Savina, A. A.; Abakumov, A. M.; Stevenson, K. J. Solid-Electrolyte Interphase Nucleation and Growth on Carbonaceous Negative Electrodes for Li-Ion Batteries Visualized with in Situ Atomic Force Microscopy. *Sci Rep* **2020**, *10* (1). https://doi.org/10.1038/s41598-020-65552-6.

(37) Edge, J. S.; O'Kane, S.; Prosser, R.; Kirkaldy, N. D.; Patel, A. N.; Hales, A.; Ghosh, A.; Ai, W.; Chen, J.; Yang, J.; Li, S.; Pang, M. C.; Bravo Diaz, L.; Tomaszewska, A.; Marzook, M. W.; Radhakrishnan, K. N.; Wang, H.; Patel, Y.; Wu, B.; Offer, G. J. Lithium Ion Battery Degradation: What You Need to Know. *Physical Chemistry Chemical Physics*. Royal Society of Chemistry April 14, 2021, pp 8200–8221. https://doi.org/10.1039/d1cp00359c.

(38) Wang, A.; Kadam, S.; Li, H.; Shi, S.; Qi, Y. Review on Modeling of the Anode Solid Electrolyte Interphase (SEI) for Lithium-Ion Batteries. *npj Computational Materials*. Nature Publishing Group December 1, 2018. https://doi.org/10.1038/s41524-018-0064-0.

(39) Wu, J.; Ihsan-Ul-Haq, M.; Chen, Y.; Kim, J. K. Understanding Solid Electrolyte Interphases: Advanced Characterization Techniques and Theoretical Simulations. *Nano Energy*. Elsevier Ltd November 1, 2021. https://doi.org/10.1016/j.nanoen.2021.106489.

(40) Adenusi, H.; Chass, G. A.; Passerini, S.; Tian, K. V.; Chen, G. Lithium Batteries and the Solid Electrolyte Interphase (SEI)—Progress and Outlook. *Advanced Energy Materials*. John Wiley and Sons Inc March 10, 2023. https://doi.org/10.1002/aenm.202203307.

(41) Adenusi, H.; Chass, G. A.; Passerini, S.; Tian, K. V.; Chen, G. Lithium Batteries and the Solid Electrolyte Interphase (SEI)—Progress and Outlook. *Advanced Energy Materials*. John Wiley and Sons Inc March 10, 2023. https://doi.org/10.1002/aenm.202203307.

(42) Liu, Q.; Du, C.; Shen, B.; Zuo, P.; Cheng, X.; Ma, Y.; Yin, G.; Gao, Y. Understanding Undesirable Anode Lithium Plating Issues in Lithium-Ion Batteries. *RSC Adv* **2016**, *6* (91), 88683–88700. https://doi.org/10.1039/c6ra19482f.

(43) Mei, W.; Zhang, Y.; Li, Y.; Zhuo, P.; Chu, Y.; Chen, Y.; Jiang, L.; Zhou, H.; Sun, J.; Wang, Q. Unveiling Voltage Evolution during Li Plating-Relaxation-Li Stripping Cycling of Lithium-Ion Batteries. *Energy Storage Mater* **2024**, *66*. https://doi.org/10.1016/j.ensm.2024.103193.

(44) Du, H.; Wang, Y.; Kang, Y.; Zhao, Y.; Tian, Y.; Wang, X.; Tan, Y.; Liang, Z.; Wozny, J.; Li, T.; Ren, D.; Wang, L.; He, X.; Xiao, P.; Mao, E.; Tavajohi, N.; Kang, F.; Li, B. Side Reactions/Changes in Lithium-Ion Batteries: Mechanisms and Strategies for Creating Safer and Better Batteries. *Advanced Materials*. John Wiley and Sons Inc July 18, 2024. https://doi.org/10.1002/adma.202401482.

(45) Wang, P.; Xiong, R.; Shen, W.; Sun, F. Aging-Induced, Rate-Independent Lithium Plating: A Complete Mechanism Analysis throughout the Battery Lifecycle. *Appl Energy* **2025**, *393*. https://doi.org/10.1016/j.apenergy.2025.126094.

(46) Liu, G.; Lu, W. A Model of Concurrent Lithium Dendrite Growth, SEI Growth, SEI Penetration and Regrowth. *J Electrochem Soc* **2017**, *164* (9), A1826–A1833. https://doi.org/10.1149/2.0381709jes.

(47) He, L.; Sun, Q.; Lu, L.; Adams, S. Understanding and Preventing Dendrite Growth in Lithium Metal Batteries. *ACS Appl Mater Interfaces* **2021**, *13* (29), 34320–34331. https://doi.org/10.1021/acsami.1c08268.

(48) Huang, Y.; Yang, H.; Gao, Y.; Chen, G.; Li, Y.; Shi, L.; Zhang, D. Mechanism and Solutions of Lithium Dendrite Growth in Lithium Metal Batteries. *Materials Chemistry Frontiers*. Royal Society of Chemistry December 16, 2023, pp 1282–1299. https://doi.org/10.1039/d3qm01151h.

(49) Wang, Q.; Liu, B.; Shen, Y.; Wu, J.; Zhao, Z.; Zhong, C.; Hu, W. Confronting the Challenges in Lithium Anodes for Lithium Metal Batteries. *Advanced Science*. John Wiley and Sons Inc September 1, 2021. https://doi.org/10.1002/advs.202101111.

(50) He, D.; Cui, W.; Liao, X.; Xie, X.; Mao, M.; Sang, X.; Zhai, P.; Zhao, Y.; Huang, Y.; Zhao, W. Electronic Localization Derived Excellent Stability of Li Metal Anode with Ultrathin Alloy. *Advanced Science* **2022**, *9* (10). https://doi.org/10.1002/advs.202105656.

(51) Jiang, T.; Xiong, Q.; Yang, H.; Chen, G. Z. Performance and Application of Si/Ti3C2T x (MXene) Composites in Lithium Ion Battery. *JPhys Energy* **2023**, *5* (1). https://doi.org/10.1088/2515-7655/acb6b4.

(52) Sun, W.; Huang, C. Elucidating the Effect of Electrode Calendering on Electrochemical Performance Using 3D Image-Based Modelling. *J Power Sources* **2024**, *611*. https://doi.org/10.1016/j.jpowsour.2024.234774.

(53) Aravindan, V.; Lee, Y. S.; Madhavi, S. Research Progress on Negative Electrodes for Practical Li-Ion Batteries: Beyond Carbonaceous Anodes. *Advanced Energy Materials*. Wiley-VCH Verlag July 1, 2015. https://doi.org/10.1002/aenm.201402225.

(54) Deng, L.; Zheng, Y.; Zheng, X.; Or, T.; Ma, Q.; Qian, L.; Deng, Y.; Yu, A.; Li, J.; Chen, Z. Design Criteria for Silicon-Based Anode Binders in Half and Full Cells. *Advanced Energy Materials*. John Wiley and Sons Inc August 1, 2022. https://doi.org/10.1002/aenm.202200850.

(55) Chavan, S.; Venkateswarlu, B.; Salman, M.; Liu, J.; Pawar, P.; Joo, S. W.; Choi, G. S.; Kim, S. C. Thermal Management Strategies for Lithium-Ion Batteries in Electric Vehicles: Fundamentals, Recent Advances, Thermal Models, and Cooling Techniques. *International Journal of Heat and Mass Transfer*. Elsevier Ltd November 1, 2024. https://doi.org/10.1016/j.ijheatmasstransfer.2024.125918.

(56) Choi, J. W.; Aurbach, D. Promise and Reality of Post-Lithium-Ion Batteries with High Energy Densities. *Nature Reviews Materials*. Nature Publishing Group March 31, 2016. https://doi.org/10.1038/natrevmats.2016.13.

(57) Liang, Y.; Zhao, C. Z.; Yuan, H.; Chen, Y.; Zhang, W.; Huang, J. Q.; Yu, D.; Liu, Y.; Titirici, M. M.; Chueh, Y. L.; Yu, H.; Zhang, Q. A Review of Rechargeable Batteries for Portable Electronic Devices. *InfoMat*. Blackwell Publishing Ltd March 1, 2019, pp 6–32. https://doi.org/10.1002/inf2.12000.

(58) Cai, W. Lithium-Ion Battery Manufacturing for Electric Vehicles: A Contemporary Overview. In *Advances in Battery Manufacturing, Services, and Management Systems*; Wiley-IEEE Press, 2016; pp 1–28. https://doi.org/10.1002/9781119060741.ch1.

(59) Aldrin, M. K. J.; Subha Editors, A. P. P. *Energy Systems in Electrical Engineering Energy Harvesting and Storage Fundamentals and Materials*.

(60) Stravova, Z.; Klvac, O.; Bana, J.; Anothumakkool, B.; Zikmund, T.; Blazek, P.; Kaiser, J.; Kazda, T. Comprehensive Study of Rapid Capacity Fade in Prismatic Li-Ion Cells with Flexible Packaging. *Sci Rep* **2024**, *14* (1). https://doi.org/10.1038/s41598-024-77673-3.

(61) Dai, F.; Cai, M. Best Practices in Lithium Battery Cell Preparation and Evaluation. *Commun Mater* **2022**, *3* (1). https://doi.org/10.1038/s43246-022-00286-8.

(62) Hu, J.; Wu, B.; Chae, S.; Lochala, J.; Bi, Y.; Xiao, J. Achieving Highly Reproducible Results in Graphite-Based Li-Ion Full Coin Cells. *Joule* **2021**, *5* (5), 1011–1015. https://doi.org/10.1016/j.joule.2021.03.016.

(63) Mu, G.; Agrawal, S.; Sittisomwong, P.; Bai, P. Impacts of Negative to Positive Capacities Ratios on the Performance of Next-Generation Lithium-Ion Batteries. *Electrochim Acta* **2022**, *406*. https://doi.org/10.1016/j.electacta.2022.139878.

(64) Chen, S.; Niu, C.; Lee, H.; Li, Q.; Yu, L.; Xu, W.; Zhang, J. G.; Dufek, E. J.; Whittingham, M. S.; Meng, S.; Xiao, J.; Liu, J. Critical Parameters for Evaluating Coin Cells and Pouch Cells of Rechargeable Li-Metal Batteries. *Joule* **2019**, *3* (4), 1094–1105. https://doi.org/10.1016/j.joule.2019.02.004.

(65) Smith, A.; Stüble, P.; Leuthner, L.; Hofmann, A.; Jeschull, F.; Mereacre, L. Potential and Limitations of Research Battery Cell Types for Electrochemical Data Acquisition. *Batter Supercaps* **2023**, *6* (6). https://doi.org/10.1002/batt.202300080.

(66) Ogunfunmi, T.; Ebechidi, N.; Ahmed, R.; Oyewole, O.; Obayemi, J.; Soboyejo, W. An Investigation into Compressive Deformation and Failure Mechanisms in a Novel Li-Ion Solid-State Electrolyte. *MRS Adv* **2021**, *6* (4–5), 154–161. https://doi.org/10.1557/s43580-021-00014-3.

(67) Zhu, G. L.; Zhao, C. Z.; Huang, J. Q.; He, C.; Zhang, J.; Chen, S.; Xu, L.; Yuan, H.; Zhang, Q. Fast Charging Lithium Batteries: Recent Progress and Future Prospects. *Small*. Wiley-VCH Verlag April 12, 2019. https://doi.org/10.1002/smll.201805389.

(68) Liu, R.; Zhou, A.; Zhang, X.; Mu, J.; Che, H.; Wang, Y.; Wang, T. T.; Zhang, Z.; Kou, Z. Fundamentals, Advances and Challenges of Transition Metal Compounds-Based Supercapacitors. *Chemical Engineering Journal*. Elsevier B.V. May 15, 2021. https://doi.org/10.1016/j.cej.2021.128611.

(69) Choi, C.; Ashby, D. S.; Butts, D. M.; DeBlock, R. H.; Wei, Q.; Lau, J.; Dunn, B. Achieving High Energy Density and High Power Density with Pseudocapacitive Materials. *Nature Reviews Materials*. Nature Research January 1, 2020, pp 5–19. https://doi.org/10.1038/s41578-019-0142-z.

(70) De Luna, Y.; Youssef, K.; Bensalah, N. Enabling Fast-Charging via Layered Ternary Transition Metal Oxide as Anode Materials for Lithium-Ion Batteries. *Mater Res Bull* **2025**, *185*. https://doi.org/10.1016/j.materresbull.2025.113325.

(71) Zhao, H.; Zuo, H.; Wang, J.; Jiao, S. Practical Application of Graphite in Lithium-Ion Batteries: Modification, Composite, and Sustainable Recycling. *Journal of Energy Storage*. Elsevier Ltd September 20, 2024. https://doi.org/10.1016/j.est.2024.113125.

(72) Li, S.; Wang, K.; Zhang, G.; Li, S.; Xu, Y.; Zhang, X.; Zhang, X.; Zheng, S.; Sun, X.; Ma, Y. Fast Charging Anode Materials for Lithium-Ion Batteries: Current Status and Perspectives. *Advanced Functional Materials*. John Wiley and Sons Inc June 1, 2022. https://doi.org/10.1002/adfm.202200796.

(73) Zor, C.; Turrell, S. J.; Uyanik, M. S.; Afyon, S. Lithium Plating and Stripping: Toward Anode-Free Solid-State Batteries. *Advanced Energy and Sustainability Research*. John Wiley and Sons Inc August 1, 2024. https://doi.org/10.1002/aesr.202300001.

(74) Mei, W.; Jiang, L.; Liang, C.; Sun, J.; Wang, Q. Understanding of Li-Plating on Graphite Electrode: Detection, Quantification and Mechanism Revelation. *Energy Storage Mater* **2021**, *41*, 209–221. https://doi.org/10.1016/j.ensm.2021.06.013.

(75) Wang, S.; Quan, W.; Zhu, Z.; Yang, Y.; Liu, Q.; Ren, Y.; Zhang, X.; Xu, R.; Hong, Y.; Zhang, Z.; Amine, K.; Tang, Z.; Lu, J.; Li, J. Lithium Titanate Hydrates with Superfast and Stable Cycling in Lithium Ion Batteries. *Nat Commun* **2017**, *8* (1). https://doi.org/10.1038/s41467-017-00574-9.

(76) Dong, H.; Yao, T.; Ji, X.; Zhang, Q.; Lin, X.; Zhang, B.; Ma, C.; Meng, L.; Chen, Y.; Wang, H. Enhancing the Lithium Storage Performance of the Nb2O5 Anode via Synergistic Engineering of Phase and Cu Doping. *ACS Appl Mater Interfaces* **2024**, *16* (17), 22055–22065. https://doi.org/10.1021/acsami.4c03044.

(77) Shi, H.; Shi, C.; Jia, Z.; Zhang, L.; Wang, H.; Chen, J. Titanium Dioxide-Based Anode Materials for Lithium-Ion Batteries: Structure and Synthesis. *RSC Advances*. Royal Society of Chemistry November 23, 2022, pp 33641–33652. https://doi.org/10.1039/d2ra05442f.

(78) Pimta, K.; Autthawong, T.; Yodying, W.; Phromma, C.; Haruta, M.; Kurata, H.; Sarakonsri, T.; Chimupala, Y. Development of Bronze Phase Titanium Dioxide Nanorods for Use as Fast-Charging Anode Materials in Lithium-Ion Batteries. *ACS Omega* **2023**, *8* (17), 15360–15370. https://doi.org/10.1021/acsomega.3c00618.

(79) Du, X.; Wang, Q.; Feng, T.; Chen, X.; Li, L.; Li, L.; Meng, X.; Xiong, L.; Sun, X.; Lu, L.; Xu, Y. One-Step Preparation of Nanoarchitectured TiO2 on Porous Al as Integrated Anode for High-Performance Lithium-Ion Batteries. *Sci Rep* **2016**, *6*. https://doi.org/10.1038/srep20138.

(80) Bai, Y.; Mora-Seró, I.; De Angelis, F.; Bisquert, J.; Wang, P. Titanium Dioxide Nanomaterials for Photovoltaic Applications. *Chemical Reviews*. American Chemical Society October 8, 2014, pp 10095–10130. https://doi.org/10.1021/cr400606n.

(81) Shi, H.; Shi, C.; Jia, Z.; Zhang, L.; Wang, H.; Chen, J. Titanium Dioxide-Based Anode Materials for Lithium-Ion Batteries: Structure and Synthesis. *RSC Advances*. Royal

Society of Chemistry November 23, 2022, pp 33641–33652. https://doi.org/10.1039/d2ra05442f.

(82) Cargnello, M.; Gordon, T. R.; Murray, C. B. Solution-Phase Synthesis of Titanium Dioxide Nanoparticles and Nanocrystals. *Chemical Reviews*. American Chemical Society October 8, 2014, pp 9319–9345. https://doi.org/10.1021/cr500170p.

(83) Wang, X.; Li, Z.; Shi, J.; Yu, Y. One-Dimensional Titanium Dioxide Nanomaterials: Nanowires, Nanorods, and Nanobelts. *Chemical Reviews*. American Chemical Society October 8, 2014, pp 9346–9384. https://doi.org/10.1021/cr400633s.

(84) Yuwono, J. A.; Burr, P.; Galvin, C.; Lennon, A. Atomistic Insights into Lithium Storage Mechanisms in Anatase, Rutile, and Amorphous TiO2Electrodes. *ACS Appl Mater Interfaces* **2021**, *13* (1), 1791–1806. https://doi.org/10.1021/acsami.0c17097.

(85) Lee, T. Y.; Lee, C. Y.; Chiu, H. T. Vapor-Solid Reaction Growth of Rutile TiO2 Nanorods and Nanowires for Li-Ion-Battery Electrodes. *ACS Omega* **2019**, *4* (14), 16217–16225. https://doi.org/10.1021/acsomega.9b02453.

(86) Nico, C.; Monteiro, T.; Graça, M. P. F. Niobium Oxides and Niobates Physical Properties: Review and Prospects. *Progress in Materials Science*. Elsevier Ltd July 1, 2016, pp 1–37. https://doi.org/10.1016/j.pmatsci.2016.02.001.

(87) Ahn, Y.; Li, T.; Huang, S.; Ding, Y.; Hwang, S.; Wang, W.; Luo, Z.; Wang, J. H.; Nam, G.; Liu, M. Mixed-Phase Niobium Oxide as a Durable and Ultra-Fast Charging Anode for High-Power Lithium-Ion Batteries. *Adv Funct Mater* **2024**, *34* (8). https://doi.org/10.1002/adfm.202310853.

(88) Budak; Geißler, M.; Becker, D.; Kruth, A.; Quade, A.; Haberkorn, R.; Kickelbick, G.; Etzold, B. J. M.; Presser, V. Carbide-Derived Niobium Pentoxide with Enhanced Charge Storage Capacity for Use as a Lithium-Ion Battery Electrode. *ACS Appl Energy Mater* **2020**, *3* (5), 4275–4285. https://doi.org/10.1021/acsaem.9b02549.

(89) Li, T.; Nam, G.; Liu, K.; Wang, J. H.; Zhao, B.; Ding, Y.; Soule, L.; Avdeev, M.; Luo, Z.; Zhang, W.; Yuan, T.; Jing, P.; Kim, M. G.; Song, Y.; Liu, M. A Niobium Oxide with a Shear Structure and Planar Defects for High-Power Lithium Ion Batteries. *Energy Environ Sci* **2022**, *15* (1), 254–264. https://doi.org/10.1039/d1ee02664j.

(90) Griffith, K. J.; Forse, A. C.; Griffin, J. M.; Grey, C. P. High-Rate Intercalation without Nanostructuring in Metastable Nb2O5 Bronze Phases. *J Am Chem Soc* **2016**, *138* (28), 8888–8899. https://doi.org/10.1021/jacs.6b04345.

(91) Yang, Y.; Zhao, J. Wadsley–Roth Crystallographic Shear Structure Niobium-Based Oxides: Promising Anode Materials for High-Safety Lithium-Ion Batteries. *Advanced Science*. John Wiley and Sons Inc June 1, 2021. https://doi.org/10.1002/advs.202004855.

(92) Lin, J.; Zhao, S.; Jervis, R.; Shearing, P. Probing the Electrochemical Processes of Niobium Pentoxides (Nb2O5) for High-Rate Lithium-Ion Batteries: A Review. *ChemElectroChem*. John Wiley and Sons Inc March 15, 2024. https://doi.org/10.1002/celc.202300581.

(93) Cunha, D. M.; Hendriks, T. A.; Vasileiadis, A.; Vos, C. M.; Verhallen, T.; Singh, D. P.; Wagemaker, M.; Huijben, M. Doubling Reversible Capacities in Epitaxial Li4Ti5O12 Thin Film Anodes for Microbatteries. *ACS Appl Energy Mater* **2019**, *2* (5), 3410–3418. https://doi.org/10.1021/acsaem.9b00217.

(94) Fang, Z.; Wang, J.; Wu, H.; Li, Q.; Fan, S.; Wang, J. Progress and Challenges of Flexible Lithium Ion Batteries. *J Power Sources* **2020**, *454*. https://doi.org/10.1016/j.jpowsour.2020.227932.

(95) Zhao, Y.; Guo, J. Development of Flexible Li-Ion Batteries for Flexible Electronics. *InfoMat*. Blackwell Publishing Ltd September 1, 2020, pp 866–878. https://doi.org/10.1002/inf2.12117.

(96) Liu, Y.; Gong, X.; Podder, C.; Wang, F.; Li, Z.; Liu, J.; Fu, J.; Ma, X.; Vanaphuti, P.; Wang, R.; Hitt, A.; Savsatli, Y.; Yang, Z.; Ge, M.; Lee, W. K.; Yonemoto, B.; Tang, M.; Pan, H.; Wang, Y. Roll-to-Roll Solvent-Free Manufactured Electrodes for Fast-Charging Batteries. *Joule* **2023**, *7* (5), 952–970. https://doi.org/10.1016/j.joule.2023.04.006.

(97) Liu, H.; Cheng, X.; Chong, Y.; Yuan, H.; Huang, J. Q.; Zhang, Q. Advanced Electrode Processing of Lithium Ion Batteries: A Review of Powder Technology in Battery Fabrication. *Particuology* **2021**, *57*, 56–71. https://doi.org/10.1016/j.partic.2020.12.003.

(98) Lu, C.; Wu, W.; Wang, L.; Tian, R.; Du, F. Thick Electrode for Energy Storage Systems: A Facile Strategy towards High Energy Density Li Ion Batteries. *Next Materials* **2024**, *4*, 100170. https://doi.org/10.1016/j.nxmate.2024.100170.

(99) Sliz, R.; Valikangas, J.; Silva Santos, H.; Vilmi, P.; Rieppo, L.; Hu, T.; Lassi, U.; Fabritius, T. Suitable Cathode NMP Replacement for Efficient Sustainable Printed Li-Ion Batteries. *ACS Appl Energy Mater* **2022**, *5* (4), 4047–4058. https://doi.org/10.1021/acsaem.1c02923.

(100) Ryu, M.; Hong, Y. K.; Lee, S. Y.; Park, J. H. Ultrahigh Loading Dry-Process for Solvent-Free Lithium-Ion Battery Electrode Fabrication. *Nat Commun* **2023**, *14* (1). https://doi.org/10.1038/s41467-023-37009-7.

(101) Mun, S. C.; Jeon, Y. H.; Won, J. H. Progress and Challenges for Replacing N-Methyl-2-Pyrrolidone / Polyvinylidene Fluoride Slurry Formulations in Lithium-Ion Battery Cathodes. *Progress in Natural Science: Materials International* **2024**, *34* (1), 194–206. https://doi.org/10.1016/j.pnsc.2024.02.013.

(102) Haghi, S.; Summer, A.; Bauerschmidt, P.; Daub, R. Tailored Digitalization in Electrode Manufacturing: The Backbone of Smart Lithium-Ion Battery Cell Production. *Energy Technology* **2022**, *10* (10). https://doi.org/10.1002/ente.202200657.

(103) Kim, E. J.; Kumar, P. R.; Gossage, Z. T.; Kubota, K.; Hosaka, T.; Tatara, R.; Komaba, S. Active Material and Interphase Structures Governing Performance in Sodium and Potassium Ion Batteries. *Chemical Science*. Royal Society of Chemistry May 18, 2022, pp 6121–6158. https://doi.org/10.1039/d2sc00946c.

(104) Gonçalves, R.; Lanceros-Méndez, S.; Costa, C. M. Electrode Fabrication Process and Its Influence in Lithium-Ion Battery Performance: State of the Art and Future Trends. *Electrochem commun* **2022**, *135*. https://doi.org/10.1016/j.elecom.2022.107210.

(105) Jiao, X.; Kirianova, A. V.; Xu, X.; Kapitanova, O. O.; Krivchenko, V. A.; Napolskiy, F. S.; Volkov, V. S.; Gallyamov, M. O.; Liu, Y. Conductive Additives for Improving the Rate Capability of Cathode Materials in Secondary Lithium Batteries. *ACS Appl Energy Mater* **2023**, *6* (5), 2855–2862. https://doi.org/10.1021/acsaem.2c03772.

(106) Jeong, H.; Jang, J.; Jo, C. A Review on Current Collector Coating Methods for Next-Generation Batteries. *Chemical Engineering Journal*. Elsevier B.V. October 15, 2022. https://doi.org/10.1016/j.cej.2022.136860.

(107) Weichert, A.; Göken, V.; Fromm, O.; Beuse, T.; Winter, M.; Börner, M. Strategies for Formulation Optimization of Composite Positive Electrodes for Lithium Ion Batteries Based on Layered Oxide, Spinel, and Olivine-Type Active Materials. *J Power Sources* **2022**, *551*. https://doi.org/10.1016/j.jpowsour.2022.232179.

(108) Plateau, T. P.; Boyer, G.; Park, J. Hyper-Thick Electrodes for Lithium-Ion Batteries Enabled by Micro-Electric-Field Process. *Advanced Science* **2025**, *12* (7). https://doi.org/10.1002/advs.202413444.

(109) Khan, F. M. N. U.; Rasul, M. G.; Mandal, N. K.; Sayem, A. S. M. Optimization of Electrode Thickness of Lithium-Ion Batteries for Maximizing Energy Density. *Journal of Solid State Electrochemistry* **2025**, *29* (2), 753–768. https://doi.org/10.1007/s10008-024-06109-9.

(110) Schumm, B.; Dupuy, A.; Lux, M.; Girsule, C.; Dörfler, S.; Schmidt, F.; Fiedler, M.; Rosner, M.; Hippauf, F.; Kaskel, S. Dry Battery Electrode Technology: From Early Concepts to Industrial Applications. *Advanced Energy Materials*. John Wiley and Sons Inc June 24, 2025. https://doi.org/10.1002/aenm.202406011.

(111) Zhu, P.; Liu, S.; Zhao, L.; Liu, L.; Huang, Y.; Li, J.; Li, F. Solvent-Free Lithium-Ion Battery Electrodes with Ultrahigh Loading Using a Reactive Epoxy Nanobinder. *J Mater Chem A Mater* **2024**, *13* (2), 1109–1122. https://doi.org/10.1039/d4ta05905k.

(112) Oh, H.; Kim, G. S.; Hwang, B. U.; Bang, J.; Kim, J.; Jeong, K. M. Development of a Feasible and Scalable Manufacturing Method for PTFE-Based Solvent-Free Lithium-Ion Battery Electrodes. *Chemical Engineering Journal* **2024**, *491*. https://doi.org/10.1016/j.cej.2024.151957.

(113) Gyulai, A.; Bauer, W.; Ehrenberg, H. Dry Electrode Manufacturing in a Calender: The Role of Powder Premixing for Electrode Quality and Electrochemical Performance. *ACS Appl Energy Mater* **2023**, *6* (10), 5122–5134. https://doi.org/10.1021/acsaem.2c03755.

(114) Lu, Y.; Zhao, C. Z.; Yuan, H.; Hu, J. K.; Huang, J. Q.; Zhang, Q. Dry Electrode Technology, the Rising Star in Solid-State Battery Industrialization. *Matter*. Cell Press March 2, 2022, pp 876–898. https://doi.org/10.1016/j.matt.2022.01.011.

(115) Lu, Y.; Zhao, C. Z.; Yuan, H.; Hu, J. K.; Huang, J. Q.; Zhang, Q. Dry Electrode Technology, the Rising Star in Solid-State Battery Industrialization. *Matter*. Cell Press March 2, 2022, pp 876–898. https://doi.org/10.1016/j.matt.2022.01.011.

(116) Schumm, B.; Dupuy, A.; Lux, M.; Girsule, C.; Dörfler, S.; Schmidt, F.; Fiedler, M.; Rosner, M.; Hippauf, F.; Kaskel, S. Dry Battery Electrode Technology: From Early Concepts to Industrial Applications. *Advanced Energy Materials*. John Wiley and Sons Inc June 24, 2025. https://doi.org/10.1002/aenm.202406011.

(117) Horst, M.; Beverborg, F.; Bahlmann, L.; Schreiber, S.; Gerk, J.; Michalowski, P.; Kwade, A. Effect of Active Material Morphology on PTFE-Fibrillation, Powder Characteristics and Electrode Properties in Dry Electrode Coating Processes. *Powder Technol* **2025**, *451*. https://doi.org/10.1016/j.powtec.2024.120451.

(118) Xia, X.; Yang, J.; Liu, Y.; Zhang, J.; Shang, J.; Liu, B.; Li, S.; Li, W. Material Choice and Structure Design of Flexible Battery Electrode. *Advanced Science*. John Wiley and Sons Inc January 25, 2023. https://doi.org/10.1002/advs.202204875.

(119) Ludwig, B.; Zheng, Z.; Shou, W.; Wang, Y.; Pan, H. Solvent-Free Manufacturing of Electrodes for Lithium-Ion Batteries. *Sci Rep* **2016**, *6*. https://doi.org/10.1038/srep23150.

(120) Feng, S. H.; Li, G. H. Hydrothermal and Solvothermal Syntheses. In *Modern Inorganic Synthetic Chemistry: Second Edition*; Elsevier Inc., 2017; pp 73–104. https://doi.org/10.1016/B978-0-444-63591-4.00004-5.

(121) Li, J.; Wu, Q.; Wu, J. Synthesis of Nanoparticles via Solvothermal and Hydrothermal Methods. In *Handbook of Nanoparticles*; Springer International Publishing, 2015; pp 1–28. https://doi.org/10.1007/978-3-319-13188-7_17-1.

(122) Sonawane, G. H.; Patil, S. P.; Sonawane, S. H. Nanocomposites and Its Applications. In *Applications of Nanomaterials: Advances and Key Technologies*; Elsevier, 2018; pp 1–22. https://doi.org/10.1016/B978-0-08-101971-9.00001-6.

(123) Jin, T.; Han, Q.; Jiao, L. Binder-Free Electrodes for Advanced Sodium-Ion Batteries. *Advanced Materials*. Wiley-VCH Verlag January 1, 2020. https://doi.org/10.1002/adma.201806304.

Chapter 2: Designing Niobium Oxide Anodes for Flexible and Fast-Charging Lithium-Ion Batteries

Abstract

Flexible lithium-ion batteries (FLIBs) are critical for powering emerging technologies such as wearable electronics, biomedical devices, and soft robotics, capable of maintaining performance under mechanical deformation while offering fast-charging capability. However, achieving both high areal capacity and structural durability remains challenging. Increasing the electrode mass loading improves energy density but typically results in mechanical brittleness and limited ionic transport, especially in conventional slurry-based fabrication methods that rely on toxic solvents like N-methyl-2-pyrrolidone (NMP). In this work, we present a flexible anode featuring mixed-phase niobium oxide, a defect-engineered material known for its excellent high-rate performance and stability. The electrode is produced through a solvent-free dry fabrication method utilizing carbon nanofibers and polytetrafluoroethylene to form a robust, fibrillated architecture. Moreover, a conductive polymer adhesive of poly(3,4-ethylenedioxythiophene):polystyrene sulfonate (PEDOT:PSS) is introduced to promote strong interfacial contact between the electrode film and various current collectors without the need for heat or pressure. This integrated design not only overcomes the limitations of rigid lithium-ion batteries (LIBs) under mechanical deformation but also addresses environmental concerns by eliminating harmful solvents. Overall, our approach demonstrates a promising strategy for realizing high-performance, readily fabricated FLIBs suitable for practical applications.

2.1 Introduction

Extensive research in the battery field has been dedicated to the development of smart devices, which demand flexibility under mechanical deformation, rapid charging capability, and reliable operational safety [1,2]. However, when conventional rigid lithium-ion batteries (LIBs) are subjected to bending or folding, mechanical stresses can lead to the detachment of the electrode from the current collector, posing risks of short circuits and safety hazards [3,4]. This limitation highlights the critical need for FLIBs. Nonetheless, the development of FLIBs presents challenges. First, electrodes are highly susceptible to mechanical failure, such as cracking and delamination, which can result in severe structural and electrochemical degradation under repeated flexing or bending [5]. Additionally, achieving high energy density while ensuring mechanical flexibility is extremely difficult [7,8]. One effective strategy to enhance energy density involves increasing the mass loading of the electrode, as it increases the proportion of active material within the electrode [9,10]. However, electrodes with higher mass loading typically exhibit increased thickness, which in turn makes them more prone to mechanical deformation due to their increased rigidity [11]. Furthermore, increasing mass loading also poses difficulties in achieving fast-charging capability [12]. As electrode thickness increases, the diffusion pathways for electrolyte ions extend, resulting in longer electron and ion transport, leading to reduced rate capability [13–15]. In order to address these challenges, the study employed a dry electrode fabrication technique combined with a fast-charging-capable active material for the electrode.

Compared to the conventional slurry-based electrode fabrication method, the dry electrode process eliminates the use of solvents [16]. In the absence of solvents, this technique enables a higher proportion of active material, thereby facilitating the fabrication of electrodes with increased mass loading [17–19]. Moreover, by eliminating volatile and toxic solvents such as N-methyl-2-pyrrolidone (NMP), the dry electrode process offers an environmentally friendly alternative, reducing environmental hazards associated with conventional electrode manufacturing [20,21]. However, a notable concern associated with dry electrode processing comes from its reliance on a hot calendaring process for the better interfacial adhesion of the dry electrode to the current collector [22,23]. This additional step can introduce undesirable side effects or potential structural damage to the electrode [24].

One of the primary rate-limiting factors is the slow diffusion of lithium ions within the active material of the anode [25]. The properties of the active material play a critical role in governing the diffusion rate [26]. Thus, this study identified selecting a suitable fast-charging anode material to optimize this process. For instance, $Li_4Ti_5O_{12}$ (LTO) has been widely studied as a fast-charging anode material because of its high-rate electrochemical kinetics [27–29]. However, research has highlighted its limitations in terms of theoretical capacity and electrical conductivity [30,31]. To overcome these limitations, alternative fast-charging anode materials, Nb-based oxides with Wadsley-Roth shear structures such as Nb_2O_5, $Nb_{16}W_5O_{55}$, and $Ti_2Nb_{10}O_{29}$, have been investigated [32–34]. Among Nb-based oxides, recent studies have highlighted the superior high-rate capability and long-term durability of defect-engineered niobium oxides even under practical conditions [35,36]. Therefore, a mixed-phase niobium oxide (d-H,M-Nb_2O_5), composed of defective crystal structures, was utilized as a fast-charging anode material in this study.

Herein, we propose a novel flexible electrode design that enables fast charging at high mass loading by incorporating niobium oxide, Nb_2O_5. The electrode will be fabricated using a solvent-free dry electrode process, employing fibrous carbon nanofiber (CNF) and polytetrafluoroethylene (PTFE) along with the chosen active material to facilitate fibrilization, ensuring both flexibility and durability against mechanical deformation. Furthermore, the application of the polymer adhesive, PEDOT: PSS, on the electrode allows for effective adhesion to various types of current collectors, demonstrating versatility and offering a simple method that does not require external pressure or heat.

2.2 Experimental Section

2.2.1 Materials

The synthesis of Nb_2O_5 was carried out using a solvothermal reaction followed by calcination. Specifically, 2g of Nb_2O_5 hydrate (CBMM Co.) was dispersed in 60 mL of ethanol and stirred using a magnetic stir bar for 1 hour. The resulting solution was transferred to a 100 mL Teflon kettle for the solvothermal reaction. Subsequently, the kettle was placed in an autoclave and heated in an oven at 200°C for 12 hours. The obtained powder was rinsed with ethanol and deionized water three times, then dried in an air oven at 70°C overnight. The dried powder was placed in an alumina crucible and inserted into a tube furnace, where it was calcined at 950°C for 3 hours with a heating ramp rate of 5°C min^{-1} under an argon gas flow of 10 sccm.

2.2.2 Electrode Preparation

The dry-processed anode was made by premixing the anode active material (Nb_2O_5) with carbon additives (CNF and SUPER P) and a binder (PTFE) using a mortar and pestle with a mass ratio of 85 (active material):10 (carbon additives):5 (binder). Three distinct electrodes were prepared: CNF 20 (2:8), CNF 50 (5:5), and CNF 80 (8:2). The number of the electrodes corresponds to the varying mass ratios of the two carbon additives used (CNF: SUPER P). The premixed powders are then transferred onto the metal board and evenly spread using a stainless-steel rolling pin. The prepared dry electrode was then applied onto current collectors, copper foil, and carbon mat, and adhered using a polymer adhesive (PEDOT: PSS dispersed in deionized water, 1.0-1.3 wt.%) with an areal mass loading of 0.01 mg cm^{-2}. For the drying process, the electrode was first oven-dried for 30 minutes at 80°C, followed by vacuum oven drying for 6 hours at the same temperature. Then the anode electrodes were punched to a diameter of 11mm.

2.2.3 Cell Preparation

2.2.3.1 Half-cell

For the half-cell fabrication, lithium metal was used as both reference and counter electrode. The MTI Corporation battery analyzer (BST8-MA) was employed to apply charging and discharging to the prepared CR 2032-coin cells. Different C-rates were applied: 0.5C, 1C, 2C, and 5C (with the current density of 1C = 200mA g^{-1}) with the 5-cycle formation at each C-rate. The prepared anode was attached onto the current collector, resulting in a mass loading level of 8-10 mg cm^{-2}. In terms of fabricating the flexible pouch full cells, anodes were prepared by blending 85 wt.% anode active material, 10 wt.% carbon additives, and 5 wt.% PTFE binder. The cathode was also prepared using the same process as the anode preparation, by mixing 90 wt.% cathode active material (NMC811), 5 wt.% carbon additives (in a 1:1 mass ratio of CNF and SUPER P), and 5 wt. % PTFE binder. The dry-processed cathode was then attached to the carbon mat current collector. 1.0M of $LiPF_6$ dissolved in EC/DMC (1:1 v/v) was used as an electrolyte, the microporous trilayer (PP/PE/PP) membrane (Celgard 2325) was used as a separator, and the lithium metal (Xiamen Tob New Energy Technology Co., LTD) was used. The coin cells were fabricated by stacking working electrode/separator/reference electrode/spacer/spring in the coin cell casing. The electrolyte was added to the stacked components.

2.2.3.2 Full-cell

For the full cell assembly, the PDMS film was prepared with a 1mm thickness through curing in a vacuum oven at 50 °C overnight. The NMC 811 and Nb_2O_5 electrodes were cut into 0.9×1.9 cm and 1.0×2.0cm, respectively. Al and Ni metal tabs were attached to the positive and negative electrodes, respectively. The flexible pouch cells were created by stacking PDMS/negative electrode/separator/positive electrode/PDMS together. Subsequently, the edge of the pouch cell was sealed with PDMS. The N/P ratio range of the fabricated full cells was 1.00 – 1.03. The electrolyte was injected into the pouch cell using a syringe, and the hole was covered with epoxy resin. The fabricated pouch cell was rested in an Ar-filled glovebox for 24 hours. The charge/discharge procedures for the developed pouch full cells were conducted using the MTI Corporation system (BST8-A6V0).

2.2.4 Mechanical Characterization

The mechanical strength of the prepared anode was determined using the Dynamic Mechanical Analyzer (TA Instruments Q800). To conduct the mechanical measurements, the electrodes were cut to dimensions of 24.21 mm × 6.38 mm × 0.1 mm (l × w × t). The elasticity of the prepared electrodes with different compositions was measured by applying a preset load of 0.001N, a ramp force of 0.05 N/min, and a maximum force of 0.35N. To examine the performance and behavioral differences of half-cell and full-cell assemblies before and after bending, a custom-made bending device was developed to apply bending to the prepared anodes.

2.2.5 Microstructural Characterization

2.2.5.1 Scanning Electron Microscopy (SEM)

Microstructural observations were conducted using surface and cross-section images obtained with the Quanta FEG 250 SEM, at a beam voltage setting of 10kV.

2.2.5.2 Raman Measurements

Raman spectroscopy was performed using Renishaw RM1000 micro-spectroscopic system with a 50× objective and an Ar laser excitation (514 nm). The wavenumber range was from 200 to 1200 cm^{-1}.

2.2.5.3 X-Ray Diffraction (XRD)

XRD patterns were obtained using Rigaku Miniflex Power XRD with a Cu Kα radiation source. The 2θ range was from 10 to 80°.

2.3 Results and Discussion

2.3.1 Design Concept of Niobium Oxide Flexible Electrode

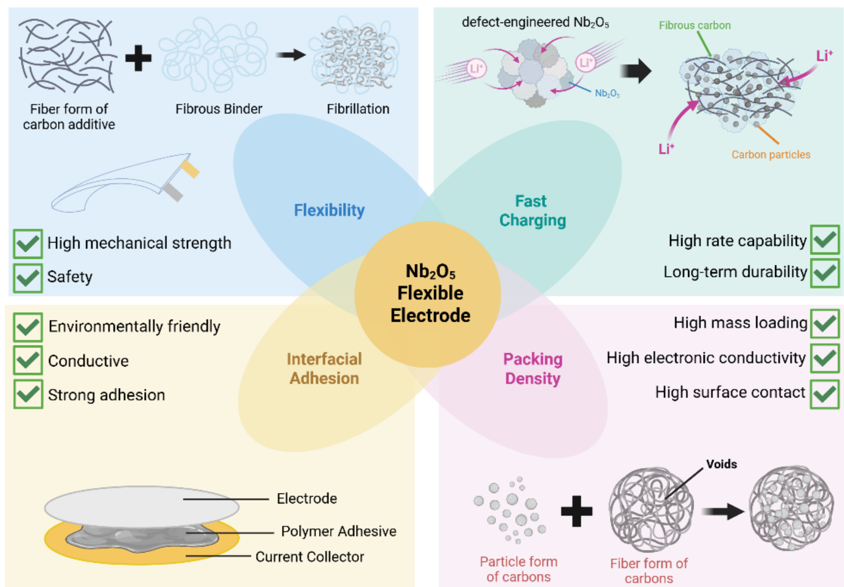

Figure 2-1. Schematic illustration of the design concept of Nb_2O_5 flexible electrode.

The flexibility of the electrode is highly dependent on the mechanical properties and morphological network of electrode components [37–39]. To enhance mechanical stability, an interconnected structure with fibrous networks induced by CNF and PTFE was designed for a flexible electrode (**Figure 1**) [40–42]. The fibrous carbon additive provides a continuous electronic pathway, facilitating long-distance electron transport in high mass loading electrodes [43]. However, the fibrous morphology of CNF can increase the porosity in the electrode due to the loose packing, leading to a poor contact surface area between the active material, conductive carbon, and binder [44]. The porosity will disconnect the continuous network of electrodes and reduce both mechanical stability and electrochemical kinetics [45]. To minimize the porosity in the electrode, carbon nanoparticles, Super P (SP), were added for the dry free-standing electrode fabrication. As a result, we obtained the free-standing film-type electrodes from the dry process (Figure S1).

The free-standing electrode offers inherent flexibility and increased volumetric-energy-density [46,47]. However, despite these benefits, free-standing electrode design also faces several limitations. Without the support of current collectors, they tend to be more fragile and prone to cracking or deformation, especially during handling or operation [48,49]. The lack of a highly conductive current collector can also lead to reduced electrical conductivity in large-scale cells, which may compromise rate capability [50]. In addition, the solvent-free processed electrode poses challenges in establishing strong contact with current collectors because of the weak interfacial adhesion of the PTFE binder [51]. Accordingly, PEDOT:PSS is selected as an additional polymer adhesive, owing to its high electrical conductivity, strong adhesion, and chemical resistance [52,53]. Hence, a small amount of PEDOT:PSS is used as a conductive binder between the free-standing electrode and current collectors, providing high electrical conductivity and strong interfacial adhesion to the free-standing electrode without thermal or high-pressure treatments.

2.3.2 Mechanical Properties of Nb_2O_5 Electrodes

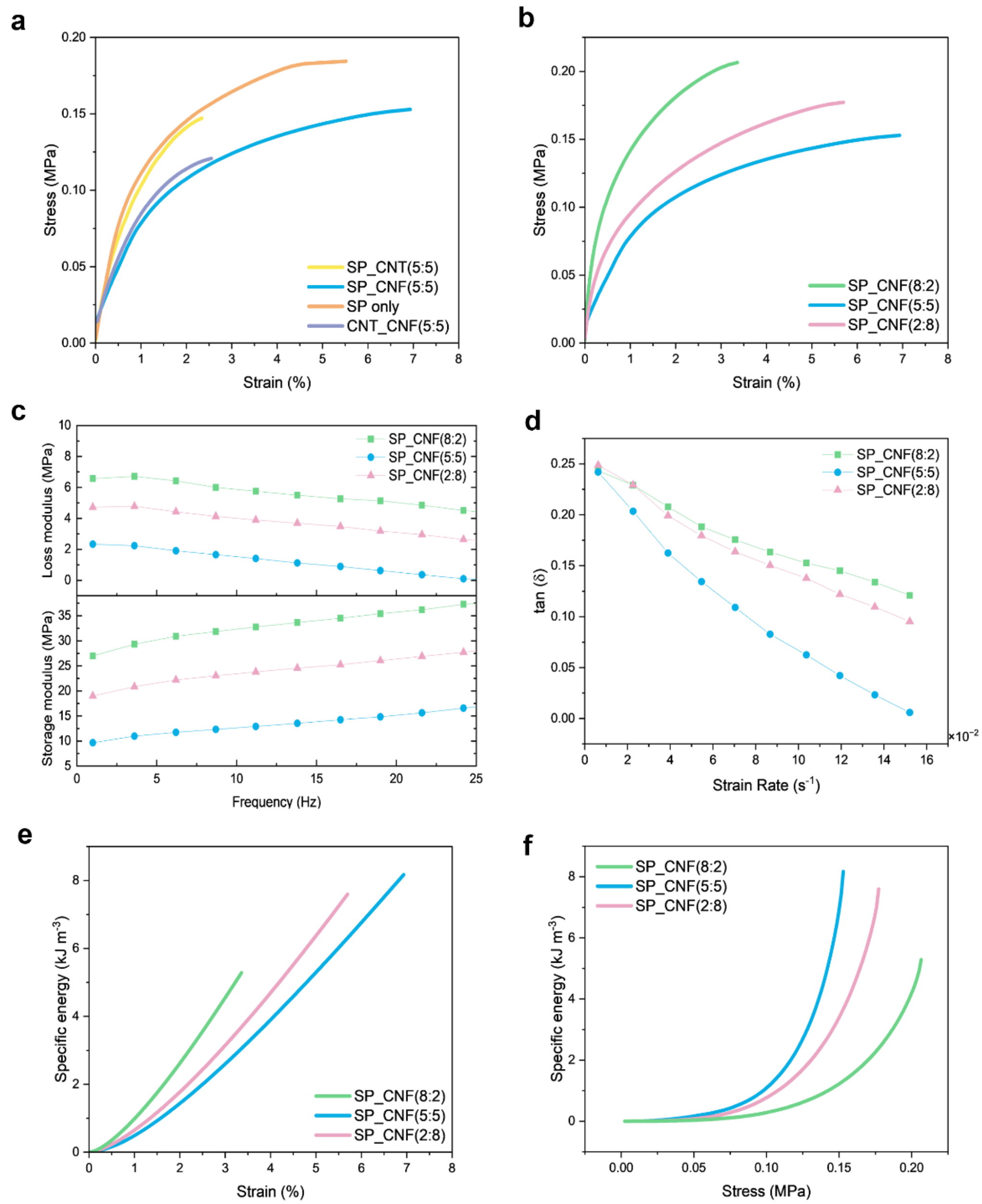

Figure 2-2. Mechanical properties of electrodes. Tensile test comparisons of different a) fibrous carbon additives and b) compositions of Super P and CNF. Dynamic mode test of electrodes with various compositions for c) storage and loss modulus, and d) damping factor. Specific energy absorbed in electrodes as function of e) strain and f) stress.

To identify the optimal electrodes exhibiting the highest mechanical flexibility and stability against mechanical deformation, the compositions of selected carbon additives were optimized by comparing various electrode formulations, along with a comparative assessment of different candidates of carbon additives was also conducted. The free-standing electrodes were used for the tests, and the mass ratio of active material, conductive carbons, and binder was 85:10:5. The crystal and bonding structures of SP_CNF(5:5) exhibited the mixed composition of niobium oxide with the Wadsley-Roth shear structure, carbon additives, and polymer binder (Figure S2). As illustrated in **Figure 2**a, a comparison was conducted between candidates containing different fiber-based carbon additives, such as carbon nanotubes (CNT) and CNF. In addition, to evaluate whether combining fiber and particle forms could enhance mechanical strength, the tests were performed using various combinations of different forms of carbon, including a sample consisting solely of carbon particles. Both SP_CNT(5:5) and CNT_CNF(5:5) exhibited similar strain values, with SP_CNT(5:5) reaching 2.34% and CNT_CNF(5:5) achieving 2.55%. On the other hand, when tensile strength was applied to the all-particle form electrode containing only Super P, a high strain of 5.52% was observed. This highlights the critical role of incorporating the particle-form carbon additive in significantly enhancing the stretchability of the electrodes. Lastly, when Super P and CNF were mixed in equal proportions, the SP_CNF(5:5) exhibited a strain of 6.93%, representing the highest stretchability observed among all tested electrode compositions, emphasizing the importance of using the combination of particle and fiber carbon to achieve even greater flexibility. Furthermore, the results show the distinct differences between CNT and CNF in terms of flexibility, as demonstrated by the significant variation in elongation between the SP_CNT(5:5) and SP_CNF(5:5) electrodes. As a result, CNF was selected over CNT for the fiber carbon additive. To optimize the electrode composition for identifying the formulation with the highest flexibility, three different ratios of both particle and fiber-type carbon additives were tested (Figure 2b). Among the three ratios, an equal ratio of particle and fiber form of carbon additives, SP_CNF(5:5), resulted in the greatest elongation, demonstrating the highest flexibility. In addition, the change in stiffness, $\Delta d\delta\ d\varepsilon^{-1}$, was also calculated from the tensile strength test for the three ratios, and SP_CNF(5:5) presented the smallest changes in terms of strain, maintaining the original stiffness at higher strain (Figure S3).

In order to validate the results of the electrode optimization obtained through tensile testing, the storage modulus, loss modulus, and damping factor were also evaluated. Given that the storage modulus represents the stiffness of a material and considering that the SP_CNF(5:5) electrode demonstrated the lowest stiffness, this further supports the elasticity observed for SP_CNF(5:5) in the tensile test results (Figure 2c). Furthermore, the lowest loss modulus observed for SP_CNF(5:5) correlates with its elastic behavior, as the loss modulus quantifies the energy dissipated as heat during deformation. This suggests that SP_CNF(5:5) demonstrates the highest elasticity, with the ability to recover energy without significant heat dissipation. This behavior is also linked to battery safety, as electrodes with higher elasticity generate less internal heat energy. Finally, the damping factor is derived from the relationship between the storage and loss modulus (Figure 2d). The lowest damping factor of SP_CNF(5:5) at all strain rates presents less internal friction and energy loss inside the electrode, highlighting its ability to return to its original form without needing to undergo significant energy dissipation, thus demonstrating its elasticity. These features show higher mechanical resilience and less degradation for electrodes, maintaining ionic/electronic pathways over repeated mechanical deformations.

For identifying the differences in mechanical behavior among the tested electrodes, specific energy as a function of strain and stress was analyzed. As shown in Figure 2e, distinct differences in the mechanical behavior of each electrode became apparent with increasing strain. Among them, SP_CNF(5:5) not only exhibited the greatest elongation but also achieved the highest overall specific energy, indicating its ability to absorb the most energy before failure and demonstrating the greatest resistance against deformation. Similarly, Figure 2f highlights the superior toughness of the SP_CNF(5:5) electrode. As shown, this electrode displayed the steepest slope of specific energy in relation to the stress, indicating its ability to absorb the greatest amount of energy with increasing applied stress. This behavior reflects the material's high ductility and thus, more flexible mechanical properties compared to the other electrode compositions.

Based on the mechanical evaluation of various electrode formulations, we can find several key conclusions. Combining particle and fiber carbon additives leads to synergistic improvements in flexibility, depending on their compositions, increasing the maximum strain and reducing the stiffness change under tensile stress. Furthermore, CNF was found to outperform CNT as a fiber additive, achieving higher mechanical stability. Dynamic mechanical analysis (DMA) further validated these results, showing that SP_CNF(5:5) had the lowest storage modulus, loss modulus, and damping factor, confirming its excellent elasticity and reduced internal friction, which are beneficial for maintaining electrode integrity and improving battery safety. Additionally, the highest specific energy and toughness of SP_CNF(5:5) reflect its strong resistance to mechanical failure and superior energy absorption under strain. Collectively, these results establish SP_CNF(5:5) as the optimal formulation for flexible electrodes with excellent mechanical stability.

2.3.3 Microscopic Observation of Nb_2O_5 Electrodes

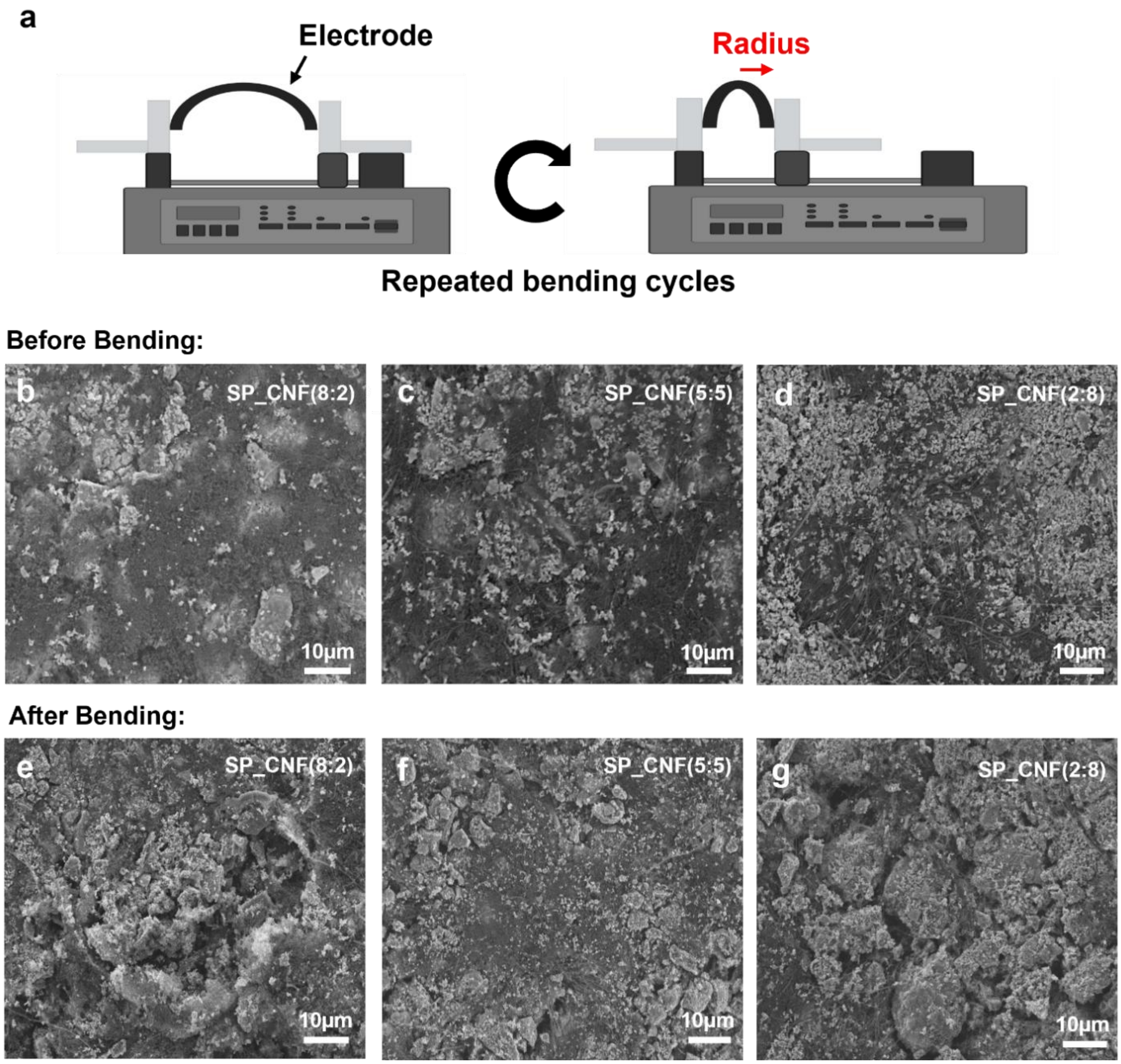

Figure 2-3. Bending test of the freestanding electrodes. a) Schematic illustration of the lab-made bending device. Microscopic observations of free-standing electrodes with different conductive carbon compositions b-d) before bending and e-g) after 100 bending cycles with a radius of 0.2 cm.

To observe the changes in each conductive carbon composition under repeated mechanical deformation, 100 bending cycles with a radius of 0.2 cm were conducted on all electrodes using the lab-made bending device (**Figure 3**a and S4). Before bending, the scanning electron microscopy (SEM) images of all electrodes exhibited dense and smooth surfaces without cracking or deformation (Figure 3b – 3d). Upon comparing the post-bending scanning SEM images (Figure 3e – 3g), the SP_CNF(5:5) electrode presented with less pronounced cracks when compared against SP_CNF(8:2) and SP_CNF(2:8), indicating its greater mechanical toughness and resistance to repeated external mechanical deformation. Additionally, the SEM image of the conventional slurry-casted electrode was also observed after the same bending conditions (Figure S5). In contrast to the SP_SNF(5:5), the conventional electrode showed severe cracking on the surface, which may result in safety issues. As confirmed in the mechanical characterization and microscopic observation, the optimal mechanical behaviors of SP_CNF(5:5) were suitable for the flexible electrode design.

2.3.4 Electrochemical Performance of Nb_2O_5 Electrodes

2.3.4.1 Freestanding Electrodes

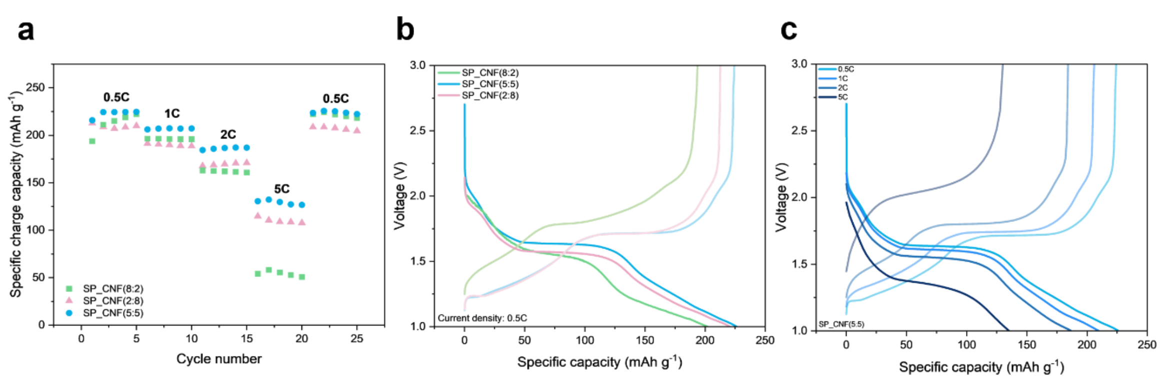

Figure 2-4. Electrochemical performance of free-standing electrodes with varied conductive carbon compositions. a) Rate capability of the electrodes at current densities of 0.5C, 1C, 2C, and 5C. b) Voltage profiles of the electrodes at 0.5 C and c) SP_CNF(5:5) voltage profiles at all C-rates. The active material mass loading for the electrodes was 8 – 9 mg cm^{-2}.

The electrochemical performance of free-standing Nb_2O_5 electrodes with varying conductive carbon compositions was evaluated at different current densities ranging from 0.5C to 5C within a voltage window of 1.0 – 3.0 V to assess their capacity at various current rates and their capability for fast charging/discharging (**Figure 4**a). The specific charge capacities of SP_CNF(8:2), SP_CNF(5:5), and SP_CNF(2:8) were determined to be 193.72 mAh g^{-1}, 224.32 mAh g^{-1}, and 212.80 mAh g^{-1} at a current density of 0.5 C, respectively (Figure 4b). At low C-rates, the specific capacity of all electrodes was not significantly different from one another, but SP_CNF(5:5) exhibited higher specific capacities and smaller voltage hysteresis at high C-rates compared to SP_CNF(2:8) and SP_CNF(8:2) (Figure 4c and S6). This result suggests that an optimal balance between fibrous and particle forms of carbon additives is critical not only for mechanical properties but also for achieving superior capacity.

2.3.4.2 Electrodes with Current Collectors

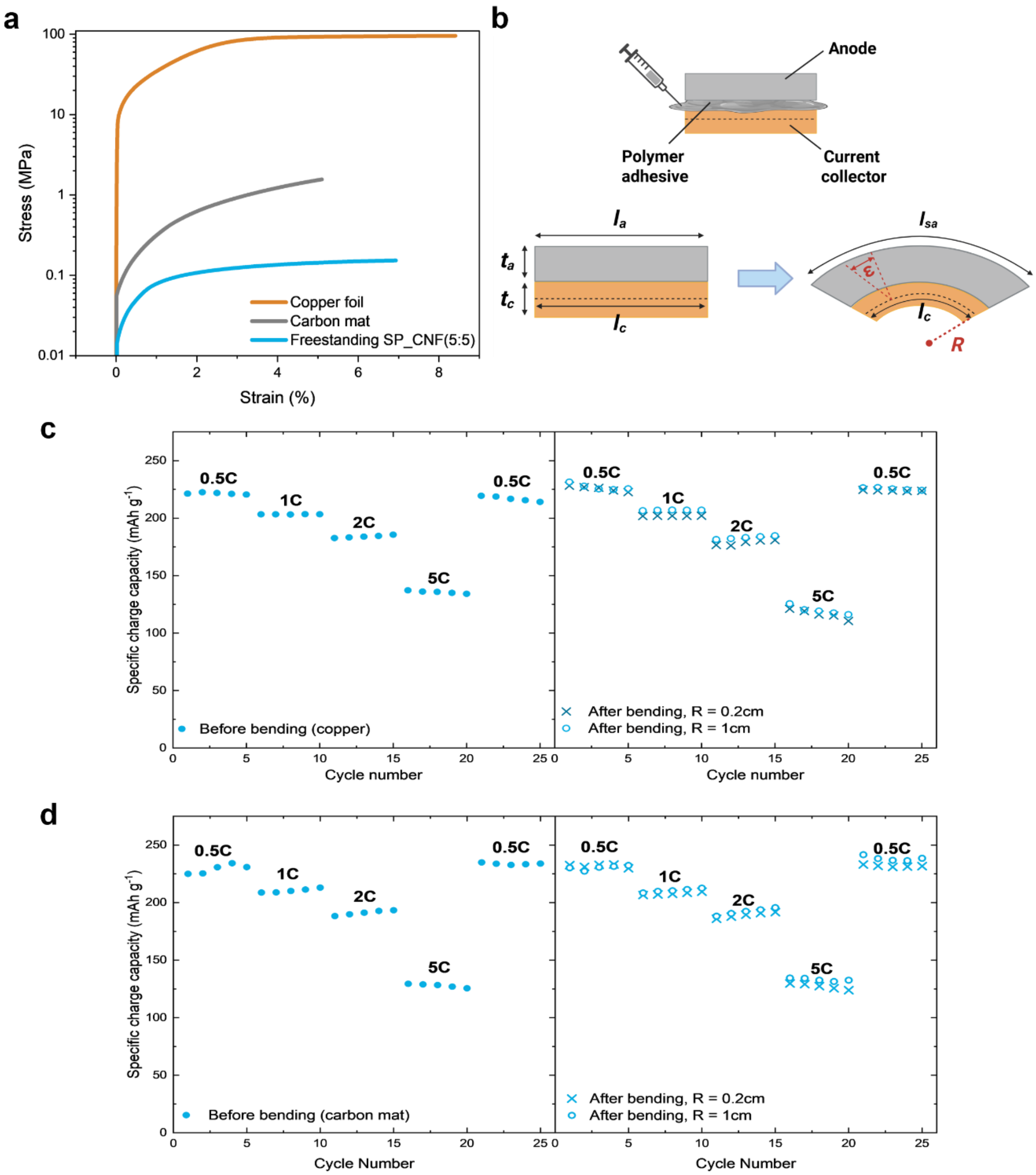

Figure 2-5. Electrochemical performance of the current collector-attached electrodes after bending. SP_CNF(5:5) with current collector a) mechanical strength comparison between free-standing SP_CNF(5:5) against different current collectors. b) Schematic illustration of the current collector attached electrode and the strain generated by the applied bending radii on the electrode. Rate capabilities of SP_CNF(5:5) electrodes on current collectors of c) copper foil and d) carbon mat before bending and after 100 bending cycles with radii of 0.2 cm and 1 cm.

Comparative analysis of mechanical strength between the free-standing electrode, copper foil, and carbon mat current collectors was conducted to demonstrate the necessity of current collectors for the free-standing electrodes to resist the externally applied mechanical deformation. Through tensile strength measurements, it was observed that the copper foil and carbon mat current collectors could withstand substantially greater stress than the free-standing electrode (**Figure 5**a). Additionally, the results indicate that pristine copper foil exhibited significantly higher ductility than the carbon mat, withstanding greater stress and undergoing more elongation prior to fracture. Accordingly, the fabricated electrode was integrated with two distinct current collectors possessing higher mechanical strength to evaluate the electrochemical performance under mechanical deformation. In order to examine the durability of the fabricated electrode when adhered to current collectors, PEDOT:PSS was used as a conductive polymer adhesive, attributed to its non-toxic nature and excellent electrical and ionic conductivity, preventing degradation of charge transport between the anode and current collectors [50]. Following the adhesion of the free-standing electrode to the current collector, cyclic bending tests were performed. To discuss the maximum theoretical strain on the electrode, the strain induced by a bending radius was calculated using Equation 1 and 2 (Figure 5b and Supplementary note 1).

$$l_{sa} = l_c + \Delta l \tag{1}$$

$$\varepsilon = \frac{l_{sa}}{l_c} - 1 = \frac{R + t_a + t_c}{R + \frac{t_c}{2}} - 1 \tag{2}$$

where *l* is a length, *a* denotes a freestanding electrode, *c* denotes a current collector, *sa* represents a bent freestanding electrode, and ε refers to strain. The maximum strain applied to current collectors was theoretically calculated based on the equations (Table 1 and Figure S7-S10**)**. The thickness of the electrode was approximately 60 μm, and the bending radii of 0.2 cm and 1 cm were selected to simulate moderate deformation and an extreme condition near folding. The thick carbon mat current collector with a small bending radius of 0.2 cm showed the highest theoretical strain, 7.60%. However, the electrode did not exhibit any significant cracking or damage on the surface under this condition (Figure S11).

Table 2-1. Calculated values of strain applied at each radius to different current collectors.

Bending radius, R (cm)	Current collector	Strain, ε (%)
0.2	Copper foil (t_c = 0.012mm)	3.29
	Carbon mat (t_c = 0.199mm)	7.60
1	Copper foil (t_c = 0.012mm)	0.66
	Carbon mat (t_c = 0.199mm)	2.07

As a result, the electrode attached to the copper foil current collector exhibited no significant difference in capacity across all applied current densities when comparing the electrochemical performance before and after bending at both radii (Figure 5c). Similarly, for the electrodes attached to the carbon mat current collector, the electrochemical performance remained consistent after bending cycles at both radii, showing no observable difference in rate capabilities before and after bending (Figure 5d).

2.3.4.3. Pouch Cell Configuration

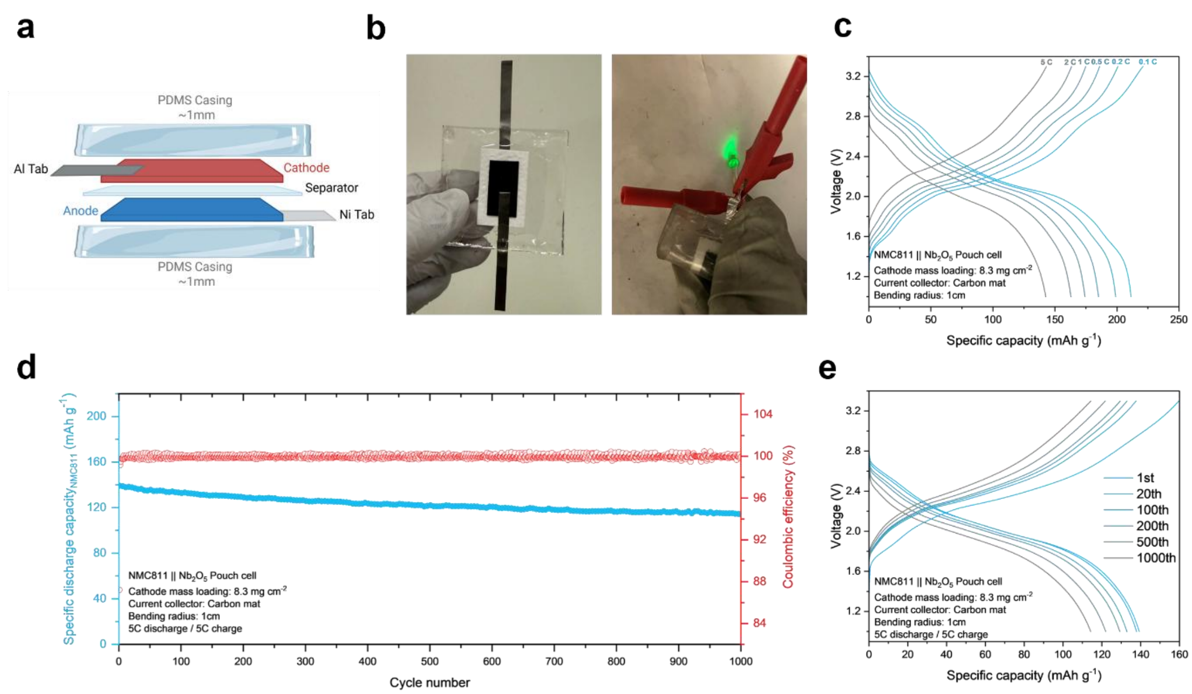

Figure 2-6. Flexible pouch cell fabrication and electrochemical performance. a) Schematic illustration of the flexible pouch full cell using a PDMS casing. b) Image of the assembled pouch cell (left) and folded cell while lighting an LED (right). c) Rate capability of the bent pouch cell

at various current densities, ranging from 0.5 C to 5 C. d) Long-term cycling of the bent pouch cell at a current density of 5C (8.3 mA cm^{-2}), and e) the corresponding voltage profiles. The flexible pouch cells were tested with a bending radius of 1 cm.

Based on the flexible electrode design of Nb_2O_5 negative electrodes, flexible $LiNi_{0.8}Mn_{0.1}Co_{0.1}O_2$ (NMC811) positive electrodes were fabricated using a dry process and a polymer adhesive attaching to the carbon mat current collector. The NMC811 flexible electrode exhibited excellent mechanical stability, showing no visible surface cracking or damage after 100 bending cycles at a bending radius of 1 cm (Figure S12).

A full cell was assembled by pairing the NMC811 and Nb_2O_5 flexible electrodes to assess electrochemical performance under fast (dis)charging conditions. To enable mechanical flexibility, polydimethylsiloxane (PDMS) films were employed as the pouch cell casing (**Figure 6**a). The assembled cell successfully powered a green light-emitting diode (LED) while being folded (Figure 6b and Figure S13), demonstrating functional operation under mechanical deformation. Electrochemical performance was evaluated with the pouch cell bent at a 1 cm bending radius. The cell exhibited specific capacities of 211, 199, 186, 175, 163, and 143 mAh g^{-1} at current rates of 0.1, 0.2, 0.5, 1, 2, and 5C (1C = 1.66 mA cm^{-2}), respectively (Figure 6c). Long-term cycling at 5C over 1,000 cycles resulted in 82.1% capacity retention (Figure 6d and 6e), indicating excellent durability under high-rate operation and mechanical deformation. Notably, the full cell maintained the high-rate capabilities even at high areal mass loadings exceeding 10 mg cm^{-2} (Figure S14).

2.4 Conclusion

In conclusion, we have designed a flexible, high-mass loading, fast-charging capable niobium oxide anode for LIBs. The engineered structural design allows mechanical resilience against external deformation, enabling the anode to maintain stable electrochemical capacity under mechanical stress without performance degradation. Bending tests conducted on both half-cell and full-cell configurations using a custom-designed bending apparatus validated the structural integrity of the anode, exhibiting no observable difference in performance before and after mechanical deformation. We also performed tensile testing on the anode using DMA, which has further shown its outstanding mechanical flexibility. In order to also show the versatility of PEDOT:PSS adhesive with various current collectors, the consistent electrochemical performance was confirmed across different current collector substrates. The anode demonstrated excellent fast-charging performance in both half-cell and full-cell, including a pouch cell configuration, further emphasizing its potential for integration into flexible lithium-ion battery applications. Overall, this study presents a next-generation fast-charging electrode design that delivers excellent rate capability, durability, and mechanical flexibility, making it a promising candidate for advanced flexible, high-power rechargeable lithium-ion batteries.

2.5 Supplementary Information

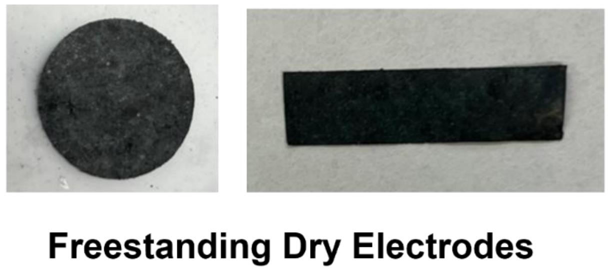

Figure S2-1. Freestanding dry electrodes in versatile shapes fabricated through a dry electrode process.

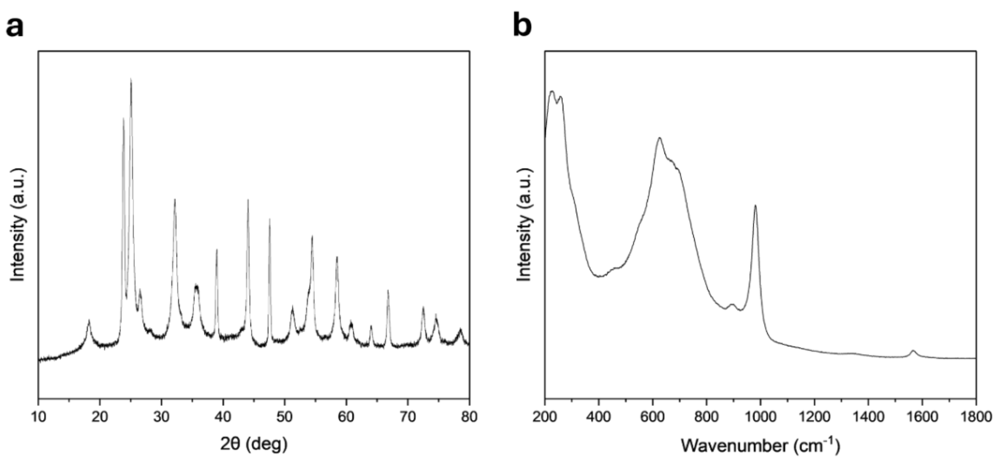

Figure S2-2. a) X-ray diffraction pattern and b) Raman spectrum of SP_CNF(5:5) sample.

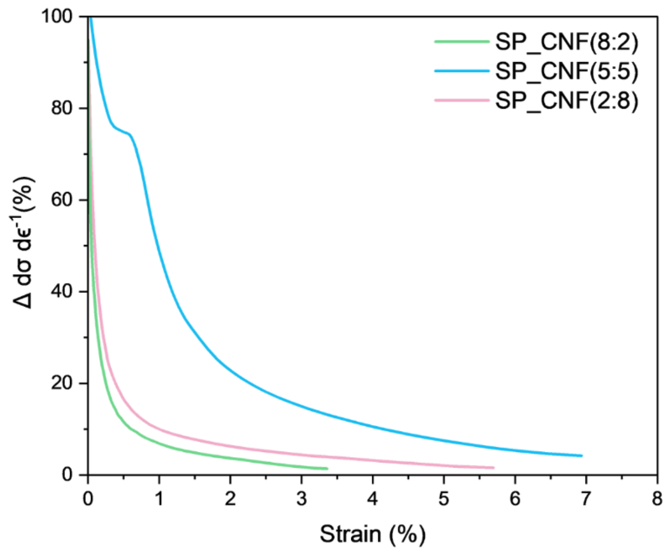

Figure S2-3. Change in stiffness of SP_CNF(8:2), SP_CNF(5:5), SP_CNF(2:8) samples in terms of strain.

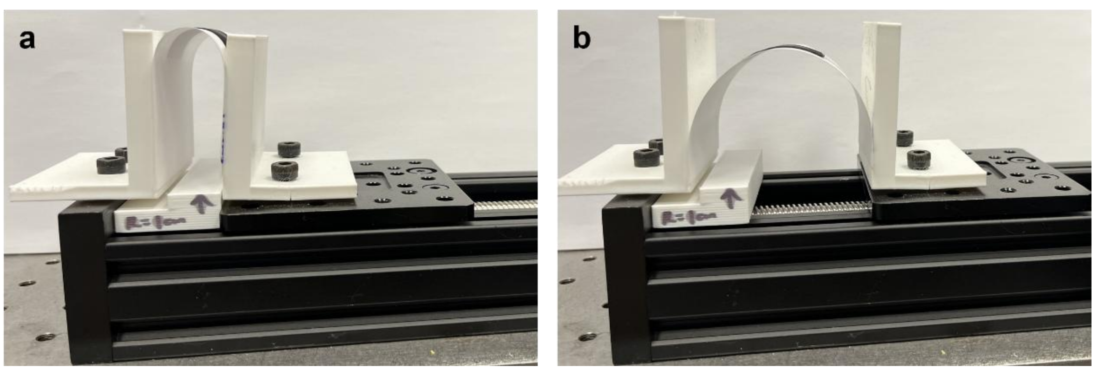

Figure S2-4. Bending device images of a) application of bending at a radius of 1cm and b) at relaxation.

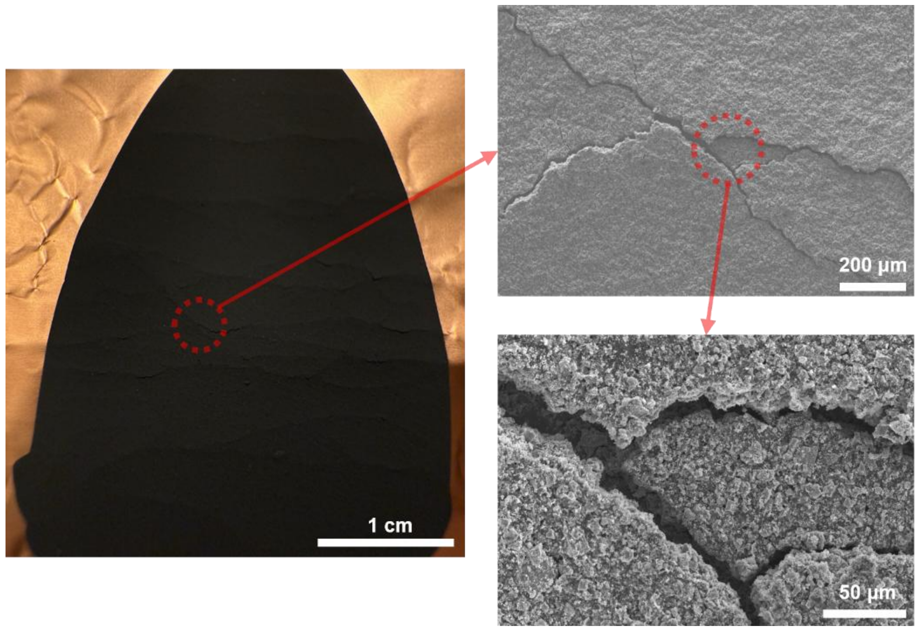

Figure S2-5. Scanning electron microscopy images of the conventional electrode after 100 bending cycles with a radius of 0.2cm. The electrode was fabricated using a conventional slurry process.

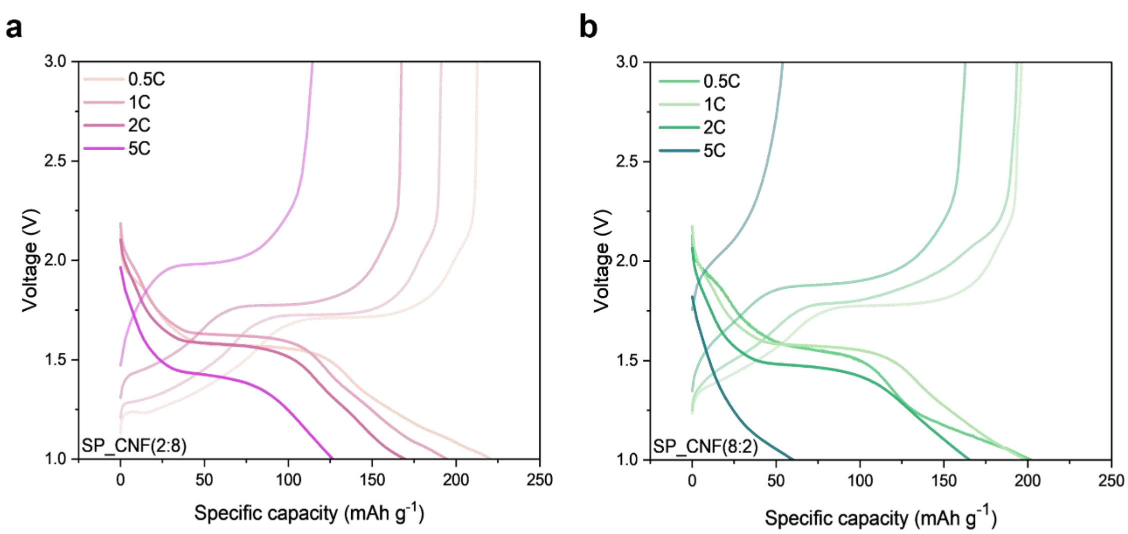

Figure S2-6. Voltage profiles of a) SP_CNF(2:8) b) SP_CNF(8:2) electrodes at current densities of 0.5 C, 1 C, 2 C, and 5 C.

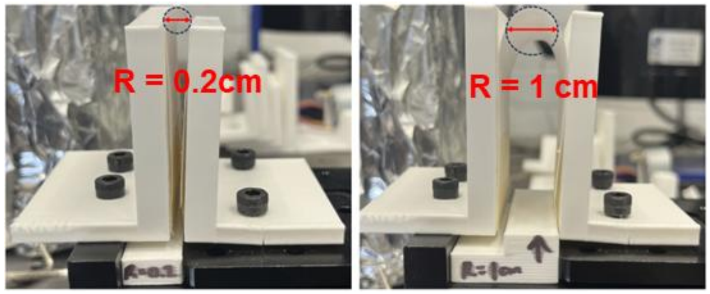

Figure S2-7. Images of the bending device with different bending radii of 0.2 cm and 1 cm.

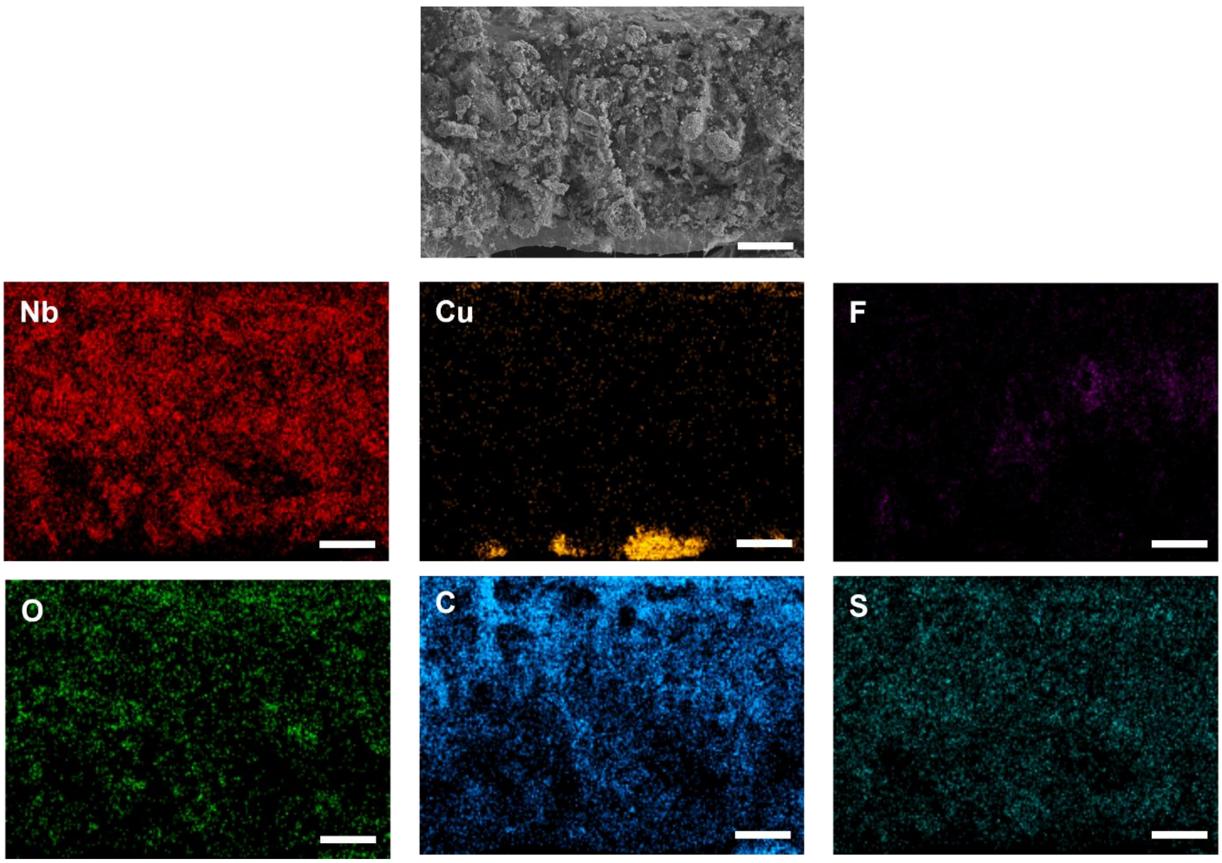

Figure S2-8. Scanning electron microscopy and energy-dispersive X-ray spectroscopy mapping images of SP_CNF(5:5) anode adhered onto copper current collector. The scale bar corresponds to 20 μm.

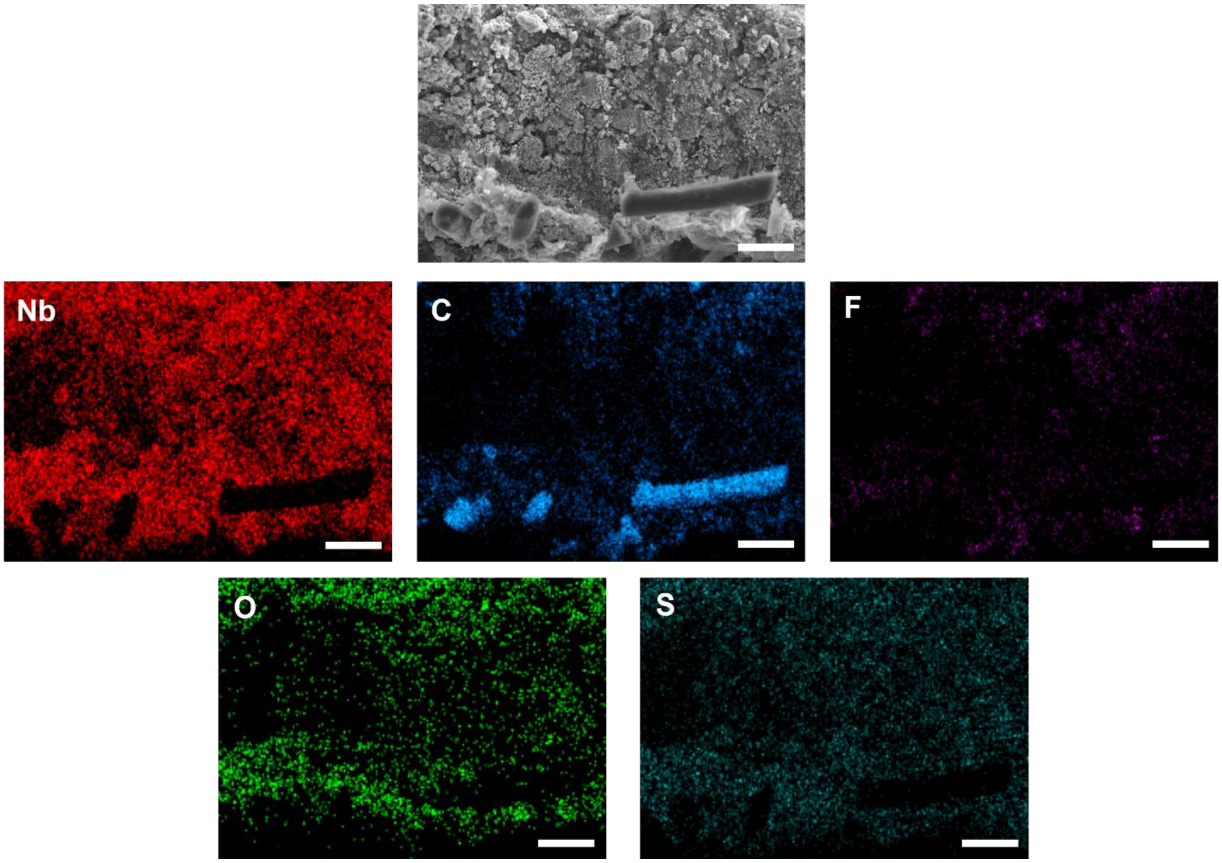

Figure S2-9. Scanning electron microscopy and energy-dispersive X-ray spectroscopy mapping images of SP_CNF(5:5) anode adhered onto carbon mat current collector. The scale bar corresponds to 20 μm.

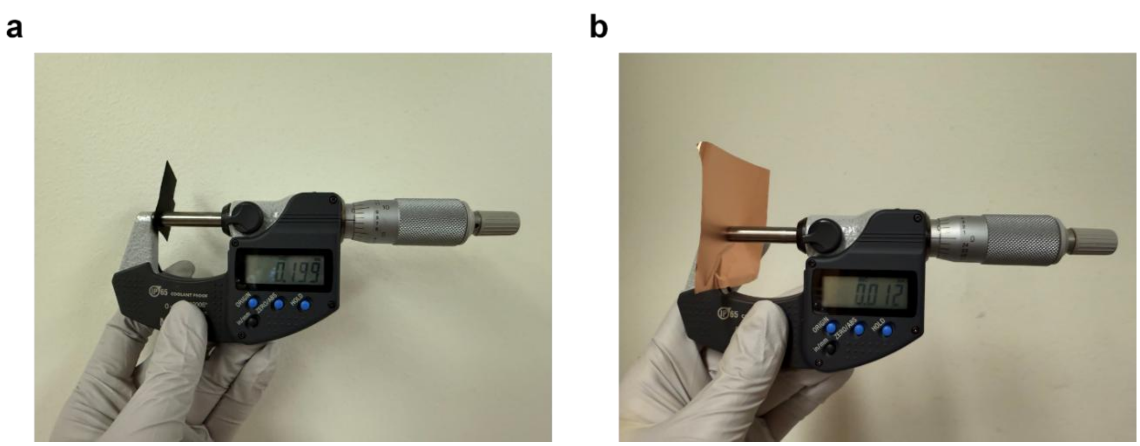

Figure S2-10. Thickness of a) carbon mat and b) copper foil current collectors for electrodes.

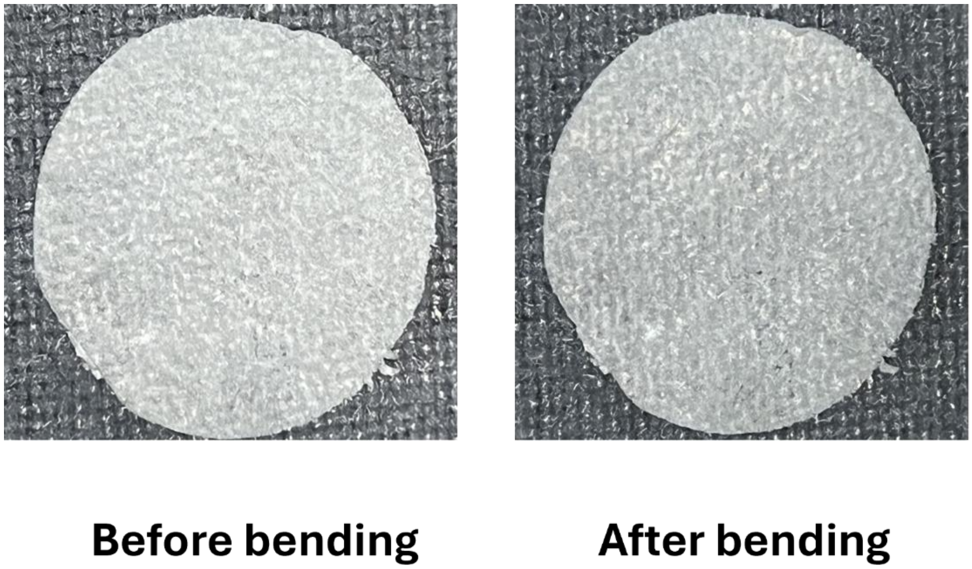

Figure S2-11. Images of SP_CNF(5:5) electrode on the carbon mat current collector a) before bending and b) after 100 bending cycles with a radius of 0.2 cm.

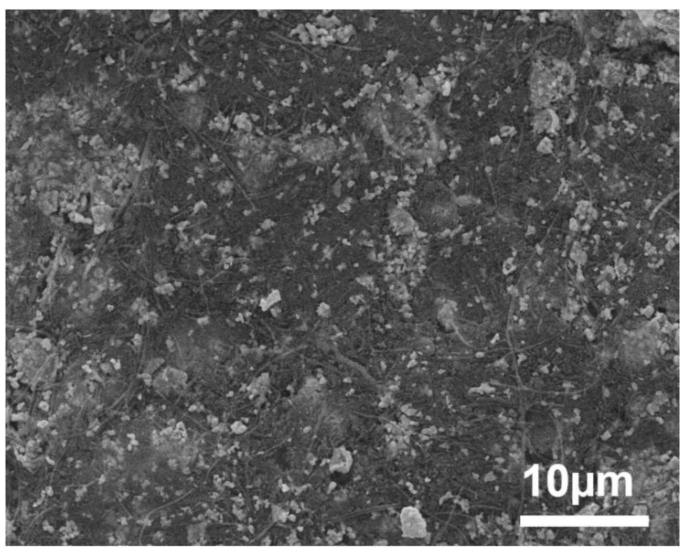

Figure S2-12. SEM image of SP_CNF(5:5) electrode attached to the carbon mat current collector after 1,000 bending cycles with a radius of 1 cm.

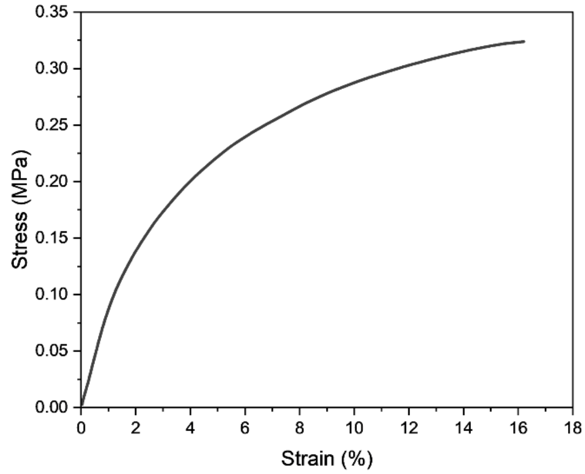

Figure S2-13. Tensile strength test result of NMC811 (LiNi0.8Mn0.1Co0.1O2) freestanding electrode fabricated with a dry electrode process.

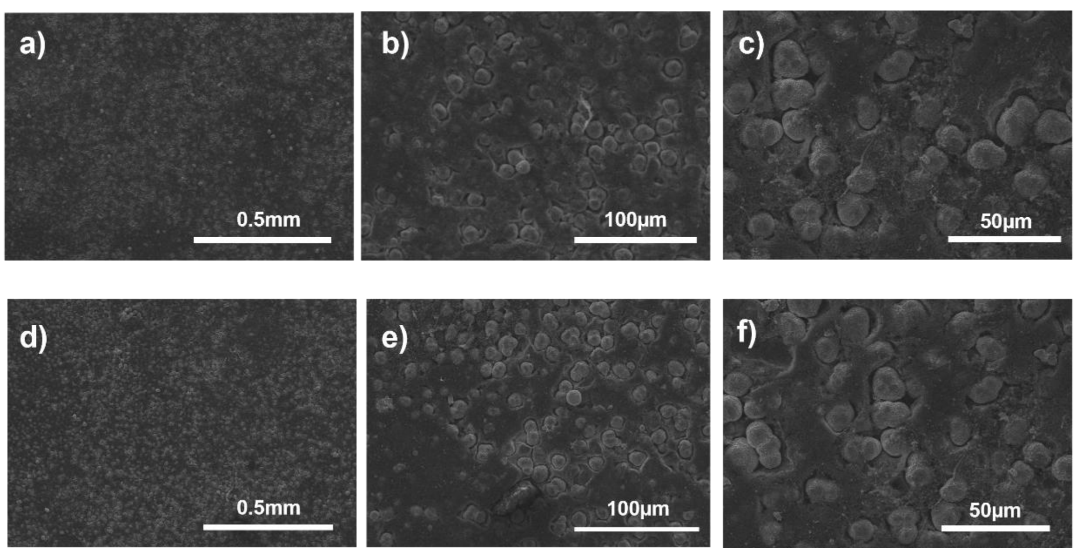

Figure S2-14. Scanning electron microscopy images of NMC811 (LiNi0.8Mn0.1Co0.1O2) cathode fabricated with a dry electrode process a-c) before bending and d-f) after 100 bending cycles with a radius of 1 cm. The electrode composition was selected based on the results of the niobium oxide flexible anode.

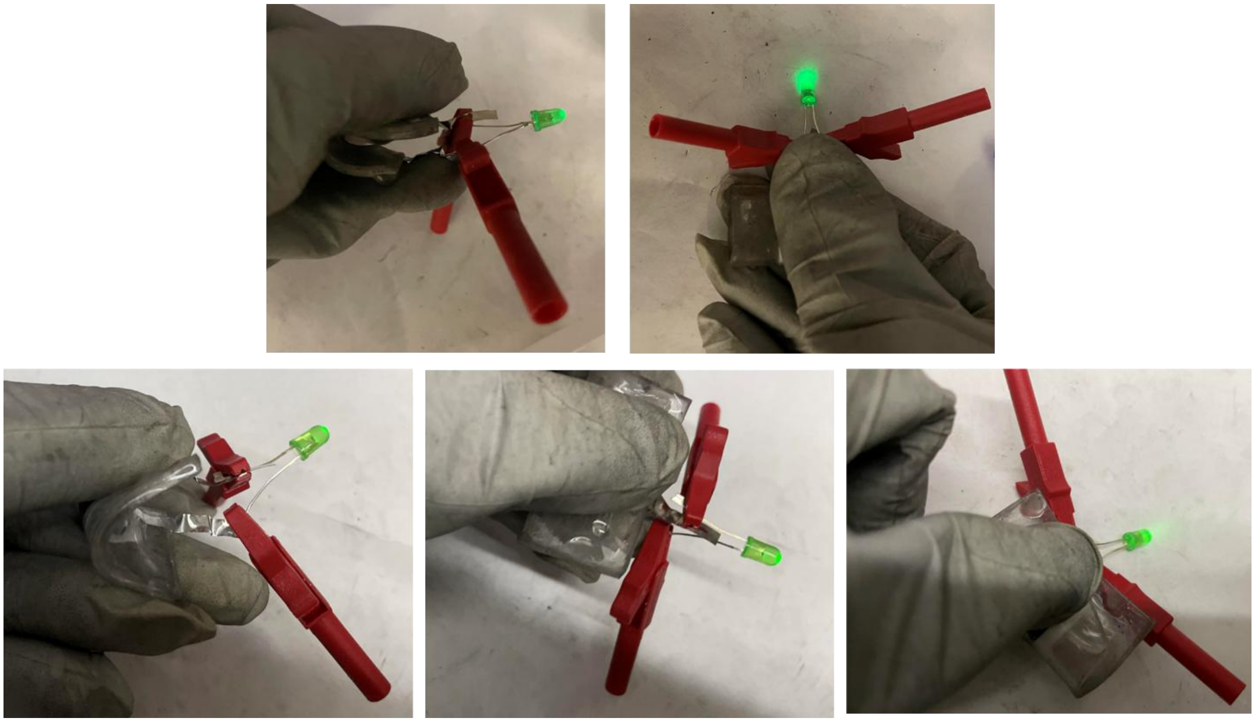

Figure S2-15. Optical images of NMC || Nb2O5 pouch cells. The cells were folded while lighting an LED.

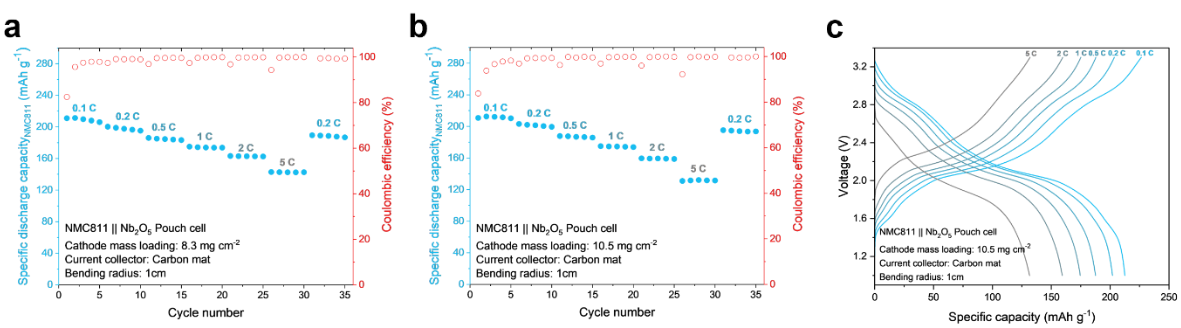

Figure S2-16. Rate capabilities of NMC811 || Nb2O5 pouch cell with mass loading of a) 8.3 mg cm-2 and b) 10.5 mg cm-2 at various current densities ranging from 0.1 C to 5 C, and c) the corresponding voltage profile for the pouch cell with a mass loading of 10.5 mg cm^{-2} at various current densities ranging from 0.1 C to 5 C, and c) the corresponding voltage profile for the pouch cell with a mass loading of 10.5 mg cm^{-2}. The pouch cells were tested while being bent with a 1 cm radius.

Supplementary note 1

Equation 1 and 2 are simplified with assumptions. Theoretically, the neutral axis at height *z* from the bottom of the laminate, where layer 1 is on top and layer 2 is on bottom, can be calculated using the following equation

$$z = \frac{E_1 t_1 \left(t_2 + \frac{t_1}{2}\right) + E_2 t_2 (\frac{t_2}{2})}{E_1 t_1 + E_2 t_2}$$

where *E* is Young's modulus and *t* is the thickness. As shown in Figure 5a, the Young's moduli of copper foil and carbon mat are significantly higher than free-standing electrodes. Based on the measurements, we assume $E_1 << E_2$. As a result, the neutral axis is located in the middle of the current collectors.

2.6 References

(1) Zhang, Q.; Gao, X. W.; Liu, X.; Mu, J. J.; Gu, Q.; Liu, Z.; Luo, W. Bin. Flexible Wearable Energy Storage Devices: Materials, Structures, and Applications, Battery Energy, 2024, 3, 20230061. https://doi.org/10.1002/bte2.20230061.

(2) Wehner, L. A.; Mittal, N.; Liu, T.; Niederberger, M. Multifunctional Batteries: Flexible, Transient, and Transparent. ACS Cent Sci 2021, 7 (2), 231–244. https://doi.org/10.1021/acscentsci.0c01318.

(3) Li, Y.; Wang, R.; Guo, Z.; Xiao, Z.; Wang, H.; Luo, X.; Zhang, H. Emerging Two-Dimensional Noncarbon Nanomaterials for Flexible Lithium-Ion Batteries: Opportunities and Challenges. Journal of Materials Chemistry A. Royal Society of Chemistry 2019, pp 25227–25246. https://doi.org/10.1039/c9ta09377j.

(4) Fu, K. K.; Cheng, J.; Li, T.; Hu, L. Flexible Batteries: From Mechanics to Devices. ACS Energy Letters. American Chemical Society November 11, 2016, pp 1065–1079. https://doi.org/10.1021/acsenergylett.6b00401.

(5) Riley, S.; Shevchuk, A.; George, C. Achieving Dynamic Stability and Electromechanical Resilience for Ultra-Flexible Battery Technology. Communications Materials. Springer Nature December 1, 2024. https://doi.org/10.1038/s43246-024-00703-0.

(6) Gong, X.; Yang, Q.; Zhi, C.; Lee, P. S. Stretchable Energy Storage Devices: From Materials and Structural Design to Device Assembly. Advanced Energy Materials. John Wiley and Sons Inc April 1, 2021. https://doi.org/10.1002/aenm.202003308.

(7) Chang, J.; Shang, J.; Sun, Y.; Ono, L. K.; Wang, D.; Ma, Z.; Huang, Q.; Chen, D.; Liu, G.; Cui, Y.; Qi, Y.; Zheng, Z. Flexible and Stable High-Energy Lithium-Sulfur Full Batteries with Only 100% Oversized Lithium. Nat Commun 2018, 9 (1). https://doi.org/10.1038/s41467-018-06879-7.

(8) Zhang, Y.; Xiao, Y.; Chen, L.; Hu, S. A Strategy to Build High-Performance Thick Electrodes for Lithium-Ion Batteries with Enhanced Compressive Modulus and Regulated Tortuosity in the Phase-Inversion Process. J Mater Chem A Mater 2024, 12 (27), 16537–16545. https://doi.org/10.1039/d4ta00589a.

(9) Kong, L.; Tang, C.; Peng, H. J.; Huang, J. Q.; Zhang, Q. Advanced Energy Materials for Flexible Batteries in Energy Storage: A Review. SmartMat. John Wiley and Sons Inc December 1, 2020. https://doi.org/10.1002/smm2.1007.

(10) Li, D.; Shen, C.; Zheng, Y.; Xu, J. Electrochemo-Mechanical Degradation and Failure of Active Particles in High Energy Density Batteries: A Review. Small. John Wiley and Sons Inc February 25, 2025. https://doi.org/10.1002/smll.202407740.

(11) Chen, X.; Zhan, R.; Chen, Z.; Wang, X.; Tu, S.; Liu, S.; Zeng, Y.; Dong, T.; Cheng, K.; Ou, Y.; Tan, Y.; Sun, Y. Enhancing Fast-Charging Capability of Thick Electrode in Lithium-Ion Batteries Through Electronic/Ionic Hybrid Conductive Additive Engineering. Adv Energy Mater 2025, No. 2500242.

(12) Zhang, Y.; Lu, S.; Wang, Z.; Volkov, V.; Lou, F.; Yu, Z. Recent Technology Development in Solvent-Free Electrode Fabrication for Lithium-Ion Batteries. Renewable and Sustainable Energy Reviews. Elsevier Ltd September 1, 2023. https://doi.org/10.1016/j.rser.2023.113515.

(13) Chen, R.; Cai, X.; He, X.; Hong, X.; Liu, Y.; So, J. K.; Wang, B.; Zhou, Y.; Cheng, L.; Shen, Z. X. High Mass-Loading CoO@NiCo-LDH//FeNiS Flexible Supercapacitor with High Energy Density and Fast Kinetics. Chemical Engineering Journal 2024, 484. https://doi.org/10.1016/j.cej.2024.149736.

(14) Shao, J.; Zheng, J.; Xing, G.; Lu, Y.; Lv, X.; Zhang, C. Design and Preparation of Thick Electrodes for Lithium-Ion Batteries. J Energy Storage 2024, 103. https://doi.org/10.1016/j.est.2024.114357.

(15) Kim, N. Y.; Kim, J. H.; Koo, H.; Oh, J.; Pang, J. H.; Kang, K. D.; Chae, S. S.; Lim, J.; Nam, K. W.; Lee, S. Y. Material Challenges Facing Scalable Dry-Processable Battery Electrodes. ACS Energy Letters. American Chemical Society November 8, 2024, pp 5688–5703. https://doi.org/10.1021/acsenergylett.4c01690.

(16) Ryu, M.; Hong, Y. K.; Lee, S. Y.; Park, J. H. Ultrahigh Loading Dry-Process for Solvent-Free Lithium-Ion Battery Electrode Fabrication. Nat Commun 2023, 14 (1). https://doi.org/10.1038/s41467-023-37009-7.

(17) Gao, Y.; Yang, Y.; Jia, S.; Luo, D.; Chen, Z. Interfacial Engineering of Solvent-Free Cathodes with High Loading for High-Energy-Density Lithium Metal Batteries. Adv Funct Mater 2025. https://doi.org/10.1002/adfm.202511636.

(18) Lee, D.; Shim, Y.; Kim, Y.; Kwon, G.; Choi, S. H.; Kim, K. S.; Yoo, D. J. Shear Force Effect of the Dry Process on Cathode Contact Coverage in All-Solid-State Batteries. Nat Commun 2024, 15 (1). https://doi.org/10.1038/s41467-024-49183-3.

(19) Sadan, M. K.; Lian, G. J.; Smith, R. M.; Cumming, D. Co, Ni-Free Ultrathick Free-Standing Dry Electrodes for Sustainable Lithium-Ion Batteries. ACS Appl Energy Mater 2023, 6 (24), 12166–12171. https://doi.org/10.1021/acsaem.3c02448.

(20) Yao, W.; Chouchane, M.; Li, W.; Bai, S.; Liu, Z.; Li, L.; Chen, A. X.; Sayahpour, B.; Shimizu, R.; Raghavendran, G.; Schroeder, M. A.; Chen, Y. T.; Tan, D. H. S.; Sreenarayanan, B.; Waters, C. K.; Sichler, A.; Gould, B.; Kountz, D. J.; Lipomi, D. J.; Zhang, M.; Meng, Y. S. A 5 V-Class Cobalt-Free Battery Cathode with High Loading Enabled by Dry Coating. Energy Environ Sci 2023, 16 (4), 1620–1630. https://doi.org/10.1039/d2ee03840d.

(21) Gyulai, A.; Bauer, W.; Ehrenberg, H. Dry Electrode Manufacturing in a Calender: The Role of Powder Premixing for Electrode Quality and Electrochemical Performance. ACS Appl Energy Mater 2023, 6 (10), 5122–5134. https://doi.org/10.1021/acsaem.2c03755.

(22) Mun, J.; Song, T.; Park, M. S.; Kim, J. H. Paving the Way for Next-Generation All-Solid-State Batteries: Dry Electrode Technology. Advanced Materials. John Wiley and Sons Inc 2025. https://doi.org/10.1002/adma.202506123.

(23) Tao, R.; Gu, Y.; Du, Z.; Lyu, X.; Li, J. Advanced Electrode Processing for Lithium-Ion Battery Manufacturing. Nature Reviews Clean Technology 2025, 1 (2), 116–131. https://doi.org/10.1038/s44359-024-00018-w.

(24) Weiss, M.; Ruess, R.; Kasnatscheew, J.; Levartovsky, Y.; Levy, N. R.; Minnmann, P.; Stolz, L.; Waldmann, T.; Wohlfahrt-Mehrens, M.; Aurbach, D.; Winter, M.; Ein-Eli, Y.; Janek, J. Fast Charging of Lithium-Ion Batteries: A Review of Materials Aspects. Advanced Energy Materials. John Wiley and Sons Inc September 1, 2021. https://doi.org/10.1002/aenm.202101126.

(25) Tian, R.; Breshears, M.; Horvath, D. V.; Coleman, J. N. The Rate Performance of Two-Dimensional Material-Based Battery Electrodes May Not Be as Good as Commonly Believed. ACS Nano 2020, 14 (3), 3129–3140. https://doi.org/10.1021/acsnano.9b08304.

(26) Griffith, K. J.; Wiaderek, K. M.; Cibin, G.; Marbella, L. E.; Grey, C. P. Niobium Tungsten Oxides for High-Rate Lithium-Ion Energy Storage. Nature 2018, 559 (7715), 556–563. https://doi.org/10.1038/s41586-018-0347-0.

(27) Sharma, N.; Puthusseri, D.; Thotiyl, M. O.; Ogale, S. Hard Carbon and Li4Ti5O12-Based Physically Mixed Anodes for Superior Li-Battery Performance with Significantly Reduced Li Content: A Case of Synergistic Materials Cooperation. ACS Omega 2017, 2 (12), 8818–8824. https://doi.org/10.1021/acsomega.7b01659.

(28) Zhang, H.; Yang, Y.; Xu, H.; Wang, L.; Lu, X.; He, X. Li4Ti5O12 Spinel Anode: Fundamentals and Advances in Rechargeable Batteries. InfoMat. John Wiley and Sons Inc April 1, 2022. https://doi.org/10.1002/inf2.12228.

(29) Deng, W.; Feng, X.; Li, X.; O'Neill, S.; Hu, L.; Liu, L.; Wong, W.; Hu, Y.-Y.; Li, C. M. Improving the Electrochemical Performance of Li4Ti5O12 Anode by Phosphorus Reduction at Relatively Low Temperature; Chemical Communications, 2018; Vol. 2019-November. https://doi.org/10.1039/x0xx00000x.

(30) Yue, J.; Badaczewski, F. M.; Voepel, P.; Leichtweiß, T.; Mollenhauer, D.; Zeier, W. G.; Smarsly, B. M. Critical Role of the Crystallite Size in Nanostructured Li4Ti5O12 Anodes for Lithium-Ion Batteries. ACS Appl Mater Interfaces 2018, 10 (26), 22580–22590. https://doi.org/10.1021/acsami.8b05057.

(31) Lakhdar, Y.; Geary, H.; Houck, M.; Gastol, D.; Groombridge, A. S.; Slater, P. R.; Kendrick, E. Optimization of Electrode and Cell Design for Ultrafast-Charging Lithium-Ion Batteries Based on Molybdenum Niobium Oxide Anodes. ACS Appl Energy Mater 2022, 5 (9), 11229–11240. https://doi.org/10.1021/acsaem.2c01814.

(32) Green, A. J.; Driscoll, E. H.; Anderson, P. A.; Kendrick, E.; Slater, P. R. High-Power Recycling: Upcycling to the next Generation of High-Power Anodes for Li-Ion Battery

Applications. J Mater Chem A Mater 2024, 12 (12), 7321–7328. https://doi.org/10.1039/d3ta07549d.

(33) Gultom, N. S.; Hsieh, T. S.; Liao, S. C.; Ko, G. Y.; Kuo, D. H. Improved Performance of Li-Added Mo-Nb Oxide as the Anode for Li-Ion Batteries with N-Carbon Coating. ACS Appl Energy Mater 2022, 5 (5), 6129–6238. https://doi.org/10.1021/acsaem.2c00534.

(34) Ahn, Y.; Li, T.; Huang, S.; Ding, Y.; Hwang, S.; Wang, W.; Luo, Z.; Wang, J. H.; Nam, G.; Liu, M. Mixed-Phase Niobium Oxide as a Durable and Ultra-Fast Charging Anode for High-Power Lithium-Ion Batteries. Adv Funct Mater 2024, 34 (8). https://doi.org/10.1002/adfm.202310853.

(35) Li, T.; Nam, G.; Liu, K.; Wang, J. H.; Zhao, B.; Ding, Y.; Soule, L.; Avdeev, M.; Luo, Z.; Zhang, W.; Yuan, T.; Jing, P.; Kim, M. G.; Song, Y.; Liu, M. A Niobium Oxide with a Shear Structure and Planar Defects for High-Power Lithium Ion Batteries. Energy Environ Sci 2022, 15 (1), 254–264. https://doi.org/10.1039/d1ee02664j.

(36) Xia, X.; Yang, J.; Liu, Y.; Zhang, J.; Shang, J.; Liu, B.; Li, S.; Li, W. Material Choice and Structure Design of Flexible Battery Electrode. Advanced Science. John Wiley and Sons Inc January 25, 2023. https://doi.org/10.1002/advs.202204875.

(37) Gaikwad, A. M.; Arias, A. C. Understanding the Effects of Electrode Formulation on the Mechanical Strength of Composite Electrodes for Flexible Batteries. ACS Appl Mater Interfaces 2017, 9 (7), 6390–6400. https://doi.org/10.1021/acsami.6b14719.

(38) Xiao, B. H.; Xiao, K.; Li, J. X.; Xiao, C. F.; Cao, S.; Liu, Z. Q. Flexible Electrochemical Energy Storage Devices and Related Applications: Recent Progress and Challenges. Chemical Science. Royal Society of Chemistry June 28, 2024, pp 11229–11266. https://doi.org/10.1039/d4sc02139h.

(39) Han, S. A.; Suh, J. H.; Park, M. S.; Kim, J. H. High-Loading Dry-Electrode for All Solid-State Batteries: Nanoarchitectonic Strategies and Emerging Applications. Electrochemical Energy Reviews. Springer December 1, 2025. https://doi.org/10.1007/s41918-025-00240-5.

(40) Qin, T.; Yang, H.; Li, Q.; Yu, X.; Li, H. Design of Functional Binders for High-Specific-Energy Lithium-Ion Batteries: From Molecular Structure to Electrode Properties. Industrial Chemistry & Materials 2024, 2 (2), 191–225. https://doi.org/10.1039/d3im00089c.

(41) Park, J.; Kim, J.; Kim, J.; Kim, M.; Song, T.; Paik, U. Sustainable and Cost-Effective Electrode Manufacturing for Advanced Lithium Batteries: The Roll-to-Roll Dry Coating Process. Chemical Science. Royal Society of Chemistry March 28, 2025, pp 6598–6619. https://doi.org/10.1039/d5sc00059a.

(42) Choi, J.; Polyzos, G.; Humphrey, H. E.; Toomey, M.; Kanbargi, N.; Naskar, A.; Belharouak, I.; Sharma, J. Long Carbon Fibers Boost Performance of Dry Processed Li-Ion Battery Electrodes. J Power Sources 2025, 640. https://doi.org/10.1016/j.jpowsour.2025.236603.

(43) Aboalhassan, A. A.; Zhang, Y.; Zahng, H.; Yan, J.; Yu, J.; Ding, B. Facile Fabrication of Flexible Carbon Nanofiber Electrodes with Both High Packing Density and Capacity for Li-Ion Batteries. Advanced Energy and Sustainability Research 2021, 2, 2100020. https://doi.org/10.1002/aesr.202100020

(44) Abdollahifar, M.; Cavers, H.; Scheffler, S.; Diener, A.; Lippke, M.; Kwade, A. Insights into Influencing Electrode Calendaring on the Battery Performance. Advanced Energy Materials 2023, 13, 2300973. https://doi.org/10.1002/aenm.202300973.

(45) Li, Z.; Ye, S.; Wang, W.; Xu, Q.; Liu, H.; Wang, Y.; Xia, Y. Free-Standing Sandwich-Structured Flexible Film Electrode Composed of Na2Ti3O7 Nanowires@CNT and Reduced Graphene Oxide for Advanced Sodium-Ion Batteries. ACS Omega 2017, 2 (9), 5726–5736. https://doi.org/10.1021/acsomega.7b01051.

(46) Li, M.; Pan, F.; Choo, E. S. G.; Lv, Y.; Chen, Y.; Xue, J. Designed Construction of a Graphene and Iron Oxide Freestanding Electrode with Enhanced Flexible Energy-Storage Performance. ACS Appl Mater Interfaces 2016, 8 (11), 6972–6981. https://doi.org/10.1021/acsami.5b10853.

(47) Zhang, Y.; Jing, S.; Shen, H.; Li, S.; Huang, Y.; Shen, Y.; Liu, S.; Zhang, Z.; Liu, F. Developments, Novel Concepts, and Challenges of Current Collectors: From Conventional Lithium Batteries to All-Solid-State Batteries. ChemElectroChem. John Wiley and Sons Inc July 15, 2024. https://doi.org/10.1002/celc.202300739.

(48) Chen, C. H.; Chiu, J. M.; Shown, I.; Wang, C. H. Simple Way of Making Free-Standing Cathode Electrodes for Flexible Lithium-Ion Batteries. RSC Adv 2022, 12 (15), 9249–9255. https://doi.org/10.1039/d1ra08993e.

(49) Yu, Y.; Tang, Z.; Wang, Y.; Zhang, H.; Zhang, H.; Li, X. Cobalt-Based Current Collectors for Flexible Electrodes and Their Application in Lithium-Sulfur Batteries. J Mater Chem A Mater 2024, 12 (10), 5760–5767. https://doi.org/10.1039/d3ta06966d.

(50) Chen, B.; Zhang, Z.; Xiao, M.; Wang, S.; Huang, S.; Han, D.; Meng, Y. Polymeric Binders Used in Lithium Ion Batteries: Actualities, Strategies and Trends. ChemElectroChem. John Wiley and Sons Inc July 15, 2024. https://doi.org/10.1002/celc.202300651.

(51) Grygiel, M.; Ratyński, M.; Czerwiński, A.; Hamankiewicz, B. PEDOT:PSS as a Conductive Polymer Binder for Ecologically and Economically Sustainable, Carbon-Free NMC Electrodes. Appl Phys A Mater Sci Process 2024, 130 (12). https://doi.org/10.1007/s00339-024-08039-9.

(52) Yoon, D. H.; Yoon, S. H.; Ryu, K. S.; Park, Y. J. PEDOT:PSS as Multi-Functional Composite Material for Enhanced Li-Air-Battery Air Electrodes. Sci Rep 2016, 6. https://doi.org/10.1038/srep19962.

Chapter 3:

Growth of Titanium Dioxide Nanowires on Flexible Carbon Fibers for High-Rate and Flexible Lithium-Ion Batteries

Abstract:

In recent years, considerable attention has shifted from conventional rigid batteries to flexible energy storage systems, driven by the demand for portable electronics that require flexibility, fast charging, and high energy density. Conventionally, electrodes fabricated using the slurry-casting method require a current collector, which limits electrode flexibility. Here, we report a flexible, freestanding anode based on titanium dioxide, designed for fast-charging applications. Specifically, nanostructured titanium dioxide was investigated to accommodate fast-charging capability. Using hydrothermal/solvothermal synthesis methods, titanium dioxide nanowires were directly grown on a flexible carbon fiber substrate, allowing for integration into flexible lithium-ion batteries. This electrode design not only reduces costs by eliminating the need for a current collector but also mitigates concerns of electrode detachment under external pressure or deformation due to its freestanding configuration. In summary, this work demonstrates an electrode design combining excellent mechanical strength, inherent flexibility, and high electronic conductivity, highlighting its great potential for integration into flexible energy storage systems.

3.1 Introduction

Growing interest in flexible devices for portable electronics, such as wearable technologies, has emerged in response to increasing consumer demands for fast-charging capability, high energy capacity, and mechanically flexible batteries [1,2]. Among different types of rechargeable batteries, lithium-ion batteries (LIBs) are most commonly adopted due to their high energy density, high output voltage, and long cycle life [3,4]. However, conventional LIBs face significant challenges in achieving mechanical flexibility due to their inherently rigid structures, which can result in the detachment of electrode materials from current collectors under external mechanical stress [5,6]. Repeated mechanical deformation, such as bending, twisting, and stretching, may further cause capacity degradation, potential device failure, and increased safety risks [7]. In addition, LIBs encounter challenges in achieving fast-charging capability [8]. While electrode materials play a critical role in determining the electrochemical performance of batteries, commercially available electrode materials continue to face limitations in supporting high rate charging [9]. For instance, graphite, the conventional anode material widely used in commercial LIBs exhibit sluggish intercalation kinetics, which restricts their ability to support fast-charging operations [10,11]. To address this limitation, metal oxides have attracted considerable attention as potential high-rate anode materials for LIBs [12]. Among various metal oxides, titanium dioxides (TiO_2) have been recognized as a promising anode material candidate to accommodate rapid lithium-ion diffusion [13]. Particularly, TiO_2 nanostructures have been extensively investigated for their potential to deliver high-rate capability [14]. The form of nanowire microstructure exhibits excellent rate capability and stable, reversible capacity, highlighting their promise as high-performance anode materials [15,16]. Moreover, one dimensional (1D) microstructure of nanowires offers structural flexibility and can be fabricated as binder-free electrodes, making them highly suitable for applications in flexible electronic devices [17]. To further ensure electrode flexibility, carbon cloth can be employed as a flexible substrate, owing to its excellent flexibility, high electrical conductivity, and mechanical robustness [18,19]. Accordingly, the direct growth of 1D nanowires on carbon cloth can help facilitate the fabrication of binder-free, flexible electrodes.

Herein, this study reports one-dimensional (1D) TiO_2 nanostructures that were directly grown on a flexible carbon cloth substrate via hydrothermal synthesis method. The resulting TiO_2 nanowire array uniformly integrated with the substrate, forming a binder-free anode for

LIBs. Systematic experimental optimizations were conducted to determine the optimal synthesis conditions at which the TiO_2 nanowire anode exhibits outstanding performance, including high-rate capability, cycling stability, and remarkable mechanical flexibility, essential for fast-charging, flexible energy storage applications.

3.2 Experimental Section

3.2.1 Electrode Preparation

To perform experimental optimizations, both hydrothermal and solvothermal routes were employed by varying the synthesis solution. Carbon fiber sheets were cut to dimensions of 3 x 5 cm and rinsed in a solution consisting of 20 mL deionized water, 20 mL acetone, and 20 mL ethanol. The rinsed samples were then dried in an oven at 70°C for 1 h to evaporate the residual rinsing solutions. The carbon fiber surface was prepared for hydrothermal/solvothermal synthesis, the cleaned carbon fiber was immersed in 50 mL of hydrochloric acid (HCl) for 12 h. Following the acid treatment, the samples were rinsed again in 20mL deionized water, 20mL acetone, and 20mL ethanol. The samples were then dried in an oven at 70°C for 1 h. The treated carbon cloth was immersed in a solution containing 50 mL ethanol and 1.1 mL titanium butoxide (TBT) for 12 h, followed by annealing at 400°C for 30 min to form a titanium oxide seed layer on the carbon cloth. For solvothermal synthesis, the two sets of prepared carbon cloths were placed in a 100 mL Teflon-lined stainless-steel autoclave containing a mixture of acetone (37.5mL), 37-38% HCl (22.5 mL), and TBT (1.5 mL), and treated at 200°C for 3 h. For hydrothermal synthesis, the two prepared carbon cloth samples were placed in a 100 mL Teflon-lined stainless-steel autoclave containing a mixture of 40 mL deionized water, 40 mL HCl, and 1.2 mL TBT, and treated at the same condition.

3.2.2 Electrochemical Characterization

In half-cell fabrication, lithium metal was employed as both the reference and counter electrode, and the prepared anode had a mass loading of 2mg cm^{-2}. The electrolyte consisted of 1.0M $LiPF_6$ in EC/DMC (1:1 v/v), a microporous trilayer PP/PE/PP membrane (Celgard 2325) separator, and lithium metal (Thermo Scientific) were used for cell assembly. Charge-discharge measurements of the assembled CR 2032-coin cells were carried out using a battery analyzer

(BST8-MA, MTI Corporation) at C-rates of 0.5C, 1C, 2C, and 5C (1C = 335 mA g^{-1}), with five formation cycles conducted at each C-rate.

3.2.3 Electrode Characterization

Mechanical Analysis: Mechanical strength measurements of the prepared anodes were conducted using a Dynamic Mechanical Analyzer (TA Instruments Q800). The loaded hydrothermal sample had dimensions of 12.36 mm x 5.50 mm x 0.30 mm, the solvothermal sample measured 12.36 mm x 4.88 mm x 0.30 mm, and the pristine carbon fibers with measurements of 9.80 mm x 4.45 mm x 0.30 mm (l × w × t). The flexibility of the prepared samples was evaluated from stress-strain curves obtained under a preset load of 1N, a ramp force of 1.5 N/min, and a maximum force of 18N.

Scanning Electron Microscopy (SEM): Microstructural surface images were acquired using a Quanta FEG 250 scanning electron microscopy (SEM) operated at a beam voltage of 10 kV.

3.3 Results & Discussion

3.3.1 Design Concept of Freestanding Titanium Dioxide Flexible Anode

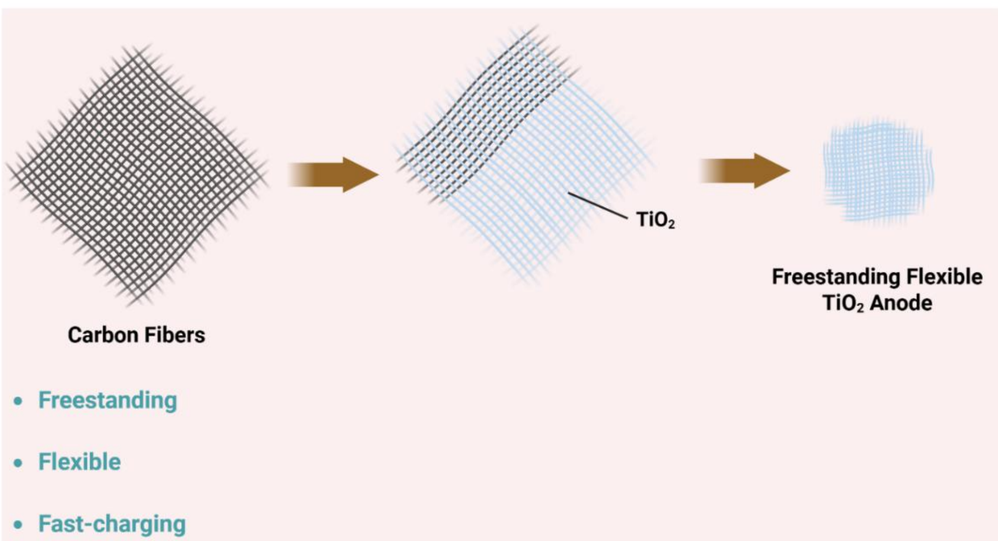

Figure 3-1. Design concept of flexible TiO_2 synthesized carbon fiber anode.

In this study, hydrothermal/solvothermal synthesis was directly carried out on a flexible carbon fiber substrate to produce a freestanding anode. The selection of carbon fiber was driven by its excellent mechanical strength, making it a promising material for flexible and wearable device applications [20]. Furthermore, its high electrical conductivity facilitates efficient electron transport during electrochemical reaction in battery systems [21]. Another advantage of the freestanding electrode lies in its ability to reduce overall weight by removing the need for a current collector, which enables higher active material mass loading and therefore, improves the energy density of the battery system [22–24]. Moreover, eliminating the need to adhere fabricated electrodes onto a current collector also allows for being environmentally friendly by avoiding the use of toxic NMP in the binder formulation [25]. The anode design not only enables a freestanding configuration but also incorporates titanium dioxide onto the carbon fiber to facilitate fast-charging performance. Overall, this study aims to develop an anode that is freestanding and flexible while supporting fast charging, with the goal of integration into flexible electronics.

3.3.2 Microstructural Observations of TiO_2 Anodes

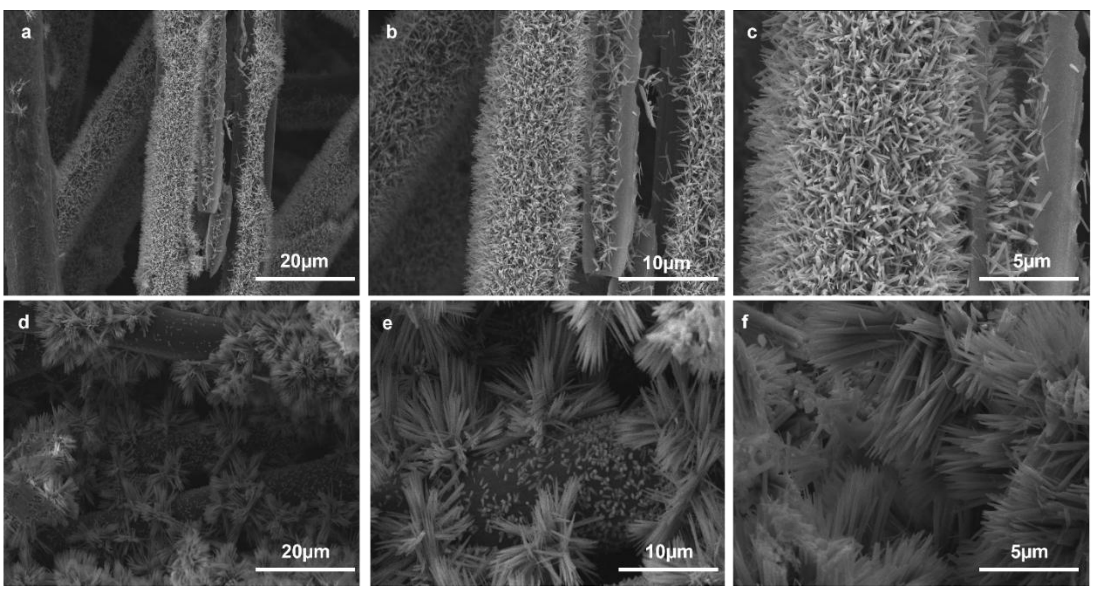

Figure 3-2. Scanning electron microscopy images of a-c) hydrothermal d-f) solvothermal synthesized TiO_2 carbon cloth.

In the course of experimental optimization, different synthesis routes were evaluated. The morphologies of TiO_2 grown on carbon fibers, prepared using the two different synthesis routes, were examined by scanning electron microscopy (**Figure 2**). TiO_2 synthesized via the hydrothermal method exhibited needle-like nanowire morphologies (Figure 2a-c), and a similar needle-like structure was observed for TiO_2 nanowires prepared through the solvothermal method (Figure 2d-f). Notably, distinct size variations in the nanowires grown on carbon fibers were observed between the two synthesis methods.

3.3.3 Mechanical Testing of TiO_2 Anodes

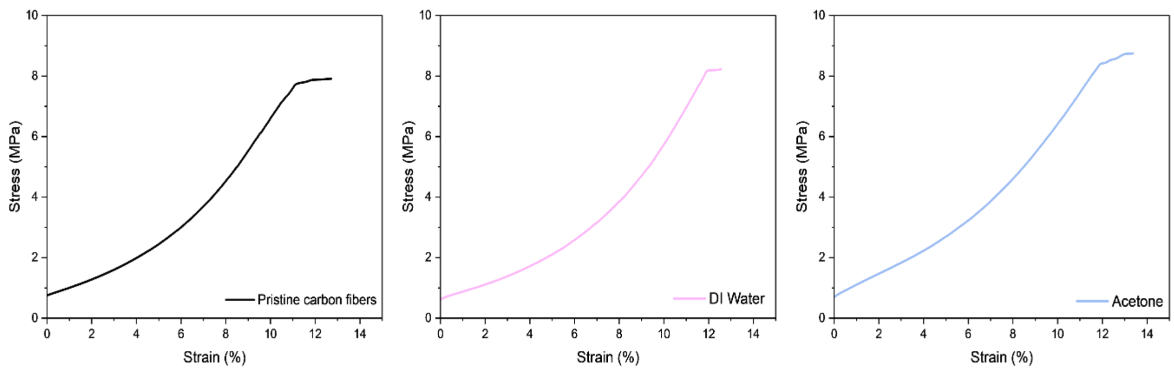

Figure 3-3. Mechanical characterization of a) pristine carbon fibers b) hydrothermal c) solvothermal synthesized TiO_2 carbon cloth.

To evaluate the flexibility of the synthesized electrodes, tensile strength measurements were performed using a dynamic mechanical analyzer (**Figure 3**). For comparison, pristine carbon fiber substrates were also subjected to tensile strength testing to assess any changes in mechanical properties before and after synthesis. The results indicate that pristine carbon fibers exhibited a yield strength of 7.74 MPa and sustained elongation up to a strain of 11.16 % (Figure 3a). Comparatively the hydrothermally synthesized electrode demonstrated a yield strength of 8.17 MPa at 11.92 % strain, while the electrode fabricated using solvothermal synthesis method showed 8.39 MPa at 11.89 % strain (Figure 3b-c). These results indicate that the mechanical strength of the electrodes remains comparable to that of the pristine carbon cloth, confirming the preservation of their excellent mechanical properties after synthesis.

3.3.4 Electrochemical Performance of TiO_2 Anodes

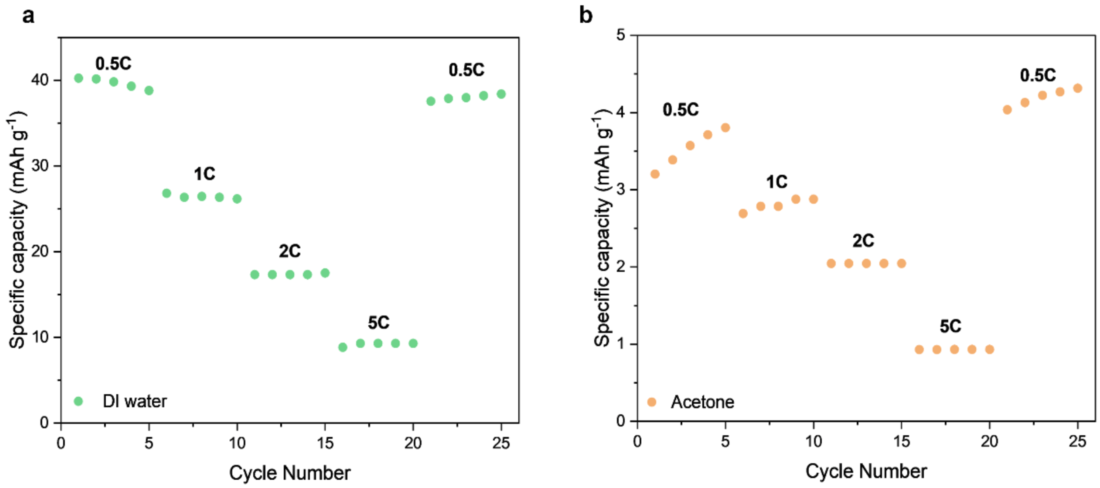

Figure 3-4. Electrochemical Performance of a) hydrothermal b) solvothermal synthesized TiO_2 carbon cloth

The electrochemical performance was evaluated at various current rates to assess fast-charging capability at high C-rate, as well as performance at lower rates. As shown in **Figure 4**, the specific capacities obtained from both hydrothermal and solvothermal synthesis method were significantly lower than the theoretical capacity (335 mAh g^{-1}). At a current rate of 0.5C within the voltage range of 1-3V, the hydrothermal sample exhibited an initial specific capacity of 40.24 mAh g^{-1}, whereas the solvothermal sample showed 3.20 mAh g^{-1}. The specific capacity typically varies depending on the crystal structure of the grown titanium dioxide however, the low values observed in Figure 4 are considerably below expectations, making it difficult to confirm successful crystal growth. Liu et al. (2012) similarly synthesized titanium dioxide nanowires on carbon fiber using a hydrothermal method. The air-annealed TiO2 sample exhibited an initial discharge capacity of 400 mAh g^{-1} and a second discharge capacity of 296 mAh g^{-1} when tested at 1C within the voltage range of 0.01-3V, further confirming that the results obtained in Figure 4 are significantly lower than expected [26]. According to the SEM images in Figure 2, particle size appears to influence the results shown in Figure 4. Specifically, the larger particles produced by solvothermal method exhibited lower electrochemical performance compared to the smaller, hydrothermally grown titanium dioxide particles. Xue et al. (2025) investigated the effect of

TiO_2 particle size in titanium niobium oxides (TNO) on the electrochemical performance of lithium-ion batteries. TNO samples with varying particle sizes of 1.09, 1.03, 1.06, 0.94, and 1.00 μm (TNO1-TNO5, respectively) were synthesized, among which TNO4 exhibited the smallest particle size. At lower current rates, TNO1 initially delivered highest capacity however, it experienced capacity decay upon extended cycling, attributed to its larger particle size. In contrast, rate capability tests demonstrated that TNO3 consistently achieved the highest capacity across all current rates among the samples evaluated [27].

3.4 Conclusion

In this study, TiO_2 nanorods were grown on carbon fibers via hydrothermal/solvothermal synthesis for the development of freestanding, flexible, and fast-charging anodes. Mechanical testing was conducted to evaluate the flexibility of the anode and to assess changes in mechanical durability before and after synthesis. Microstructural observations revealed that the morphological difference from differences in nanorod size influences the electrochemical performance. However, the measured capacity remained significantly lower than the theoretical value, possibly suggesting that the crystal structures were not successfully achieved. Despite the overall low capacity, the smaller particle size obtained through hydrothermal synthesis exhibited higher capacity than the larger particle size produced by solvothermal synthesis. Moving forward, further experimental optimization is required, including adjustment of solvent ratios, confirmation of crystallinity, and the potential implementation of surface treatments of conductive coatings to enhance the overall capacity.

3.5 Supplementary Information

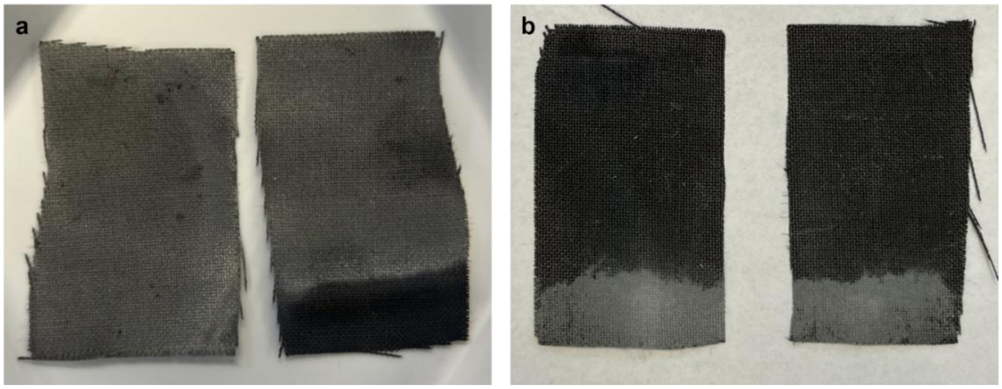

Figure S3-1. TiO_2 Synthesis Images of a) hydrothermal b) solvothermal synthesized TiO2 carbon cloth.

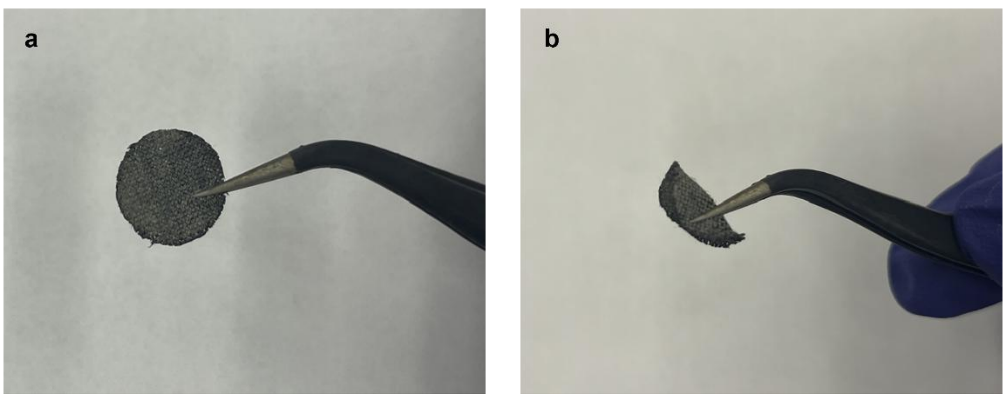

Figure S3-2. Fabricated electrode a) before bending b) after bending.

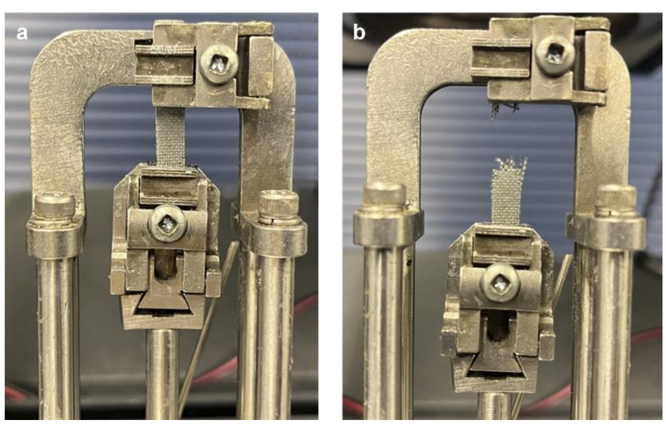

Figure S3-3. Tensile strength testing a) before b) after fracture.

3.6 References

(1) Qian, G.; Liao, X.; Zhu, Y.; Pan, F.; Chen, X.; Yang, Y. Designing Flexible Lithium-Ion Batteries by Structural Engineering. *ACS Energy Letters*. American Chemical Society March 8, 2019, pp 690–701. https://doi.org/10.1021/acsenergylett.8b02496.

(2) Park, M. H.; Noh, M.; Lee, S.; Ko, M.; Chae, S.; Sim, S.; Choi, S.; Kim, H.; Nam, H.; Park, S.; Cho, J. Flexible High-Energy Li-Ion Batteries with Fast-Charging Capability. *Nano Lett* 2014, *14* (7), 4083–4089. https://doi.org/10.1021/nl501597s.

(3) Kim, M.; Kim, J. Advanced Integrated Fast-Charging Protocol for Lithium-Ion Batteries by Considering Degradation. *ACS Sustain Chem Eng* 2024, *12* (17), 6786–6796. https://doi.org/10.1021/acssuschemeng.4c01673.

(4) Gao, Z.; Song, N.; Zhang, Y.; Li, X. Cotton-Textile-Enabled, Flexible Lithium-Ion Batteries with Enhanced Capacity and Extended Lifespan. *Nano Lett* 2015, *15* (12), 8194–8203. https://doi.org/10.1021/acs.nanolett.5b03698.

(5) Zhao, Y.; Guo, J. Development of Flexible Li-Ion Batteries for Flexible Electronics. *InfoMat*. Blackwell Publishing Ltd September 1, 2020, pp 866–878. https://doi.org/10.1002/inf2.12117.

(6) Li, H.; Wang, H.; Chan, D.; Xu, Z.; Wang, K.; Ge, M.; Zhang, Y.; Chen, S.; Tang, Y. Nature-Inspired Materials and Designs for Flexible Lithium-Ion Batteries. *Carbon Energy*. John Wiley and Sons Inc September 1, 2022, pp 878–900. https://doi.org/10.1002/cey2.187.

(7) Shi, Y.; Wang, Z.; Wen, L.; Pei, S.; Chen, K.; Li, H.; Cheng, H. M.; Li, F. Ultrastable Interfacial Contacts Enabling Unimpeded Charge Transfer and Ion Diffusion in Flexible Lithium-Ion Batteries. *Advanced Science* 2022, *9* (10). https://doi.org/10.1002/advs.202105419.

(8) Li, C.; Liang, Z.; Wang, L.; Cao, D.; Yin, Y. C.; Zuo, D.; Chang, J.; Wang, J.; Liu, K.; Li, X.; Luo, G.; Deng, Y.; Wan, J. Superwettable Electrolyte Engineering for Fast Charging Li-Ion Batteries. *ACS Energy Lett* 2024, *9* (3), 1295–1304. https://doi.org/10.1021/acsenergylett.3c02572.

(9) Wang, R.; Wang, L.; Liu, R.; Li, X.; Wu, Y.; Ran, F. "Fast-Charging" Anode Materials for Lithium-Ion Batteries from Perspective of Ion Diffusion in Crystal Structure. *ACS Nano*. American Chemical Society January 30, 2024, pp 2611–2648. https://doi.org/10.1021/acsnano.3c08712.

(10) Ding, X.; Zhou, Q.; Li, X.; Xiong, X. Fast-Charging Anodes for Lithium Ion Batteries: Progress and Challenges. *Chemical Communications* 2024, *60* (18), 2472–2488. https://doi.org/10.1039/d4cc00110a.

(11) Kim, N.; Chae, S.; Ma, J.; Ko, M.; Cho, J. Fast-Charging High-Energy Lithium-Ion Batteries via Implantation of Amorphous Silicon Nanolayer in Edge-Plane Activated Graphite Anodes. *Nat Commun* 2017, *8* (1). https://doi.org/10.1038/s41467-017-00973-y.

(12) Fu, W.; Zhao, E.; Ma, R.; Sun, Z.; Yang, Y.; Sevilla, M.; Fuertes, A. B.; Magasinski, A.; Yushin, G. Anatase TiO2 Confined in Carbon Nanopores for High-Energy Li-Ion Hybrid Supercapacitors Operating at High Rates and Subzero Temperatures. *Adv Energy Mater* 2020, *10* (2). https://doi.org/10.1002/aenm.201902993.

(13) Liang, S.; Wang, X.; Qi, R.; Cheng, Y. J.; Xia, Y.; Müller-Buschbaum, P.; Hu, X. Bronze-Phase TiO2 as Anode Materials in Lithium and Sodium-Ion Batteries. *Advanced Functional Materials*. John Wiley and Sons Inc June 1, 2022. https://doi.org/10.1002/adfm.202201675.

(14) Wang, H. E.; Lu, Z. G.; Xi, L. J.; Ma, R. G.; Wang, C. D.; Zapien, J. A.; Bello, I. Facile and Rapid Synthesis of Highly Porous Wirelike TiO 2 as Anodes for Lithium-Ion Batteries. *ACS Appl Mater Interfaces* 2012, *4* (3), 1608–1613. https://doi.org/10.1021/am2017738.

(15) Shi, H.; Shi, C.; Jia, Z.; Zhang, L.; Wang, H.; Chen, J. Titanium Dioxide-Based Anode Materials for Lithium-Ion Batteries: Structure and Synthesis. *RSC Advances*. Royal Society of Chemistry November 23, 2022, pp 33641–33652. https://doi.org/10.1039/d2ra05442f.

(16) Autthawong, T.; Chimupala, Y.; Haruta, M.; Kurata, H.; Kiyomura, T.; Yu, A. S.; Chairuangsri, T.; Sarakonsri, T. Ultrafast-Charging and Long Cycle-Life Anode Materials of TiO2-Bronze/Nitrogen-Doped Graphene Nanocomposites for High-Performance Lithium-Ion Batteries. *RSC Adv* 2020, *10* (71), 43811–43824. https://doi.org/10.1039/d0ra07733j.

(17) Liu, Y.; Yang, Y. Recent Progress of TiObased Anodes for Li Ion Batteries. *Journal of Nanomaterials*. Hindawi Publishing Corporation 2016. https://doi.org/10.1155/2016/8123652.

(18) Tjandra, R.; Li, G.; Wang, X.; Yan, J.; Li, M.; Yu, A. Flexible High Performance Lithium Ion Battery Electrode Based on a Free-Standing TiO2 Nanocrystals/Carbon Cloth Composite. *RSC Adv* 2016, *6* (42), 35479–35485. https://doi.org/10.1039/c6ra03262a.

(19) Balogun, M. S.; Li, C.; Zeng, Y.; Yu, M.; Wu, Q.; Wu, M.; Lu, X.; Tong, Y. Titanium Dioxide@titanium Nitride Nanowires on Carbon Cloth with Remarkable Rate Capability for Flexible Lithium-Ion Batteries. *J Power Sources* 2014, *272*, 946–953. https://doi.org/10.1016/j.jpowsour.2014.09.034.

(20) Zhao, C.; Zheng, J.; Wang, Y.; Rui, P.; Yang, G.; Zhao, C.; Xu, S. Vaporized Hydrothermal Functionalization of Carbon Fiber and Its Superior Supercapacitor Performance. *Energy and Fuels* 2022, *36* (7), 4052–4064. https://doi.org/10.1021/acs.energyfuels.2c00261.

(21) Akter, M.; Hossain, I.; Howlader, M.; Shahriar, F.; Saima, U. H. Recent Research Advancements in Carbon Fiber-Based Anode Materials for Lithium-Ion Batteries. *Energy Technology*. John Wiley and Sons Inc March 1, 2025. https://doi.org/10.1002/ente.202401426.

(22) Cui, L. F.; Hu, L.; Choi, J. W.; Cui, Y. Light-Weight Free-Standing Carbon Nanotube-Silicon Films for Anodes of Lithium Ion Batteries. *ACS Nano* 2010, *4* (7), 3671–3678. https://doi.org/10.1021/nn100619m.

(23) Zoller, F.; Häringer, S.; Böhm, D.; Illner, H.; Döblinger, M.; Sofer, Z.; Finsterbusch, M.; Bein, T.; Fattakhova-Rohlfing, D. Overcoming the Challenges of Freestanding Tin Oxide-Based Composite Anodes to Achieve High Capacity and Increased Cycling Stability. *Adv Funct Mater* 2021, *31* (43). https://doi.org/10.1002/adfm.202106373.

(24) Shen, C.; Fang, X.; Ge, M.; Zhang, A.; Liu, Y.; Ma, Y.; Mecklenburg, M.; Nie, X.; Zhou, C. Hierarchical Carbon-Coated Ball-Milled Silicon: Synthesis and Applications in Free-Standing Electrodes and High-Voltage Full Lithium-Ion Batteries. *ACS Nano* 2018, *12* (6), 6280–6291. https://doi.org/10.1021/acsnano.8b03312.

(25) Zhao, Z.; Wang, F.; Li, B.; Chen, Z.; Zhou, H.; Wen, X.; Ye, M. Rational Fabrication Strategies of Freestanding/Binder-Free Electrodes for Efficient Capacitive Deionization. *Materials Advances*. Royal Society of Chemistry April 19, 2023, pp 2247–2268. https://doi.org/10.1039/d2ma01100j.

(26) Liu, Y.; Liu, C.; Li, J. Flexible Free-Standing Hydrogen-Treated Titanium Dioxide Nanowire Arrays as High Performance Anode for Lithium Ion Batteries; Royal Society of Chemistry, 2012; Vol. 2019-November. https://doi.org/10.1039/C4TA03495C.

(27) Xue, Z.; Li, T.; Sun, H.; Tang, Q.; Yu, Y.; Zhu, K. Influence of TiO2 Particle Size on the Synthesis of Titanium-Niobium Oxides and Their Electrochemical Performance in Lithium-Ion Cells. *ACS Omega* 2025, *10* (15), 15744–15752. https://doi.org/10.1021/acsomega.5c01447.

Chapter 4: Conclusion

4.1 Closing Remarks

In recent years, the use of lithium-ion batteries has been rapidly increasing due to their versatility, particularly in response to the rising demand for technologies such as portable electronics and electric vehicles. Moreover, the increasing incorporation of lithium-ion batteries in the automotive sector has positioned rechargeable battery development as a critical driver in the transition toward green energy, reducing reliance on fossil fuels. Although, as technology advances toward integration with flexible or non-traditionally shaped electronics, conventional lithium-ion batteries present significant challenges due to their inherent rigidity. Accordingly, the development of flexible lithium-ion batteries is essential to align with the progression of next-generation electronics and address emerging consumer demands. As a result, the overarching objective of this thesis was to explore the design of a flexible, fast-charging anode to enable its application in next-generation flexible and wearable electronic devices.

Study 1 employed fast-charging capable niobium oxide (Nb_2O_5) to fulfill the study's objective. A solvent-free electrode fabrication method was selected to support the anode design. This approach was chosen for its environmentally friendly characteristics, offering a sustainable alternative to the conventional slurry-casting method, which typically involves the use of toxic solvents. In addition, removing the solvent from the process facilitated high mass loading of the electrode, increasing the amount of active material and playing a critical role in enhancing electrochemical performance. In this experimental methodology, both particle and fibrous form of carbon additives were utilized to ensure sufficient fibrilization and minimize void spaces within the electrode structure. The ratios of these carbon additives were optimized to achieve high electrochemical performance while maintaining excellent flexibility and mechanical durability. Based on both tensile and electrochemical testing, the optimal composition was determined to be an equal ratio of carbon fibers to carbon particles (**SP_CNF(5:5)**). In a half-cell configuration assembled in a coin-cell format with a mass loading of 8-10 mg cm^{-2}, the SP_CNF(8:2), SP_CNF(5:5), and SP_CNF(2:8) samples delivered specific capacities of 193.72 mAh g^{-1}, 224.32 mAh g^{-1}, and 212.80 mAh g^{-1}, respectively, when tested at a current rate of 0.5C within the voltage range of 1 to 3V. Cyclic bending was subsequently applied to the optimal sample, SP_CNF(5:5) electrode, to further evaluate its mechanical robustness and the resulting impact on electrochemical performance. The results demonstrated no notable change in electrochemical performance before and after cyclic bending, confirming the electrode's mechanical resilience under external deformation. In addition, full-cell testing in a pouch cell configuration, assembled with the fabricated anode and an NMC 811 cathode, demonstrated a specific capacity of 186 mAh g^{-1} at 0.5C. Moreover, the full cell demonstrated strong potential as a flexible pouch cell, maintaining 82.1% capacity retention after 1,000 cycles under a fast-charging rate of 5C, highlighting its capability for long-term cycling.

Study 2 reported preliminary work on a freestanding, flexible, and fast-charging TiO2 anode. Using hydrothermal/solvothermal synthesis, TiO2 was directly grown on carbon fiber, enabling the fabrication of a mechanically durable and flexible anode. Comparative analysis of the two synthesis routes demonstrated that particle size directly influences electrochemical performance. Mechanical flexibility was evaluated through comparative tensile strength assessments of pristine carbon fiber and samples synthesized by two different methods. Pristine carbon fiber exhibited a yield strength of 7.74 MPa with 11.16% strain, while the hydrothermal and solvothermal samples showed yield strength of 8.17 MPa (11.92% strain) and 8.39 MPa (11.89% strain), respectively. These results indicate that the mechanical properties remained unchanged after synthesis, confirming the excellent mechanical flexibility of the anode. Furthermore, electrochemical performance analysis in conjunction with microstructural observations revealed that particle size had a direct influence on electrochemical performance. The initial specific capacity achieved by hydrothermal synthesis was 40.24 mAh g^{-1}, and solvothermal synthesis was 3.20 mAh g^{-1} when tested at a current rate of 0.5C from within the voltage range of 1-3V. Thus, the smaller particles obtained via hydrothermal synthesis clearly exhibited superior electrochemical performance compared to the larger particles produced by solvothermal synthesis. However, further experimental optimization is required, as the electrochemical performance obtained from both synthesis methods remained well below the theoretical specific capacity (335 mAh g^{-1}). Moreover, the significantly low values, when compared against literature values, make it difficult to confirm that successful crystal growth occurred on carbon fiber.

4.2 Future Work

In the first study, to further demonstrate the practicality of the pouch cell configuration, similar to the optimization done on anode side, optimization of the cathode's flexibility, along with electrochemical analysis can be performed. Furthermore, beyond simply lighting an LED with the pouch cell, integrating it into a wearable device such as an LED watch and demonstrating its functional operation can confirm its operation as a flexible battery.

For the second study, plasma treatment can be employed as an alternative to acid treatment, to provide a more uniform and controlled surface modification to promote improved titanium dioxide growth on the carbon fiber substrate. In addition to the pre-synthesis treatment, the introduction of post-growth surface treatment steps could potentially improve electrical conductivity and further enhance electrochemical performance. For instance, techniques such as elemental doping or surface coating may be employed to achieve these improvements. Also, the mass loading can be increased to improve on electrochemical performance by adjusting the dimensions of the carbon fiber substrate inserted into the autoclave, or by varying the amounts of active material and solvent used during synthesis. Next, exploring alternative flexible substrates, such as nanowire films, beyond carbon fiber could further optimize both electrochemical capacity and mechanical durability. Once the synthesis is optimized using the methods suggested above, the flexibility of the synthesized anode can be further assessed by subjecting the electrode to rigorous mechanical folding or bending, followed by evaluating of its post-bending performance, similar to experiments done in the first study. Another experiment could involve evaluating the long-term cycling performance of the cell to assess the capacity retention after extensive cycling. Finally, testing full-cell configurations using a pouch cell assembly can more effectively demonstrate the cell's potential as a flexible battery.